# THE ROLE OF INTERSPECIFIC INTERACTIONS IN THE MITIGATION OF VECTOR-BORNE DISEASE

CASE STUDIES ON *AEDES AEGYPTI* AND *AEDES ALBOPICTUS*




**ROBERT STEPHEN PATON**

Balliol College

University of Oxford

A thesis submitted for the degree of

*Doctor of Philosophy*

Trinity Term 2019

This thesis is dedicated to the memory of
my grandmother, *Nan Martin*,
for always believing in me.

# ACKNOWLEDGEMENTS

I would like to thank Michael Bonsall, my supervisor, for the opportunity to join the group and for his enthusiasm and patience throughout my DPhil. I am grateful to my second supervisor, Anthony Wilson, for his help during my time conducting experiments at the Pirbright Institute. Sebastian Shimeld, my college advisor, has been a tremendous support while at Oxford and I owe him greatly for the opportunity to be a lecturer at Balliol. I would like to thank Owen Lewis and Simon Gubbins for being thorough, friendly and fair examiners. Jason Matthiopoulos at the University of Glasgow taught me what it was to be quantitative ecologist; I certainly would not be where I am now without his inspiration and guidance.

By far, I owe the most to my parents. This thesis is as much the achievement of my mum, Susan, and dad, Robert, as it is mine. I could not have asked for more enthusiasm, love and support; I am monumentally fortunate and proud to be their son. My marvellous little sister, Laura, has always been a huge source of love and support. My beautiful partner, Claire Davies, has been the most loving and sassy companion I could have asked for through the journey of writing a DPhil; she has helped me through all of the highs and lows of the past 4 years.

My paternal grandmother and grandfather, Nan and Thomas Paton, and maternal grandfather James Martin were a huge part of my life growing up and I miss them dearly. My maternal grandmother, Nan Martin, was my second mum. She was more important than anyone other than my parents growing up, and she always believed in me. I miss her every day.

Phil Williams, Debby Nixon-Williams and Alban Schmid are Balliol's finest, and their friendship and support has meant so much. Katie Heath and I have together counted *precisely* $\infty$ mosquito larvae, a feat we have no desire to repeat. Her friendship and advice has kept me going through my DPhil. Tom Brewer has been a great friend; he is always generous, both with his time in reviewing manuscripts and with the whisky measures he pours. In the Mathematical Ecology Research Group, Thom Rawson, Sean Hackett and Chris Terry have been exceptionally intelligent and supportive friends. Ash Sendell-Price and Kaja Fenn kept me sane by giving me some of my biggest laughs (and hangovers) of my DPhil. Emma Darroch and Sandy Thomson are life-long friends and have always been a source of motivation, support and good times.

Finally, my dog Thumper was my partner in crime right up to the final year of my DPhil. He was my biggest source of laughs and love when I was feeling low, and I will always miss him.

*To everyone who made this possible, thank you.*

# STATEMENT OF ORIGINALITY AND THESIS FORMAT

I hereby certify that the work in this thesis is entirely my own, other than the exceptions listed below. This thesis is presented as an integrated thesis, which means work chapters are written as papers. Chapter 2 is published in the *Journal of the Royal Society Interface*, Chapter 3 has received reviewer comments from *Ecology and Evolution* and Chapter 4 is in preparation for submission to a journal.

*Chapter 1*

I wrote the introduction. Tom Brewer offered very useful comments on writing style and structure. Michael Bonsall made corrections and suggestions.

*Chapter 2*

I developed the concept and models, with advice from Michael Bonsall. I carried out the analysis and wrote the paper. Michael Bonsall reviewed the paper and made suggestions for the final text. Comments from two anonymous reviewers improved the work. Tom Brewer also provided helpful comments on early drafts of the manuscript. The code used to generate the results for this chapter is available at https://doi.org/10.17605/OSF.IO/MZDWG.

*Chapter 3*

Katherine Heath and I designed the experiments and developed the concept and ideas, with advice from Michael Bonsall and Anthony Wilson. Katherine Heath and I carried out the experiments, with help from Derek Park and Jo Stoner. I designed and conduced the analysis, and wrote the paper. Katherine Heath, Michael Bonsall and Anthony Wilson reviewed the paper and made helpful suggestions for the final text. Chris Terry also made helpful comments on the manuscript, as did three anonymous reviewers. The data and code for this chapter is available at https://doi.org/10.17605/OSF.IO/V49NJ.

*Chapter 4*

I conceived the idea for the study and designed and analysed the model. Michael Bonsall made recommendations on the final text. The code used to generate the results for this chapter is available at https://doi.org/10.17605/OSF.IO/XZBJG.

*Chapter 5*

I wrote and reviewed the discussion.

## ABSTRACT

Vector-borne disease is a significant source of mortality and morbidity, and disproportionately affects those who are most socially and economically vulnerable. The mosquitoes *Aedes aegypti* and *Aedes albopictus* are vectors of arboviruses such as dengue and Zika, with wide-ranging distributions that cover much of the tropics. There have been calls to manage *Aedes* populations using methods such as sterile and genetically-modified insect releases, with the efficacy of control contingent on a robust understanding of mosquito ecology.

*Ae. aegypti* and *Ae. albopictus* compete as larvae through resource competition and as adults through reproductive interference, but the relative roles of these mechanisms had not yet been investigated in an *Aedes*-specific model. This motivated my second chapter, where I built a theoretical model that not only included these competitive mechanisms, but also modelled the process of host choice. I demonstrated that host preference both directly mediated pathogen transmission by changing biting rates while also determining the strength of reproductive interference. This led to complex patterns of coexistence and competitive exclusion that could not be predicted by simpler models of competition.

Experimental and field evidence suggests that the costs of larval competition are context-dependent. Therefore, in Chapter 3, I conducted a set of experiments to measure the consequences of larval competition under a particular per-capita feeding regime. These experiments revealed interesting aspects of larval biology – even when there were sufficient resources for all larvae to pupate, demographic variation in resource uptake led to interspecific competition. While examining particular biotic interactions in isolation is valuable, I did so in a laboratory under tightly controlled conditions. In reality, mosquito distributions arise from a complex multivariate function of both biotic and abiotic drivers.

One such driver is temperature; as mosquitoes are exothermic, they exhibit a number of temperature-dependent ecological and epidemiological traits. No model had yet examined how temperature-dependent rates could interact with competition to cause patterns of coexistence and exclusion. Therefore, in Chapter 4, I developed a multi-species model that included species-specific ecological and epidemiological responses to temperature, along with the competitive mechanisms explored in Chapter 2. The model predicted that *Ae. albopictus* larvae would out-compete *Ae. aegypti* in climates where competitive displacements have occurred in the past. I also demonstrated that the hydra-effect – the counter-intuitive increase in population size due to diminished reproductive output – could occur in some climates due to reproductive interference (but only if there were no costs of larval competition). The model also reveals temperature-dependent patterns of disease outbreaks that would be impossible to predict using simpler, temperature-invariant models.

The work in my thesis has elucidated the relative importance of two competitive mechanisms that govern the distributions of these prolific disease vectors. I determined that outcomes of competition are sensitive to temperature and biotic processes (such as host preference). These insights will be vital for those aiming to manage insect populations in the present, and for those seeking to predict distributions in the future.

# CONTENTS

**1 Introduction** **1**
Background and motivation . . . 1
The biology of *Ae. aegypti* and *Ae. albopictus* . . . 2
Life history . . . 2
The distribution of *Aedes* mosquitoes . . . 3
Abiotic determinants of distributions . . . 3
Biotic interactions and *Aedes* distributions . . . 5
Pathogen transmission . . . 7
Vector control . . . 8
Insecticides . . . 9
Sterile insect technique . . . 9
Genetic modification . . . 9
Self-limiting strategies . . . 9
Self-sustaining . . . 10
*Wolbachia*-infected mosquito releases . . . 11
Synthesis and summary . . . 11

**2 Modelling reproductive interference** **13**
Background . . . 14
Methods . . . 17
Ecological Models . . . 17
Behavioural responses to hosts . . . 18
Sterilised Females . . . 19
Epidemiological Models . . . 21
Model analysis . . . 21
Boundaries for coexistence and isoclines . . . 21
Deriving the intrinsic growth rate of the pathogen . . . 23
Stochastic simulations . . . 23
Results . . . 24
Ecology . . . 24
Epidemiology . . . 27
Discussion . . . 32
Ecological insights . . . 32
Sterilised females . . . 34
Epidemiological consequences . . . 35
Insights, assumptions and extensions . . . 36
Conclusion . . . 37

**3 Costs of larval competition** **39**
Introduction . . . 40
Competing vectors . . . 41
Mechanisms of larval competition . . . 42
Methods . . . 43
Routine colony maintenance . . . 43
Experimental protocols . . . 43
Analysis . . . 44

Survival . . . 45
Development time . . . 46
Selecting predictors and model structures . . . 47
Gibbs variable selection . . . 47
Results . . . 49
Survival . . . 49
Development Time . . . 51
Discussion . . . 52
Conclusion . . . 56

**4 A temperature-dependent model of *Aedes* population dynamics and epidemiology 59**
Introduction . . . 60
The vectors – *Ae. aegypti* and *Ae. albopictus* . . . 60
Competition between *Aedes* mosquitoes . . . 61
Larval competition . . . 61
Reproductive interference . . . 62
Modelling temperature-dependent traits . . . 62
Methods . . . 64
Model outline . . . 64
Ecology . . . 64
Epidemiology . . . 65
Temperature-dependence . . . 67
Temperature responses . . . 67
Describing temperature changes . . . 67
Simulations . . . 69
Results . . . 71
Species-specific responses to temperature . . . 71
Interactions between larval competition and climate . . . 72
Interactions between reproductive interference and climate . . . 75
Interactions between larval competition and reproductive interference . . . 76
The sensitivity of vectorial capacity to thermal limits . . . 76
Discussion . . . 80
Insights into the ecological and epidemiological climatic niches of *Ae. aegypti* and *Ae. albopictus* 80
Climate interacts with larval competition – to the benefit of *Ae. albopictus* . . . 81
Reproductive interference counter-intuitively *increases* population size, and varies with climate 82
Changes to thermal limits: interactions between competition and climate . . . 82
Model assumptions and potential extensions . . . 83
Conclusion . . . 85

**5 Discussion 87**
The interplay of ecological and epidemiological dynamics . . . 87
Climate-dependent competition . . . 88
The spatio-temporal dynamics of larval competition . . . 89
Lessons for vector control . . . 90
Conclusions . . . 91

**Bibliography 93**

**A Supplementary material for Chapter 3 103**
Isocline derivation for equations 3 and 4 . . . 103
Derivation of the pathogen intrinsic growth rate, $R$ . . . 104

**B Supplementary material for Chapter 3** **105**
Pilot study . . . 105
Procedure . . . 105
Results . . . 105
Conclusions . . . 105
Priors . . . 106
Gibbs Variable Selection (GVS) . . . 107

**C Supplementary material for Chapter 4** **113**
Model derivation . . . 113

# LIST OF FIGURES


2.1 Boundaries of coexistence for $\delta_i$, $Q$ and behavioural responses . . . 25
2.2 Boundaries of coexistence for $\beta_i$, $\delta_i$, $Q$ and behavioural responses . . . 26
2.3 Zero-net-growth isoclines for species *A* and *B* derived from equations 2.5 and 2.6 under different competitive scenarios . . . 28
2.4 Surfaces exploring the potential for disease outbreaks under different competitive scenarios 30
2.5 Example stochastic simulations of multi-vector ecological and epidemiological dynamics . . 31
2.6 Violin plots showing the distribution of stochastic simulations of multi-vector epidemiological dynamics . . . 33

3.1 Experimental design summary schematic . . . 45
3.2 Model fit of the beta-binomial survival model for within-species competition . . . 50
3.3 Model fit of the beta-binomial survival model for between-species competition . . . 50
3.4 Model fit for within-species competition in the development time model . . . 53
3.5 Model fit for between-species competition in the development time model . . . 54

4.1 Estimated climate responses for each location . . . 70
4.2 *Aedes* adult female and juvenile responses to climate . . . 73
4.3 Epidemiological responses to climate . . . 74
4.4 Interactions between reproductive interference and climate . . . 75
4.5 Interactions between reproductive interference and climate . . . 76
4.6 Interactive effects of larval competition and reproductive interference on coexistence and exclusion . . . 77
4.7 Barplots showing the sensitivity of vectorial capacity to different thermal niches and larval competition . . . 78
4.8 Barplots showing the sensitivity of vectorial capacity to different thermal niches and reproductive interference . . . 79

B.1 Pilot study binomial model fit . . . 106
B.2 Plot of the parameter estimates for the binomial model of survival after variable selection . 110
B.3 Plot of the parameter estimates for the beta-binomial model of survival after variable selection 110
B.4 Plot of the parameter estimates for the gamma-distributed model of development times after variable selection . . . 111
B.5 Plot showing the uncertainly associated with the between-species competition estimated in the beta-binomial model of survival . . . 111
B.6 Plot showing the uncertainly associated with the between-species competition estimated in the gamma-distributed model of development times . . . 112

C.1 Temperature responses for *Ae. aegypti* and *Ae. albopictus* taken from Mordecai et al. (2017) . . 114
C.2 Sensitivity of adult population sizes to the sharpness of temperature changes . . . 115
C.3 Sensitivity of juvenile population sizes to the sharpness of temperature changes . . . 116
C.4 Timing of adult population peaks . . . 117
C.5 The effect of larval competition on adult population size . . . 117
C.6 The effect of larval competition on peak outbreak size . . . 118
C.7 The effect of reproductive interference on adult population size . . . 118
C.8 The effect of reproductive interference on peak outbreak size . . . 119

# LIST OF TABLES

2.1 Table of behavioural responses . . . . . 20
2.2 Table of parameter values . . . . . 22

3.1 Table of experimental larval density conditions . . . . . 44
3.2 Parameter estimates for the survival model . . . . . 51
3.3 Parameter estimates for the development time model . . . . . 52

4.1 Table of the temperature-dependent functions taken from Mordecai et al. (2017) . . . . . 68
4.2 Table of state-variables for equations 4.1 to 4.17, along with the initial values used for the simulations . . . . . 69

B.1 Priors used in the Bayesian analysis of larval survival and development times . . . . . 106
B.2 Gibbs Variable Selection results for the binomial model of survival . . . . . 107
B.3 Gibbs Variable Selection results for the beta-binomial model of survival . . . . . 108
B.4 Results of the Gibbs Variable Selection procedure for the gamma-distributed model of development times . . . . . 109

C.1 Parameters – taken from Mordecai et al. (2017) – to parameterise the temperature-dependent functions . . . . . 120
C.2 Table of parameter values for country temperature fits . . . . . 121

# 1 | INTRODUCTION

## Background and motivation

Vector-borne diseases are a tremendous source of mortality and morbidity, particularly for those in developing nations (Liang et al., 2015). Vectors are organisms that transmit pathogens from infected to uninfected hosts, with arthropods the most common intermediary for humans. Pathogen-arthropod transmission systems develop as a result of some species of female arthropods requiring a blood meal from a vertebrate host in order to reproduce, facilitating infection and transmission. Indeed, many vector-borne pathogens are unable to transmit directly between hosts in the absence of a vector. Arthropods are responsible for transmitting parasites such as the malaria-causing *Plasmodium* (anopheline mosquitoes), the causative bacteria of Lyme disease (*Ixodes* ticks) and viruses such as dengue and yellow fever (*Aedes* mosquitoes) (Gubler, 1998a).

It is the major arbovirus vectors *Aedes aegypti* and *Aedes albopictus* that motivate the work in this thesis. The Cuban physician Carlos Juan Finlay was the first to implicate *Ae. aegypti* as the cause of yellow fever outbreaks, drawing a link between mosquito habitat preference and seasonal abundance with outbreaks of the virus (Finlay, 1881). Finlay was an early advocate of vector control as a means of disease mitigation; his work was instrumental in convincing the US Army Yellow Fever Board to embark on a programme of controlling *Ae. aegypti*. On the importance of Finlay's discovery, the then US military Governor of Cuba, General Leonard Wood, stated:

> "*The confirmation of Dr. Finlay's doctrine is the greatest step forward made in medical science since Jenner's discovery of the vaccination*".

Subsequently, Ronald Ross's discovery that anopheline mosquitoes vectored malaria consolidated the understanding that mosquitoes could be the agents of pathogen transmission (Ross, 1897). He went on to develop a mathematical model of malaria transmission, with his research still forming the foundations of many models of vector-borne disease today (Ross, 1911). The work of Finlay and Ross can be considered the inception of the field of vector ecology and control: the pursuit of a greater understanding of where mosquitoes are found, how they transmit pathogens and – most importantly – how disease transmission can be prevented. Despite more than a century of rapid developments in mosquito ecology and control, vector-borne diseases remain a significant global public health problem (Liang et al., 2015).

Indeed, *Ae. aegypti* and *Ae. albopictus* are responsible for an estimated 390 million annual dengue infections (Bhatt et al., 2013) and the recent outbreak of Zika virus in Brazil (Faria et al., 2016). Vaccine development for arboviruses remains slow, with the notable exception of yellow fever (Eidex, 2004). The complexities

of between-serotype cross-reactivity in host immune responses has slowed progress towards a dengue vaccine (Christofferson and Mores, 2015). Despite being discovered as early as 1947, Zika vaccine development only began following the outbreak in Brazil; it was previously thought to be a mild, inconsequential infection (Cohen, 2016). Vaccine coverage for many arboviruses remains poor, principally due to do a lack of funds or political incentives (Yen et al., 2015).

*Aedes* mosquitoes are crepuscular (dawn/dusk) biters (Nelson, 1986), which reduces the effectiveness of the insecticide-treated bed-nets that yielded significant reductions in malaria incidence (in contrast, *Anopheles* bite at night) (Snow et al., 1988). Moreover, a growing prevalence of insecticide resistance threatens the most commonly deployed response to *Aedes*-driven disease outbreaks (Liu, 2015). This has led to a focus on innovative forms of population control, such as the release of sterile, transgenic or *Wolbachia*-infected mosquitoes to suppress or replace wild populations. Such methods require a strong understanding of mosquito ecology in order to maximise efficacy and avoid unintended consequences (Alphey and Alphey, 2014). In the case of *Ae. aegypti* and *Ae. albopictus*, the species are known to compete in the wild (Juliano, 2009), leading to different patterns of spatial segregation, coexistence and competitive exclusion (Lounibos and Juliano, 2018).

Here, I review our knowledge of the ecology of *Ae. aegypti* and *Ae. albopictus*. In particular, I highlight that they occupy the same ecological niche, resulting in interspecies competition. I then discuss control methods, emphasising that, in order for control to be effective, we must understand the ecological interactions between these mosquitoes.

## The biology of *Ae. aegypti* and *Ae. albopictus*

### Life history

The development of *Ae. aegypti* and *Ae. albopictus* involves several distinct life stages. Female mosquitoes require a blood meal from a vertebrate host in order to lay eggs; males are attracted to the same hosts – even though they do not bite – to facilitate mating (Nelson, 1986). After mating, females lay eggs in either natural or man-made pools of freshwater. *Aedes* are known to practice "skip-oviposition", whereby a female oviposits a single batch of eggs across multiple pools (Colton et al., 2003; Reiter, 2007). These eggs are desiccation resistant, allowing them to remain viable even if the pool temporarily evaporates (Nelson, 1986). Hatching is triggered by bacterial activity in the water (either through a reduction in oxygen or chemical cues), which signals that there is a food source for emerging larvae (Ponnusamy et al., 2011). Larvae filter feed on microorganisms suspended in the water column and moult into pupae when they accrue sufficient resources (pupae do not feed). The length of time spent as a larva is contingent on abiotic (e.g. temperature) and biotic (e.g. larval density) factors; durations are around 5 days under optimal conditions, varying to more than 2 weeks when conditions are sub-optimal. Pupae emerge as adult mosquitoes within a few days, with females generally able to mate and take a blood meal around 24 hours later. Conditions experienced at the larval stage can affect other life stages; for instance larval stage density-dependent competition can reduce adult lifespan (Reiskin and Lounibos, 2009).

A notable between-species difference is that female *Ae. albopictus* respond to reduced day lengths and cooling temperatures by laying eggs in a state of embryonic diapause (Diniz et al., 2017). These eggs are refractory to hatching stimuli, more desiccation resistant (can persist through dry spells) and have a higher lipid content (more resources to live on during diapause and after emergence). This adaption allows *Ae. albopictus* populations to persist in more temperate climates, as these eggs can hatch when seasonal conditions become favourable (Bonizzoni et al., 2013).

### The distribution of *Aedes* mosquitoes

*Ae. aegypti* has a pan-tropical distribution, but is invasive in much of this range (Kraemer et al., 2015; Lounibos and Juliano, 2018; Powell, 2018). Native to Africa, *Ae. aegypti* populations were originally forest dwelling, laying eggs in the pools of water that form in tree holes and feeding on non-human hosts (Powell, 2018). As African communities began storing water for permanent settlements, these human-made larval habitats likely proved useful for mosquito populations, particularly during the dry season. Consequently, *Ae. aegypti* thrived in human settlements, developing a strong preference for taking blood meals from human hosts (Scott and Takken, 2012). It was this "domesticated" form of *Ae. aegypti* that was transported via European slave ships to the tropical west, bringing with it yellow fever. *Ae. aegypti* arrived in Asia later – probably in the nineteenth century – via international shipping (Lounibos and Juliano, 2018). Some draw a distinction between sub-species of *Ae. aegypti*; *Ae. aegypti formosus* denotes the forest-dwelling sub-species, while *Ae. aegypti aegypti* is the anthropophilic domesticated sub-species (Mattingly, 1967).

*Ae. albopictus* has a tropical to mild-temperate distribution, colonising every continent other than Antarctica (Bonizzoni et al., 2013). Its expansion from a native range in East Asia and the Western Pacific islands began in the $20^{th}$ century, facilitated by international shipping (Lounibos and Juliano, 2018). It was first found in Europe in 1979, the continental USA in 1985 (O'Meara et al., 1995), Africa in 1989 (Cornel and Hunt, 1991) and Central and South America since the 1980s (Bonizzoni et al., 2013). This extensive distribution means that 5.1 *billion* people live in countries occupied by *Ae. albopictus* (Bonizzoni et al., 2013).

#### Abiotic determinants of distributions

*Aedes* distributions are principally determined by climate. As ectotherms, *Aedes* exhibit a number of temperature-dependent life-history traits that limit their extent (Kraemer et al., 2015; Mordecai et al., 2017). Similar sensitivities also exist to humidity and precipitation; humidity helps prevent egg desiccation, while the timing of precipitation must provision larval habitats to coincide with reproduction (Kraemer et al., 2015; Messina et al., 2015). Vegetation cover has also been shown to be a determinant of distributions, with evidence suggesting that *Ae. aegypti* has a preference for urbanised areas, whereas *Ae. albopictus* prefers peri-urban areas with more vegetation (Braks et al., 2003; Lounibos et al., 2016; Paupy et al., 2010; Rey et al., 2006).

*Aedes* distributions will inevitably shift as a consequence of anthropogenic climate change (Kraemer et al., 2019). However, predicting these expansions will be challenging. While overall climatic trends are for warmer

temperatures, there will be complex climatic feedback mechanisms that will increase weather extremes. Areas presently occupied by *Aedes* may become too arid, with rainfall patterns failing to provision larval habitats while temperatures are suitable. In contrast, previously unoccupied temperate areas may become more suitable as average temperatures rise. The self-powered dispersal abilities of *Ae. aegypti* and *Ae. albopictus* are relatively limited, though both the distance and speed of dispersal will likely be determined by habitat; patchy and exposed environments in arid climates will impede travel relative to contiguous urban extents in tropical regions (e.g. Muir and Kay (1998) vs Honório et al. (2003)). Human-mediated dispersal events are necessary for significant range expansions of *Aedes* mosquitoes; international shipping can transport eggs and adults to new continents, while domestic transport and travel can spread *Aedes* to new climatically suitable areas within countries or regions (Eritja et al., 2017). Expanding urban environments will prove pivotal for the range expansion of *Aedes*, with human-modified landscapes providing access to human hosts and ample artificial larval habitats (Kraemer et al., 2019; Messina et al., 2015).

Abiotic variables shape the *fundamental* niche of these mosquitoes; the set of conditions that precisely define the environmental limits of mosquito reproduction and survival. However the *realised* niche of *Aedes* also accounts for biotic interactions, such as those between mosquito species (Hutchinson, 1957). These interactions play a significant role in determining the distribution and abundance of *Ae. aegypti* and *Ae. albopictus*, but tend to receive less attention than correlative investigations of the abiotic factors driving mosquito presence (Lounibos and Juliano, 2018). Correlative studies typically use statistical models to describe *Aedes* occurrence data as a function of abiotic variables (such as temperature, precipitation or humidity, e.g. Kraemer et al. (2015)). The covariates in these models can be extrapolated to predict future changes in species ranges (Kraemer et al., 2019). These methods are broadly termed species distribution models (Elith and Leathwick, 2009) and, at least for *Aedes*, rarely are biotic interactions *explicitly* included. Instead, the data used to fit the models will, to an extent, reflect the *outcome* of biotic interactions. The outcomes of biotic interactions are therefore only reflected as artefacts in the magnitude and uncertainly of model coefficients associated with abiotic variables. For instance, the statistically inferred temperature niche of *Ae. aegypti* will be based on data that is also driven by competitive displacements. Consequently, areas that are climatically suitable will be unoccupied, changing the statistical estimates of the effect of temperature on *Ae. aegypti*. It is therefore critical that biotic interactions are also considered when discussing mosquito distributions (Lounibos and Juliano, 2018).

Distributional shifts in *Aedes* populations have been associated with the spread of competing mosquito species (Lounibos and Juliano, 2018). These shifts have principally resulted in the competitive displacement of *Ae. aegypti* upon the arrival of *Ae. albopictus*, though the global picture is more complex. When *Ae. albopictus* arrived in Houston, Texas, in the late 1980s, existing populations of *Ae. aegypti* began to rapidly decline (O'Meara et al., 1995). The North American range of *Ae. aegypti* is now restricted to urbanised areas of the Southern states, with *Ae. albopictus* dominating elsewhere. Similar declines of *Ae. aegypti* in response to *Ae. albopictus* invasion were documented in Bermuda (U.K.) (Kaplan et al., 2010). The species live in sympatry

on tropical islands, such as Reunion (Bagny et al., 2009), Hawaii (Winchester and Kapan, 2013) and the Seychelles (Lambrecht, 1971). On all three islands, there have been documented reductions in the range of *Ae. aegypti* in response to the arrival of *Ae. albopictus*, showing similar habitat segregation patterns to the USA. Madagascar is a unique case. It has been suggested that the *Ae. aegypti* on the island are the feral sub-species (*Ae. aegypti formosus*) and the reverse of the typical distribution is observed; *Ae. albopictus* is found in urban areas, while *Ae. aegypti* is found in dry forested areas (Raharimalala et al., 2012; Ratsitorahina et al., 2008). Historic examples of *Ae. aegypti* displacing native *Ae. albopictus* populations are rare, but have been documented in Bangkok (Stanton, 1920), Kuala Lumpur (Rudnick, 1965), and Kolkata (Gilotra et al., 1967).

### Biotic interactions and *Aedes* distributions

Species distributions are driven by both abiotic and biotic processes that can interact in complex and unpredictable ways (Leisnham and Juliano, 2009). Biotic interactions can take many forms, including predator-prey, parasite-host, within- and between-species competition. Such interactions are critical in determining the abundance and distribution of communities of organisms (Chesson, 2000). In order to explain patterns of co-occurrence and competitive exclusion in *Aedes*, researchers have considered two types of biotic interactions; interspecies competition and apparent competition. The former is mediated by competition at the larval stage (through resource scarcity and interference) and at the adult stage by reproductive interference. Apparent competition describes the phenomenon whereby a newly introduced species leads to an increased density of shared predators, resulting in a concurrent reduction in an ecologically similar species (Bonsall and Hassell, 1997). I restrict my discussion to interspecies competition at the adult and juvenile life stages due to the strength of evidence for these mechanisms (Juliano, 1998).

At the larval stage, there is clear evidence of resource-driven competition (Juliano, 2009). This occurs as eggs are laid and hatch at different times, resulting in a spectrum of different larval stages occupying the same pool. Different sizes of larvae will have different resource uptake rates, with older larvae depleting the available resources for younger larvae. In Chapter 3, I consider the differences in resource uptake rate between individuals of the *same* age; individuals in a larval cohort may express accelerated developmental pheneotypes, depriving other larvae of the requisite resources for survival in an environment with finite resources. The net effects of larval competition is the reduced survival of the larval cohort and increased development times of those that do survive (Juliano, 2009). Downstream consequences of crowded larval conditions are also observed, with the surviving larvae emerging as smaller adults (Alto et al., 2005), with shorter lifespans (Bara et al., 2015; Reiskin and Lounibos, 2009) and higher probabilities of disseminating infection (Alto et al., 2005, 2008).

There are numerous studies – many of which are summarised in Juliano (2010) – that aimed to describe the outcomes of competitive interactions between *Aedes* species. Most rear single- and mixed-species cohorts and assess the resultant changes in survivorship and development time, comparing the effects of conspecific and heterospecific larvae. Many studies have demonstrated a competitive advantage for *Ae. albopic-*

*tus*. Evidence from the field (Braks et al., 2004; Juliano, 1998) and lab (Barrera, 1996) concluded that *Ae. albopictus* larvae grew faster and suffered from lower mortality when reared on leaf detritus. Juliano's (2010) meta-analysis of *Aedes* larval competition studies suggested that competitive outcomes could be context-dependent, with *Ae. albopictus* the superior competitor when resource quality was low, and competitive equivalence when resource quality was high. Leisnham et al. (2009) demonstrate differences in competitive ability between different mosquito populations, which could facilitate sympatry among spatially-segregated populations. Moreover, differences in other life-stages could manifest in context-dependent outcomes of competition. Laboratory evidence presented by Costanzo et al. (2005) suggested that the outcome of interspecies competition is dependent on the desiccation tolerance of eggs. The authors exposed eggs to different drying regimes, finding that *Ae. aegypti* eggs were more likely to survive periods of heat stress, subsequently gaining a competitive advantage at the larval stage by emerging in greater numbers than *Ae. albopictus*. Indeed, Leisnham and Juliano (2009) suggest that coexistence of *Ae. aegypti* and *Ae. albopictus* in urban areas in the Southern USA could be mediated by differences in competitive outcome across the season; reduced egg desiccation in the dry seasons could favour *Ae. aegypti*, before it suffers from the competitive superiority of *Ae. albopictus* larvae later on in the wet season. It is likely that a myriad of mechanisms interact with climate to produce complex patterns of competitive outcomes; spatially heterogeneous landscapes will support a wide-variety of larval habitats with different abiotic and biotic conditions. Indeed, a mathematical analysis of *Aedes* competition on Bermuda found that larval competition was unable to *fully* explain the pace of the displacement of *Ae. aegypti* by *Ae. albopictus* (Kaplan et al., 2010).

In addition to resource-mediated larval competition, some evidence suggests that interference competition could also operate. Studies from Moore and Fisher (1969) and Moore and Whitacre (1972) demonstrated that *Ae. albopictus* larvae in high-density, mixed-species cohorts took far longer to develop. Neither study limited larval resources, leading the authors to suggest that *Ae. aegypti* larvae may produce a chemical product that retarded larval development of *Ae. albopictus*. This hypothesis was not, however, supported in experiments by Dye (1982). Dye (1984a) suggests instead that other habitat-related differences, such as the volume of water in the larval habitat, could account for differences in development times.

Ribeiro and Spielman (1986) described a phenomenon whereby a species suffers from a reduced reproductive output because it cross-mates with another species, but produces no offspring. The authors term this satyrization, due to the Greek mythological figure the satyr, who was part man, part goat and mated indiscriminately. In my thesis, I refer to this phenomenon as reproductive interference, as do many in the literature (Gröning and Hochkirch, 2008). Gröning and Hochkirch (2008) present signal jamming, heterospecific rivalry, misdirected courtship, heterospecific mating attempts, erroneous female choice, heterospecific mating, and hybridisation as mechanisms of reproductive interference. Arthropods are known to suffer from reproductive interference (Kishi et al., 2009; Shuker et al., 2015) and models have assessed its potential effect on species coexistence (Kishi and Nakazawa, 2013; Kuno, 1992; Kyogoku and Sota, 2017; Paton and Bonsall, 2019; Ribeiro and Spielman, 1986). These models assess the costs of reproductive interference with respect

to competition at other life stages (Kishi and Nakazawa, 2013), host-choice and female sterilisation (Paton and Bonsall, 2019) and heterospecific density (Kyogoku and Sota, 2017).

Tripet et al. (2011) were the first to discover that reproductive interference could occur between *Ae. aegypti* and *Ae. albopictus*, reporting low levels of cross-mating in the field. Upon mating, male *Aedes* inject proteins that turn females refractory to further mating attempts, and induce egg-laying. The author's were able to demonstrate that the injection of *Ae. albopictus* accessory gland proteins induced female *Ae. aegypti* to become refractory to further mating attempts, even though they had not been successfully fertilised. This did not occur in the reverse case; *Ae. albopictus* females would generally go on to mate again after injections of *Ae. aegypti* male accessory gland proteins. A subsequent study by Bargielowski et al. (2013) found that – in mixed laboratory populations – *Ae. aegypti* was more likely to mis-mate than *Ae. albopictus* (conclusions supported by Marcela et al. (2015)). Moreover, Bargielowski et al. (2013) compared cross-mating rates in populations that had previously encountered heterospecifics with naive populations; they found that populations that had previously been exposed to the competitor mis-mated at a lower rate. They postulated that *Aedes* populations have evolved to differentiate between conspecific and heterospecific mates in response to the costs of reproductive interference. Of the mechanisms of reproductive interference presented by Gröning and Hochkirch (2008), there is evidence that misdirected courtship, heterospecific mating attempts, erroneous female choice and heterospecific mating occur between *Ae. aegypti* and *Ae. albopictus*. Reproductive interference is a mechanism I consider in both Chapters 2 and 4, by building mathematical models that explicitly account for how this mechanism operates in *Aedes* populations.

### Pathogen transmission

The arboviral transmission cycle is initiated by a female mosquito taking a blood meal from a viraemic host. The viral titre of this infectious blood meal can determine the probability of becoming infected and the length of the extrinsic incubation period (the time taken for the mosquito to become infectious) (Bara et al., 2015). A key determinant of transmission is that the mosquito outlives the extrinsic incubation period and goes on to take further blood meals and transmit the pathogen (Bara et al., 2015). If the mosquito lives long enough to become infected, then the infection must reach its salivary glands; when the mosquito bites a host, it injects an anti-coagulant saliva to facilitate feeding. It is this injection of saliva into a susceptible host that transmits the virus and initiates the intrinsic incubation period – the time taken for a human to become infectious.

Vectortorial capacity (the competence of the mosquito in transmitting disease) is a multi-faceted concept, taking into account the sequence of probabilistic steps leading to infection (biting an infected host, becoming infected, outliving the extrinsic incubation period and biting a susceptible host) (Brady et al., 2016; Dye, 1992; Garrett-Jones, 1964; MacDonald, 1957). Mathematical analyses of disease transmission models suggest that biting rate is a crucial determinant of vectorial capacity, as it appears as a square term in the expression:

$$V = \frac{RB^2CL^E}{-ln(L)}. \tag{1.1}$$

Here, the vectorial capacity, $V$ is a function of the ratio of vectors to humans ($R$), the biting rate ($B$), the vector competency ($C$ – the probability of becoming infectious), the daily adult survival probability $L$ and the extrinsic incubation period ($E$). This is intuitive, as a mosquito has to both bite an infected *and* a susceptible host in order to transmit. The biting rate term is dependent on mosquito resting behaviour and host choice; it can be broken down such that $B = fQ$, where $f$ is the overall biting rate and $Q$ is the proportion of these bites taken from a human host (Brady et al., 2016; Garrett-Jones, 1964). *Ae. aegypti* is widely considered the primary arbovirus vector, as it has a strong preference for human hosts, choosing to bite and rest indoors (Ponlawat and Harrington, 2005; Scott and Takken, 2012). In contrast, *Ae. albopictus* bites and rests outdoors, taking bloodmeals from a wider variety of hosts (Paupy et al., 2009; Richards et al., 2006). However, some *Ae. albopictus* populations have been documented to be anthropophilic (Delatte et al., 2010), it is able to transmit over 26 different arboviruses (Paupy et al., 2009) and it has been implicated as the sole vector in *some* disease outbreaks (Paupy et al., 2010). In Chapter 2, I discuss how host choice can have multiple effects, driving both biting rates and ecological interactions.

High vectorial capacity therefore consists of many traits; a preference for biting humans ($B$), a susceptibility for disease ($C$) and a lifespan long enough that transmission can occur before death ($L$ and $E$). This becomes more complex due to a multitude of biotic and abiotic drivers of mosquito ecological and epidemiological vital rates (Alto et al., 2008; Bara et al., 2015; Mordecai et al., 2017). For instance, higher temperatures can increase the probability of becoming infectious and shorten the extrinsic incubation period, but can also shorten adult lifespan (Bara et al., 2015; Mordecai et al., 2017). Therefore changes in rates can potentially work to promote or inhibit vectorial capacity. The interactive effects of climate on arbovirus epidemiology are explored in Chapter 4. Biotic interactions can also affect transmission; *Ae. albopictus* larvae exposed to high densities have shorter adult lifespans (Bara et al., 2015), but can be more susceptible to dengue infection (Alto et al., 2008).

## Vector control

The burden of vector-borne disease has motivated the development of a number of novel vector control methods. While these methods are presented as distinct strategies, in reality it is often more practical to consider multiple vector-management approaches – coupled with vaccination where available – to reduce arbovirus transmission. Indeed, while technological solutions to vector control are attractive, rigorously-enforced area-wide larval habitat management can be extremely effective, particularly if paired with other methods of population suppression.

### Insecticides

Early attempts to control mosquito populations relied principally on insecticides. DDT (dichlorodiphenyltrichloroethane) was a widely used insecticide in the early control of *Ae. aegypti*, proving efficacious on islands in the South Pacific and the Americas (Weetman et al., 2018). While successful in reducing or suppressing *Ae. aegypti*, spraying came at a high cost; non-target native insects were also affected, with potentially severe up- and downstream ecosystem consequences. Coupled with concerns over the effects of spraying on human health, the use of DDT has been drastically reduced (it is now banned globally for use in agriculture). Modern insecticide-based management strategies are based on larviciding (insecticides targeting larval habitats) and indoor spraying (of pyrethroids and organophosphates), and are the most commonly used means of *Aedes* control. However, growing resistance to one or more of these modern insecticides risks the future utility of these methods (Moyes et al., 2017). Given the ecological consequences of insecticides and growing resistance, there is a clear motive for an environmentally friendly, targeted form of population suppression.

### Sterile insect technique

Edward F. Knipling was the first to propose the sterile insect technique (SIT) as a species-specific and environmentally friendly form of pest population control (Knipling, 1959). The strategy involves mass-rearing male insects and sterilising them by exposure to $\gamma$-radiation. On release, wild populations of the target species would suffer from a reduced reproductive output by mating with sterile males (Alphey et al., 2010). SIT was effective in eliminating the screwworm, *Cochliomyia hominivorax*, from Central America and the Southern USA, and stymied its invasion of North Africa (Lindquist et al., 1992). Sterile mosquito releases offer advantages over insecticide sprays as the mosquitoes actively seek-out mates, removing the reliance on insecticide sprays successfully reaching their target. There are, however, compromises with SIT; irradiation incurs fitness costs in released males, including reduced mating competitiveness and lifespan. Consequently, radiation doses need to be carefully balanced with fitness costs (Alphey et al., 2010).

Models of sterile male releases revealed that there could be counter-intuitive outcomes to SIT if released insects induced only a small penalty in reproductive rate. When modelling releases of sterile tsetse fly (*Glossina palpalis*) – the vector of sleeping sickness – Rogers and Randolph (1984) illustrated that it was possible that for low levels of population sterility, population sizes could actually *increase*. This was because larvae would suffer from a reduced density-dependent mortality as fewer eggs were laid, increasing larval survival to adulthood. I return to this concept – termed the hydra-effect (Abrams, 2009) – in the context of ecological interactions in Chapters 2 and 4.

### Genetic modification

#### Self-limiting strategies

Motivated by deficiencies in the sterile insect method, arguments were made for the exploration of genetic methods to control mosquito populations (Alphey, 2002). Self-limiting transgenic modifications work on the

same principles as SIT; mass releases of genetically sterile males with the aim to reduce reproductive output in wild populations due to failed copulations. However, unlike the compromised males used in SIT, transgenic males can successfully compete for mates in the field (Harris et al., 2012) and have similar longevity to wild-types (Lacroix et al., 2012). This motivated the development of a genetically sterile strain of *Ae. aegypti* (Phuc et al., 2007), based on developments first made in *Drosophila* (Thomas et al., 2000). Transgenic mosquitoes also brought an additional benefit; as opposed to immediate sterility, transgenic mosquitoes could be engineered to produce offspring that would abort at a late-larval stage. Mathematical models comparing transgenic to sterile mosquito releases showed that late-acting lethality was more effective because transgenic offspring will contribute to density-dependent competition and inhibit the survival of wild-type larvae (Phuc et al., 2007). This late-acting mechanism alleviates the risk of the undesirable SIT effects uncovered by the modellers of sterile insect releases (e.g. Rogers and Randolph (1984)). Phuc et al. (2007) engineered a transgenic strain of *Ae. aegypti* with late-acting larval mortality; this strain became the principle technology for the company Oxitec, founded to produce and release modified insects to suppress populations of vectors and agri-pests. To date, pilot releases have been successful on the Cayman Islands (Harris et al., 2012), Malaysia (Lacroix et al., 2012), and Brazil (Carvalho et al., 2015). There is, however, a risk that suppressing *Ae. aegypti* may competitively release *Ae. albopictus* populations. Data from field trials in Brazil do not show evidence of facilitation, though the trial was over a relatively short time-frame and in an area where *Ae. albopictus* colonisation is ongoing (Gorman et al., 2016). There is an legislative advantage of self-limiting form of genetic control; the public are generally uneasy with genetic modification, but this strategy aims to *suppress*, not *replace*, vector populations.

### Self-sustaining

Unlike self-limiting genetic strategies – where the modification will become extinct with the cessation of releases – self-sustaining strategies aim to modify wild-mosquitoes in order to change vectorial capacity. Self-sustaining strategies are seen as more risky due to the permanent modification of populations, but offer clear benefits as – if successful – the modification does not need to be maintained by continuous releases (Alphey, 2014). Gene-drives promote the inheritance of traits (encoded in "cargo" genes) at a greater than Mendelian rate, propagating a modification through the population (Gantz et al., 2015). Two principle philosophies apply to population-modifying gene-drive systems; first, the gene-drive could promote the inheritance of otherwise deleterious traits (such as sterility or reduced lifespan), leading to suppression. Second, the gene-drive could promote a modification that alters mosquito susceptibility to pathogens. Gantz et al. (2015) successfully demonstrated that a gene-drive system in *Anopheles* could promote two anti-*Plasmodium falciparum* effector genes. Candidate anti-arboviral cargo genes have been identified; a Zika-resistance mechanism has been engineered for *Ae. aegypti* that could be incorporated into a gene-drive (Buchman et al., 2019).

### *Wolbachia*-infected mosquito releases

The release of *Wolbachia*-infected mosquitoes is a form of population modification that aims to reduce vectorial capacity. *Wolbachia* is a maternally-inherited gut bacterium with a wide prevalence in insect populations (including *Ae. albopictus*), but not *Ae. aegypti*. McMeniman et al. (2009) infected *Ae. aegypti* with a strain of *Wolbachia*, finding that infected adults had shorter adult lifespans; this is of critical importance as adults must live longer than the extrinsic incubation period to transmit disease. Moreover, Moreira et al. (2009) find that both dengue and chikungunya infections were inhibited by *Wolbachia* in infected *Ae. aegypti*. *Wolbachia* spreads with a powerful inheritance mechanism, known as cytoplasmic incompatibility (CI); matings between uninfected females and infected males are inviable, whereas infected females are able to mate with either infected or uninfected males, producing infected offspring. This gives infected females a frequency dependent mating advantage, increasing the rate of inheritance. Encouraging trials in Australia observed that *Wolbachia* infection went to fixation in targeted *Ae. aegypti* populations (Hoffmann et al., 2011). Both biotic and abiotic interactions affect the spread of *Wolbachia* infections through populations. For instance, Hancock et al. (2016) demonstrated that density-dependent larval competition could slow the inheritance of *Wolbachia*, while the CI inheritance mechanism can be disrupted by the temperature and shading of larval habitats (Ross et al., 2019). This emphasises the importance of understanding the effects of mosquito ecology for population modification and control.

## Synthesis and summary

Mathematical models have played a pivotal role in both the development (Phuc et al., 2007) and the planning (Alphey et al., 2011) of vector control (Alphey and Alphey, 2014). All such models must include an ecological representation of the target vector, with useful models succeeding on two fronts. First, they must identify the level of complexity required to capture the most important ecological processes for the target mosquito. This includes selecting an appropriate number, functional form and parameterisation of biotic and abiotic relationships. Second, they must assess the robustness of model-predicted outcomes to the particular parameterisation of these relationships. Rarely do mathematical models of vector control include interspecific interactions. Bonsall et al. (2010) analyse a model of SIT and transgenic mosquito releases acting on *Ae. aegypti* in combination with larval competition with *Ae. albopictus*. While this model sheds light on the potential for interactions between control and competition, it was written prior to the recognition of reproductive interference as a critical mechanism of competition between *Aedes* mosquitoes. Moreover, the complex context-dependence of inter-*Aedes* competition makes it challenging to parameterize models appropriately.

From the evidence presented in this review, the motivation for my thesis emerges:

- *Ae. aegypti* and *Ae. albopictus* are both competent vectors of arboviruses, with expansive distributions driven by both abiotic and biotic factors.

- Interspecific interactions are critical in determining their distributions, with evidence of multiple mechanisms (larval competition and reproductive interference) and a range of context-dependent competitive outcomes. This context dependence could be driven by abiotic conditions, such as climate.

- The effective implementation of vector control programmes is contingent on accurately modelling the ecology of the vector, but models rarely consider interspecies interactions. This can be due to a lack of understanding of competitive mechanisms, or a paucity of model parameters from experimental or field studies.

The principle aim of this thesis is to explore and elucidate the nature and mechanism of the biotic interactions between *Ae. aegypti* and *Ae. albopictus*. In Chapter 2, I build a mathematical model of reproductive interference and larval competition, examining the relative importance of these two mechanisms for *Aedes* competition. This model also incorporates *Aedes*-specific processes such as host choice and female sterilisation from cross-mating. Chapter 3 aims to elucidate the nature of larval competition between *Ae. aegypti* and *Ae. albopictus* by conducting experiments that aimed to determine the superior larval stage competitor under fixed feeding regimes. In Chapter 4, I address the sensitivity of competitive outcomes to climate by building a variable delay model which takes into account species-specific temperature-dependent responses in mosquito vital rates. I conclude by describing on how these work chapters advance our understanding of vector dynamics, improving the scope for well-informed vector control programmes.

# 2 | THE ECOLOGICAL AND EPIDEMIOLOGICAL CONSEQUENCES OF REPRODUCTIVE INTERFERENCE BETWEEN THE VECTORS *AEDES AEGYPTI* AND *AEDES ALBOPICTUS*

Vector ecology is integral to understanding the transmission of vector-borne diseases, with processes such as reproduction and competition pivotal in determining vector presence and abundance. The arbovirus vectors *Aedes aegypti* and *Aedes albopictus* compete as larvae, but this mechanism is insufficient to explain patterns of coexistence and exclusion. Inviable interspecies matings – known as reproductive interference – is another candidate mechanism. Here, we analyse mathematical models of mosquito population dynamics and epidemiology which include two *Aedes*-specific features of reproductive interference. First, as these mosquitoes use hosts to find mates, reproductive interference will only occur if the same host is visited. Host choice will, in turn, be determined by behavioural responses to host availability. Second, females can become sterilised after mis-mating with heterospecifics. We find that a species with an affinity for a shared host will suffer more from reproductive interference than a less selective competitor. Costs from reproductive interference can be "traded-off" against costs from larval competition, leading to competitive outcomes difficult to predict from empirical evidence. Sterilisations of a self-limiting species can counter-intuitively lead to *higher* densities than a competitor suffering less sterilisation. We identify that behavioural responses and reproductive interference mediate a concomitant relationship between vector ecological dynamics and epidemiology. Competitors with opposite behavioural responses can maintain disease where human hosts are rare, due to vector coexistence facilitated by a reduced cost from reproductive interference. Our work elucidates the relative roles of the competitive mechanisms governing *Aedes* populations and the associated epidemiological consequences.

**Citation**: Paton, R.S. and Bonsall, M.B. (2019) The ecological and epidemiological consequences of reproductive interference between the vectors *Aedes aegypti* and *Aedes albopictus*. 16, *J. R. Soc. Interface*. https://doi.org/10.1098/rsif.2019.0270

## Background

An estimated 390 million annual cases of dengue and the emergence of Zika has motivated policy makers, NGOs and academics to call for the management of vector populations (Bhatt et al., 2013; Yakob and Walker, 2016). Effective disease mitigation requires that vector occurrence and abundance can be accurately predicted (Bhatt et al., 2013), making it essential that we understand the ecological processes driving the distributions of the principal vectors of Zika, dengue and chikungunya – *Aedes aegypti* and *Aedes albopictus*.

Both species are obligate hematophages, meaning that females must take a blood meal from a vertebrate host in order to reproduce. *Ae. aegypti* is widely considered the primary vector of urban flaviviruses transmission systems (Black et al., 2002; Chouin-Carneiro et al., 2016; Yang et al., 2014), with a propensity for biting and living in proximity to humans (Scott and Takken, 2012). Native to Africa, *Ae. aegypti* has become established across Asia and the Americas (Kraemer et al., 2015). In contrast, *Ae. albopictus* is considered by some to be a secondary vector, but is still capable of transmitting over 26 different pathogens (Paupy et al., 2009). *Ae. albopictus* originates from Asia (Gratz, 2004) and is better able to colonise temperate environments because its eggs can undergo embryonic diapause to survive extreme weather, such as low winter temperatures (Diniz et al., 2017; Kraemer et al., 2015). *Ae. albopictus* is considered an opportunistic feeder (Paupy et al., 2009; Richards et al., 2006), however in some locations it has been shown it to be anthropophilic (Delatte et al., 2010; Ponlawat and Harrington, 2005).

Human activities, such as international shipping, have expanded the distributions of *Ae. aegypti* and *Ae. albopictus* (Lounibos and Juliano, 2018), leading to the species coming into contact as they establish in new regions. They share a similar ecological niche, with females laying eggs in small (often ephemeral) pools of water which hatch into a mobile larval stage. Early introductions of *Ae. aegypti* to Asia resulted in the displacement of *Ae. albopictus* in places such as Bangkok and Kuala Lumpur, but more recently *Ae. albopictus* rapidly displaced *Ae. aegypti* from all but urban areas in the Southern United States (Lounibos and Juliano, 2018; O'Meara et al., 1995). Both Braks et al. (2004) and Simard et al. (2005) document co-occurrence in Brazil and Cameroon respectively, albeit in segregated habitats. Habitat segregation is supported by Rey et al. (2006), who found *Ae. aegypti* to have a preference for urban landscapes and *Ae. albopictus* for suburban areas with more vegetation. It is widely accepted that these species compete in the wild, leading to different patterns of coexistence and competitive exclusion (Lounibos and Juliano, 2018).

The most obvious stage for this competition is as larvae, where individuals will compete for food and space. The importance of density-dependent larval-stage competition in regulating *Aedes* populations has long been recognised (Dye, 1984b; Southwood et al., 1972), but the exact strength and form is difficult to quantify in wild populations (Legros et al., 2009). This has led researchers to investigate populations of mosquitoes in lab or semi-field settings (many are reviewed in Juliano (2009)). Most studies rear populations of *Ae. aegypti* and *Ae. albopictus* in different density conditions and assess the penalties in survival and development time. In 2010, Juliano conducted a meta-analysis of larval competition studies, finding that the

magnitude and sign of inter-specific larval competition depends on the resources that the larvae were reared on. Subsequent studies (e.g. Reiskind et al. (2012)) have supported this resource-dependent variation in competitive outcome. Costanzo et al. (2005) documented that competitive outcomes can vary with climate; in lab experiments, *Ae. albopictus* was the superior competitor in wet conditions, while *Ae. aegypti* was superior in dry conditions. Differences in the costs of competition could therefore vary across seasons, as documented by Camara et al. (2016). Leisnham et al. (2009) hypothesised that differences in competitive outcomes between *Aedes* may be dependent on whether the source population originated from areas where the species coexist, or areas of competitive displacement. However, while they found that spatially distinct populations experienced context-dependent outcomes of competition, this variation did not consistently map onto the areas of coexistence or exclusion. In the absence of a consistent rule for the competitive exclusion and coexistence of these disease vectors, another mechanism has increasingly been explored: reproductive interference.

Reproductive interference (termed satyrisation by Ribeiro and Spielman (1986)) occurs when heterospecifics engage in mating activities (e.g. courtship, copulation) that reduce the fitness of one or both parties (Burdfield-Steel and Shuker, 2011). It has been documented in a range of different species, including arthropods (Kishi et al., 2009; Shuker et al., 2015). In their review, Gröning and Hochkirch (2008) describe seven types of reproductive interference; signal jamming, heterospecific rivalry, misdirected courtship, heterospecific mating attempts, erroneous female choice, heterospecific mating, and hybridisation.

Erroneous mate selection is known to occur in *Aedes*. Tripet et al. (2011) found that non-viable interspecies matings between *Ae. aegypti* and *Ae. albopictus* occurred at low rates in the field when screening for heterospecific sperm. In lab experiments, Bargielowski et al. (2013) found far higher rates than were observed in the field, as well as a propensity for *Ae. aegypti* females to be more likely to mis-mate than *Ae. albopictus*. In the same experiment, *Ae. aegypti* strains taken from populations which have not encountered *Ae. albopictus* (allopatric) mis-mated more frequently than those from populations sympatric with the competitor, suggesting an differential penalty in reproductive interference that may be selecting for more discerning *Ae. aegypti* females in the wild. *Ae. aegypti* was similarly found to mis-mate more often in lab experiments by Marcela et al. (2015). While the higher rates found in the lab will be at least partially attributable to "cage effects" – whereby females are harassed due to crowding – it is possible that there is a true discrepancy in interspecies mating rates in the field. These interspecies matings do not produce viable offspring, and incur a penalty in wasted courtship/handling time and fitness costs to females through harassment. From this evidence, it is clear that at least four of the seven forms of reproductive interference that Gröning and Hochkirch (2008) describe are found in *Aedes*: misdirected courtship, heterospecific mating attempts, erroneous female choice and heterospecific mating. All of these factors will contribute to a diminished reproductive rate when in the presence of heterospecifics. We do not explore signal interference here, but it is well understood that the harmonisation of harmonic wing-beat frequencies of *Ae. aegypti* males and females increases copulation success (Cator et al., 2009), a process which is yet to be examined between *different Aedes* species.

*Ae. albopictus* females mis-mated to *Ae. aegypti* males will re-mate with a higher frequency than in the reverse case, with *Ae. aegypti* females sometimes becoming refractory to further mating attempts (Tripet et al., 2011). We refer to this effect as sterilisation. Moreover, sterilisation can be induced in *Ae. aegypti* females solely by the injection of *Ae. albopictus* accessory gland proteins, without the successful transfer of sperm (Carrasquilla and Lounibos, 2015). Sterilisation could therefore be induced more widely than is typically observed when screening only for the presence of heterospecific sperm in spermatheca. Should female mosquitoes become refractory in the wild, these mis-mated females will not contribute to the larval population, consequently diminishing the regulatory impact of density-dependence.

Unlike anopheline mosquitoes which mate in crepuscular swarms, *Aedes* mosquitoes use hosts as beacons to swarm and find mates (Nelson, 1986; Yuval, 2006). However, not all vectors respond in the same way to host availability, with some showing generality and others a high degree of specificity. This means that the overlap in the behavioural responses of *Ae. aegypti* and *Ae. albopictus* to hosts will scale the number of heterospecifics that will be encountered, as the process of reproduction is mediated by host choice. Mosquitoes are known to use a diverse range of hosts, even when they have a strong preference for a particular species (Takken and Verhulst, 2012). For example, *Anopheles gambiae* shows a strong preference for human hosts (Pates et al., 2001) but can use others if required (Lyimo et al., 2012; White et al., 1972). *Ae. albopictus* can also show plastic responses to host availability (Sivan et al., 2015; Valerio et al., 2010) taking blood meals from a wide variety of hosts (Richards et al., 2006). In contrast, *Ae. aegypti* is more consistently anthropophilic (Paupy et al., 2009; Richards et al., 2006) but will take blood meals form other species if necessary (Edman, 1971; Takken and Verhulst, 2012).

Any model of *Aedes* reproduction would therefore need to include a flexible function to describe how the encounter rate between the two species changes with the availability of shared hosts. The epidemiological importance of behavioural responses to host availability was explored in detail by Yakob (2016), where a function capable of describing the range of host selection processes exhibited by biting insects was developed. Using a mathematical model, Yakob (2016) was able to show that host behavioural responses can have profound effects on the epidemiology of vector-borne pathogens, determining the level of control required to prevent transmission. We link this same host behavioural response to vector population dynamics; host choice will both determine patterns of vector coexistence and exclusion, while also altering biting rates and changing transmission.

A differential costs of reproductive interference is now considered by many to be an important driver of coexistence and competitive exclusion in *Aedes*, particularly in the absence of a consistent rule for the outcome of larval competition (Bargielowski and Lounibos, 2016; Lounibos and Juliano, 2018). Studies on *Aedes* have hitherto had to rely on *general* models of reproductive interference to make inference on the relative roles of reproductive interference and larval competition (Lounibos and Juliano, 2018). For instance, Kuno (1992) presented a theoretical model of the combined effects of mating interference and standard Lotka-Volterra competition (later revisited in detail by Kishi and Nakazawa (2013)). The model includes a frequency-

dependent function which scales the reproductive rate of a species with increasing numbers of heterospecifics. They demonstrated that the process of reproductive interference can diminish the possibility of coexistence and introduce priority effects, which make invasions challenging. This model has provided great insight into this process, but does not include the *Aedes*-specific features described above; namely that encounter rates will vary with host availability, and females could become refractory after heterospecifc matings. In this study, we use a mathematical model to explore these two aspects of *Aedes* reproductive biology. First, we examine how behavioural responses to host availability could alter the encounter rate of heterospecific mosquitoes and, in turn, the feasibility of coexistence. Second, we consider how different ratios of females becoming sterilised after heterospecific matings can lead to different patterns of coexistence and exclusion. We conclude by examining the consequences of these ecological processes for the transmission of a vector-borne disease.

## Methods

In this research we build two mathematical models of *Aedes* population dynamics; first we include behavioural responses to host availability, then female sterilisation by heterospecific copulations. We do not assign either *Ae. aegypti* or *Ae. albopictus* to a particular state variable and instead discuss our findings in the context of species "*A*" and "*B*". This allows us to draw overarching conclusions about the nature of the processes we examine without using species-specific model parameterisations from particular lab or field studies, which would risk obfuscating conclusions. Shared parameters (such as birth and death rates) are therefore taken to be of a "general" *Aedes* mosquito.

We proceed to add a model of vector-borne disease dynamics to our population dynamics model. This epidemiological model used parameters from the literature on dengue. Again, we use the same parameters across both species so that conclusions can be drawn about the processes of interest.

### Ecological Models

Kuno (1992) presented a model of reproductive interference which was further analysed by Kishi and Nakazawa (2013):

$$\frac{dA(t)}{dt} = r_A A(t)\left(\frac{A(t)}{A(t) + \delta_A B(t)}\right) - \alpha_A A(t)[A(t) + \beta_A B(t)] - d_A A(t) \tag{2.1}$$

$$\frac{dB(t)}{dt} = r_B B(t)\left(\frac{B(t)}{B(t) + \delta_B A(t)}\right) - \alpha_B B(t)[B(t) + \beta_B A(t)] - d_B B(t) \tag{2.2}$$

where $A$ and $B$ are the densities of the $i^{th}$ species, with $r_i$ the reproductive rate, $d_i$ the death rate, $\alpha_i$ the strength of intraspecific competition, $\beta_i$ the *relative* strength of interspecific competition and $\delta_i$ the strength of reproductive interference. The parameters for reproductive interference, $\delta_i$, is part of a frequency-dependent function describing the proportional reduction in reproductive rate with increasing densities of heterospecifics. Equations 2.1 and 2.2 have two single-species dominant roots which are stable $\left(A^* = \frac{r_A - d_A}{\alpha_A}, B^* = 0\right.$ and

$A^* = 0, B^* = \frac{r_B - d_B}{\alpha_B}\Big)$, and an unstable trivial ($A^* = 0, B^* = 0$) root. Should interspecific competition exceed intraspecific competition, there will be one unstable multi-species root. If intraspecific is greater than interspecific, then there will be one stable coexistence point and two unstable coexistence points (Kishi and Nakazawa, 2013; Kuno, 1992). These unstable "saddle-points" are caused by regions of the phase-space where the effects of interspecific competition outweigh intraspecific competition, leading to an *Allee* effect. This manifests as a priority effect, whereby the frequency-dependent costs of reproductive interference make it difficult for a species to invade from rare as it suffers a large penalty in reproductive interference from a more abundant competitor.

### Behavioural responses to hosts

In order to include host behavioural responses, the model had to reflect that heterospecifics will only be encountered by mosquitoes utilising the same hosts:

$$\frac{dA(t)}{dt} = r_A A(t)\left((1 - f_A(Q)) + \frac{f_A(Q)A(t)}{A(t) + \delta_A f_B(Q)B(t)}\right) - \alpha_A A(t-\tau_A)[A(t-\tau_A) + \beta_A B(t-\tau_A)] - d_A A(t) \quad (2.3)$$

$$\frac{dB(t)}{dt} = r_B B(t)\left((1 - f_B(Q)) + \frac{f_B(Q)B(t)}{B(t) + \delta_B f_A(Q)A(t)}\right) - \alpha_B B(t-\tau_B)[B(t-\tau_B) + \beta_B A(t-\tau_B)] - d_B B(t) \quad (2.4)$$

This form is similar to Kuno's (1992) model but has three key modifications. First, the model is now time-lagged to represent the delay in the adult recruitment due to the larval stage of *Aedes* mosquitoes. Therefore larvae of the $i^{th}$ species experience density-dependent intra- and interspecific competition at time $t-\tau_i$, while female egg laying and adult deaths occur in the present time. Second, the parameter $\beta_i$ now corresponds to the relative strength of interspecific *larval* competition in relation to intraspecific competition ($\alpha_i$). Third, the process of reproductive interference is now mediated by the behavioural response to host availability (taken from Yakob (2016), inspired by Real (1977)), through the function $f_i(Q)$:

$$f_i(Q) = \frac{Q}{Q + \lambda_i(1-Q)^{\mu_i}}$$

where Q ($Q \in [0,1]$) is the proportion of the shared host in relation to all other hosts, and $\lambda_i$ and $\mu_i$ are the shape parameters which describe how the $i^{th}$ species utilises the shared host. A description of these parameters and an illustration of the scenarios explored here are given in Table 2.1. As this function is independent of host density, the implicit assumption is made that the available hosts will be used in proportion to preference. If *all* hosts are at a low density, then the low encounter rate of hosts is likely to mean that preference yields to necessity to feed, and less preferred hosts may be used (Takken and Verhulst, 2012).

The functions $f_i(Q)$ ensure that only the fraction of the population using a shared host will be exposed to heterospecifics and suffer from reproductive interference. This allows the proportion of successful matings to be described as:

$$\underbrace{(1 - f_i(Q))}_{\text{Unexposed to heterospecifics}} + \underbrace{\frac{f_i(Q)N_i(t)}{N_i(t) + \delta_i f_j(Q)N_j(t)}}_{\text{Exposed to heterospecifics}} .$$

The first part of this expression gives the proportion of the population of the $i^{th}$ species which is not utilising the shared host and will therefore not suffer from reproductive interference. Note that, like epidemiological models of vector-borne pathogens, we assume that inter- or intraspecific competition will *not* impede access to the host, as the host is many orders of magnitude larger than the vector. The unexposed term will tend to zero when the shared host is the only host available ($Q \longrightarrow 1$ therefore $f_i(Q) \longrightarrow 1$). In the second part, the numerator is the number of the $i^{th}$ species using the shared host, and the denominator the sum of conspecifics and heterospecific matings with individuals of the $j^{th}$ species. In our model, we make the simplifying assumption that the shared host is a human, and that the mosquitoes will not encounter each other at other vertebrate hosts. As described in Table 2.1, we limit our behavioural responses to linear, anthropophilic and zoophilic. While both species are known to bite other animal hosts, they do so with different preferences which vary between species and strain. Therefore, the "true" behavioural response would be a complex aggregate of the responses to *all* shared hosts, and maybe different for different mosquito strains.

### Sterilised Females

Equations 2.1 and 2.2 were also modified to reflect that some female *Aedes* do not go on to find a conspecific mate after mating with a heterospecifics. Sterilisation can be modelled by scaling the strength of density-dependent larval competition by the fraction of females contributing eggs (and therefore larvae) to shared pools of water:

$$\frac{dA(t)}{dt} = r_A A(t)\left(\frac{A(t)}{A(t) + \delta_A A(t)}\right) - \alpha_A A(t-\tau_A)\left(\frac{A(t-\tau_A) + \epsilon_A\delta_A B(t-\tau_A)}{A(t-\tau_A) + \delta_A B(t-\tau_A)}\right)$$
$$\left[A(t-\tau_A)\left(\frac{A(t-\tau_A) + \epsilon_A\delta_A B(t-\tau_A)}{A(t-\tau_A) + \delta_A B(t-\tau_A)}\right) + \beta_A B(t-\tau_A)\right] - d_A A(t) \quad (2.5)$$

$$\frac{dB(t)}{dt} = r_B B(t)\left(\frac{B(t)}{B(t) + \delta_B A(t)}\right) - \alpha_B B(t-\tau_B)\left(\frac{B(t-\tau_B) + \epsilon_B\delta_B A(t-\tau_B)}{B(t-\tau_B) + \delta_B A(t-\tau_B)}\right)$$
$$\left[B(t-\tau_B)\left(\frac{B(t-\tau_B) + \epsilon_B\delta_B A(t-\tau_B)}{B(t-\tau_B) + \delta_B A(t-\tau_B)}\right) + \beta_B A(t-\tau_B)\right] - d_B B(t) \quad (2.6)$$

The terms describing the larval stage density-dependent interactions are now scaled by the effects of reproductive interference (as refractory females will not lay eggs in the future). The parameter $\epsilon_i$ is the *proportion* of females of the $i^{th}$ species that *do not* become refractory after a copulation with a heterospecific male, and contribute larvae to the next generation ($\epsilon_i \in [0, 1]$).

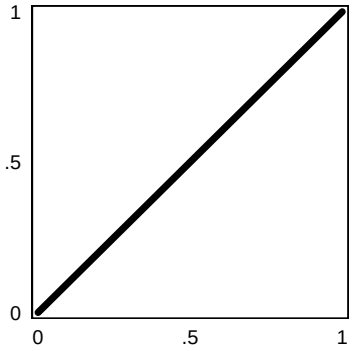
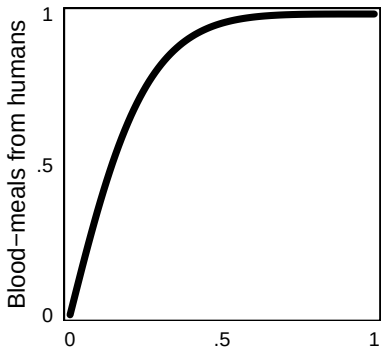
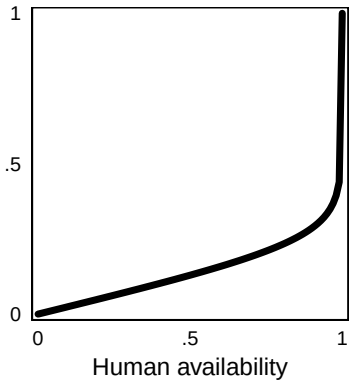
| response | shape | description | parameters |
|---|---|---|---|
| type I |  | linear response to human host availability | $\lambda = 1$ & $\mu = 1$ |
| type II |  | anthropophilic (preference for human hosts). even when rare, humans will still be sought-out | $\lambda < 1$ & $\mu \geq 1$ |
| type IV |  | zoophilic (avoidance of human hosts). humans are only bitten when other hosts are very rare | $\lambda > 1$ & $\mu \leq 1$ |



Table 2.1: Table of the of behavioural responses explored in this paper using Yakob's (2016) function, $f(Q) = Q/(Q+\lambda(1-Q)^{\mu})$. The proportional availability of human hosts, $Q$, is shown on the x-axis while the proportion of blood-meals taken from human hosts ($f(Q)$) is on the y-axis. Other functional forms are possible, but for conciseness we only draw the distinction between linear, anthropophilic and zoophilic.

### Epidemiological Models

We were interested in examining the implications of our ecological models on the epidemiology of a theoretical vector-borne pathogen. It was necessary for this model to include how behavioural responses to host availability alters biting rates (akin to the system explored by Yakob (2016)). The transmission of a pathogen in this two-vector system can therefore be described by modifying the Ross-MacDonald model of vector-borne disease transmission:

$$\frac{dI_A(t)}{dt} = \rho_A \kappa_A f_A(Q)[A(t) - I_A(t)]\frac{I_H(t)}{H} - d_A I_A(t) \tag{2.7}$$

$$\frac{dI_B(t)}{dt} = \rho_B \kappa_B f_B(Q)[B(t) - I_B(t)]\frac{I_H(t)}{H} - d_B I_B(t) \tag{2.8}$$

$$\frac{dI_H(t)}{dt} = (\rho_A \gamma_A f_A(Q) I_A(t) + \rho_B \gamma_B f_B(Q) I_B(t))\left[\frac{H - I_H(t)}{H}\right] - m I_H(t) \tag{2.9}$$

The state variables $I_A$ and $I_B$ are the density of infected mosquitoes of species $A$ and $B$, while $I_H$ is the density of infected hosts. The parameter $\rho_i$ is the biting rate (scaled by the behavioural response to hosts $f_i(Q)$), $\kappa_i$ the rate at which bites on infected hosts lead to an infection and $\gamma_i$ the rate at which bites from an infected mosquito infecting a human for the $i^{th}$ mosquito species. $H$ is the *fixed* density of hosts in the system and $m$ the rate of recovery of hosts. The death rate of infected mosquitoes is given by $d$ (such that infected mosquitoes die at an equal rate to uninfected mosquitoes and do not recover from infection). Parameter descriptions and values are given in Table 2.2.

### Model analysis

All mathematical derivations were confirmed in the software Mathematica (version 11.3.0.0) (Wolfram Research, 2018) and all calculations and simulations were conducted in the statistical software R (version 3.5.1) (R Core Team, 2019). All R code has been made available online (https://doi.org/10.17605/OSF.IO/MZDWG) and the Mathematica notebook provided as a supplementary file.

#### Boundaries for coexistence and isoclines

We solved equations 2.3 and 2.4 for $dA(t)/dt = 0$ and $dB(t)/dt = 0$ to give two quadratic expressions (see the supplementary material). The positive solution of these expressions described the zero-net-growth isoclines for the system. Substituting the solution for species $A$ into the solution for species $B$, and vice-versa, yielded two cubic expressions for which the three roots are the potential equilibrium population sizes of the respective species. The discriminant of these expressions reveals the nature of these roots; if the discriminant of both is greater than 0, then there are three non-zero real roots (one stable flanked by two unstable) and coexistence is possible (Kishi and Nakazawa, 2013). Otherwise there is an *unstable* coexistence point, where coexistence is unsustainable. By examining the regions of the parameter space where these conditions are met, we can examine the requisite conditions for coexistence. These expressions are given in the appendix and the supplementary Mathematica file. We also derived cubic isoclines for equations 2.5 and 2.6. For both

| parameter | definition | value | reference |
|---|---|---|---|
| *ecological parameters* | | | |
| $r$ | reproductive rate | 1.31 | Dye (1984b); Southwood et al. (1972) |
| $d$ | death rate | 0.12 | Dye (1984b); Southwood et al. (1972) |
| $\alpha$ | strength of density-dependent (intraspecific) larval competition | 1 | - |
| $\beta_i$ | relative strength (in relation to intraspecific) of interspecific larval competition | varied | - |
| $\delta_i$ | strength of reproductive interference | varied from 0 to 1 | Kishi and Nakazawa (2013) |
| $\lambda_i, \mu_i$ | shape parameters of the behavioural response | see table 2.1 | Yakob (2016) |
| $Q$ | the proportional availability of human hosts | varied | Yakob (2016) |
| $\epsilon_i$ | the proportion of females that contribute larvae to the next generation after interspecific matings | varied from 0 to 1 | - |
| $\tau$ | time from an egg to adult emergence | assumed 0 in simulations | - |
| *epidemiological parameters* | | | |
| $\rho$ | the biting rate of adult mosquitoes | 0.5 | Alphey et al. (2011) |
| $\kappa$ | the probability of a bite from an infected mosquito converting into an infection in a human | 0.38 | Alphey et al. (2011) |
| $\gamma$ | the probability of a bite on an infected human converting into an infection in the mosquito | 0.38 | Alphey et al. (2011) |
| $m$ | the recovery rate of infected humans | 0.17 | Alphey et al. (2011) |
| $H$ | the density of human hosts | varied | - |

Table 2.2: Table of parameter values examined in this paper. Sub-scripted parameters indicate that these were varied between the two species. Otherwise, they were always the same for both.

sets of isoclines, the stability of the equilibria was determined from the dominant eigenvalue of the Jacobian matrix of the linearised system, which is given in the supplementary Mathematica file.

### Deriving the intrinsic growth rate of the pathogen

The equations 2.7, 2.8 and 2.9 can be used to determine the intrinsic growth rate of the pathogen, $R$, in a system where vector populations are at equilibrium. If both mosquito populations are at equilibrium ($A(t) = A^*$, $B(t) = B^*$), and the infected populations tend to zero ($I_A(t)$, $I_B(t)$ and $I_H(t) \longrightarrow 0$) we can derive a Jacobian matrix using equations 2.7 to 2.9 to determine the stability of this disease-free state:

$$R = Det \begin{bmatrix} -m & \rho_A \gamma_A f_A(Q) & \rho_B \gamma_B f_B(Q) \\ \frac{\rho_A \kappa_A f_A(Q) A^*}{H} & -d_A & 0 \\ \frac{\rho_B \kappa_B f_B(Q) B^*}{H} & 0 & -d_B \end{bmatrix} \tag{2.10}$$

When the determinant of this matrix is less than zero, then the disease-free equilibrium is stable. If the determinant is greater than zero then it is unstable. A full derivation is given in the supplementary material.

### Stochastic simulations

Stochastic simulations demonstrate how a system of differential equations respond to random perturbations. In our case, this is particularly interesting given that our system yields multi-stable population dynamics; determining the asymptotic stability *precisely* at an equilibrium does not fully communicate what the *global* stability of this equilibrium is relative to other states (Nolting and Abbott, 2016). For instance, transitions between asymptotically stable equilibrium can occur when stochastic perturbations "knock" the state of the system beyond the domain of attraction of one equilibrium into the domain of another. This can demonstrate the *relative* stability of equilibrium in multi-stable systems.

The delay-differential equations given above (2.3 to 2.9) are of the form

$$\frac{dX(t)}{dt} = f(X(t), X(t-\tau)).$$

We can perturb $\frac{dX(t)}{dt}$ using discrete increments ($dW$) of a Wiener random walk process ($W$) where each $dW$ is taken from a normal distribution with a zero mean and variance $dt$ (Higham, 2001). For our multi-variate example (species $A$ and $B$ and infecteds), the differential equations can be re-written in the form:

$$d\mathbf{X}(t) = g(\mathbf{X}(t), \mathbf{X}(t-\tau))dt + \sigma(\mathbf{X}(t))d\mathbf{W} \tag{2.11}$$

where $\mathbf{X}$(t) is a column vector of $N$ state variables at time $t$, $\mathbf{X}(t-\tau)$ are the time-lagged state variables, and $\mathbf{W}$ a vector of $N$ independent Wiener processes (one for each variable). The function $g$ is the deterministic component of the processes described by equations 2.3 through 2.9, while the function $\sigma$ describes the way in which the Wiener process acts on the state variables (Higham, 2001). Note that the term $\frac{dW}{dt}$ is absent here as the Wiener process is almost always not differentiable. The function $\sigma(\mathbf{X}(t))$ describes how the increments

of noise ($d\mathbf{W}$) impact each of the state variables. We assume that the function $\sigma$ is the same for each state variable;

$$\sigma(\mathbf{X}(t)) = \boldsymbol{\psi}\mathbf{X}(t) + \boldsymbol{\chi}\,. \tag{2.12}$$

The effect of demographic noise (as a function of the the current population density) for each state-variable is described by the parameter vector $\boldsymbol{\psi}$, while exogenous sources of noise (e.g. migration) are described by the vector of parameters $\boldsymbol{\chi}$. Numerical simulations were conducted using a Euler-Maruyama scheme, as outlined in Higham (2001).

## Results

### Ecology

The strength of reproductive interference changes the region of parameter space in which coexistence is possible. In Figure 2.1, this is shown across different combinations of behavioural responses (linear, anthropophilic or zoophilic) in the rows and host availability in the columns. In all cases, increasing the cost of reproductive interference ($\delta_i$) reduces the possibility of coexistence. Reducing host availability ($Q$) expands the region where coexistence is possible. This expansion is symmetric when both species share a linear behavioural responses in panels A to C. However, when the species have different behavioural responses and humans are not the only available host ($Q < 1$), the region of coexistence changes asymmetrically (observed in panels E, F, H, I, K and L). In cases where the species have different behavioural responses, the species which is disinclined to use a shared host can suffer a greater cost of reproductive interference while still coexisting with an anthropophilic competitor. This is most pronounced in the panels E, F, K and L. Panels H and I are the only cases where the region of coexistence is smaller in comparison to panels B and C. This occurs as encounter rates in this scenario are *higher* than the linear/linear default case. Increases/decreases in $\beta_i$ simply shrink/grow the overall area of the coexistence region of while retaining the same overall patterns (not shown, analogous to Kishi and Nakazawa (2013)).

The interactive effect of reproductive interference and larval competition on the potential for coexistence are summarised in Figure 2.2. A scenario where species share linear behavioural responses (white regions) is contrasted with one where species $A$ is anthropophilic and $B$ is zoophilic (blue regions). Increasing the strength of larval competition decreases the possibility of coexistence, as does increasing the strength of reproductive interference (down the rows). Decreasing the proportion of human hosts available will increase the possibility of coexistence (across columns), as it will reduce the encounter rates between the two species. When the species do not have the same behavioural responses to hosts (blue regions), as humans become rarer, the zoophilic species is able to suffer a far greater penalty from larval competition and still coexist with an anthropophilic species. This is due to the zoophilic species utilising human hosts less and, therefore, encountering fewer heterospecifics. The discrepancy is greatest in panels H and I, where the cost of reproductive interference is greatest.

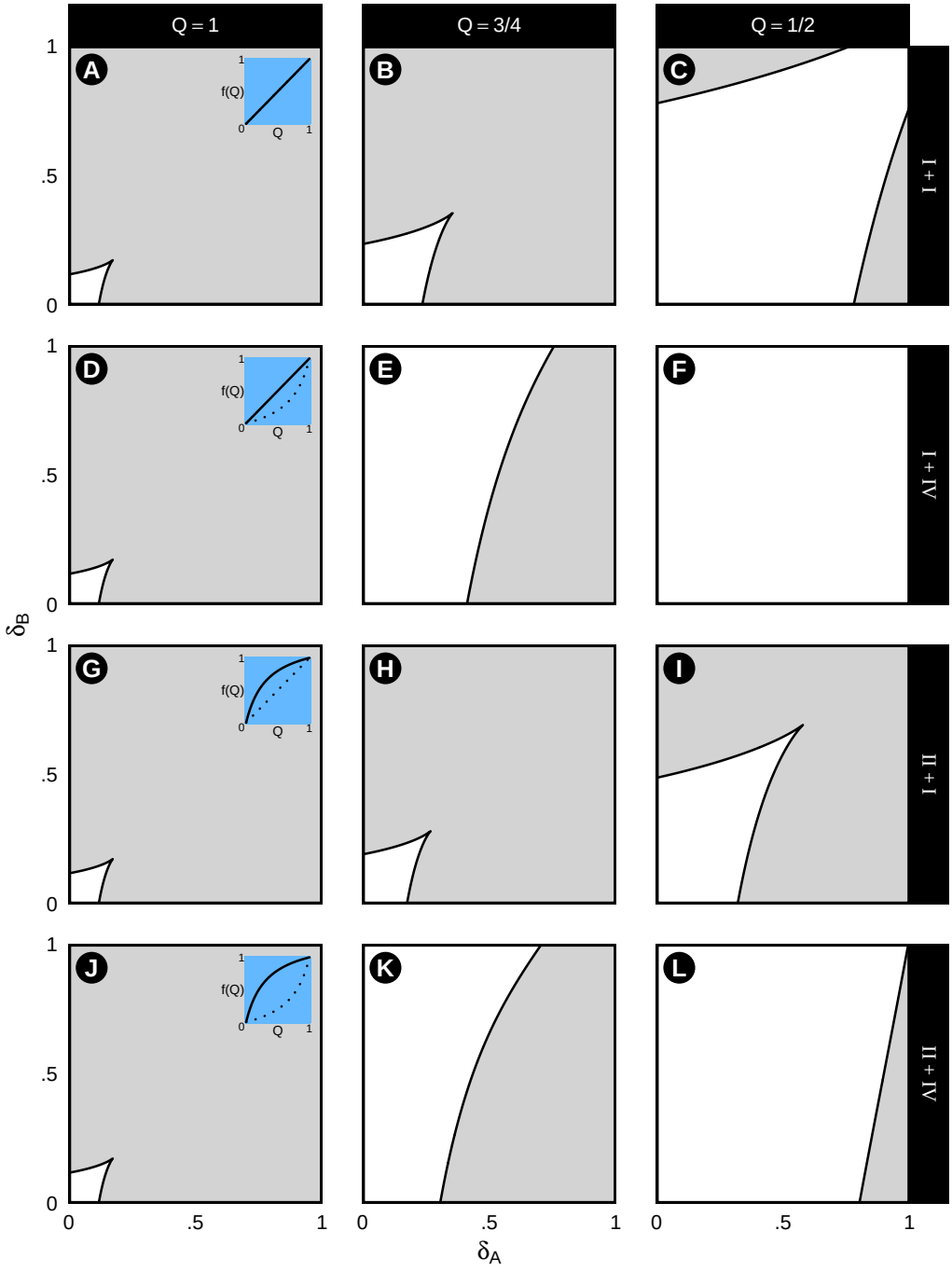



Figure 2.1: Parameter-space plots showing the boundaries of coexistence for equations 2.3 and 2.4 as a function of the strength of reproductive interference suffered by species *A* ($\delta_A$) and *B* ($\delta_B$). Regions where coexistence is possible are denoted in white. Panel rows show different combinations of behavioural responses for *A* and *B* (*A* is given first, then *B*), which can be linear (type I, $\lambda_i = 1$ and $\mu_i = 1$), anthropophilic (type II, $\lambda_i = \frac{1}{4}$ and $\mu_i = 1$) or zoophilic (type IV $\lambda_i = 4$ and $\mu_i = 1$). Panel columns show different levels of host availability $\left(Q = \{1, \frac{3}{4}, \frac{1}{2}\}\right)$. Small interior plots show how the behavioural responses differ in each of the rows, with the response for *A* shown as a solid line and that for *B* as a dotted line. The first column is the baseline, where $f_A(Q)$ and $f_B(Q)$ both equal 1, and the dynamics of Kishi and Nakazawa's (2013) model (equations 2.1 and 2.2) are retrieved. In all cases, the possibility of coexistence increases as host availability is reduced. In panels E, F, H, I, K and L the behavioural responses differ between species and $Q < 1$. Here species *B* is able to suffer higher costs of reproductive interference while still coexisting with *A*. Unvaried parameter values used are given in Table 2.2, otherwise $\alpha = 1$, $\beta_A = \beta_B = \frac{1}{2}$.

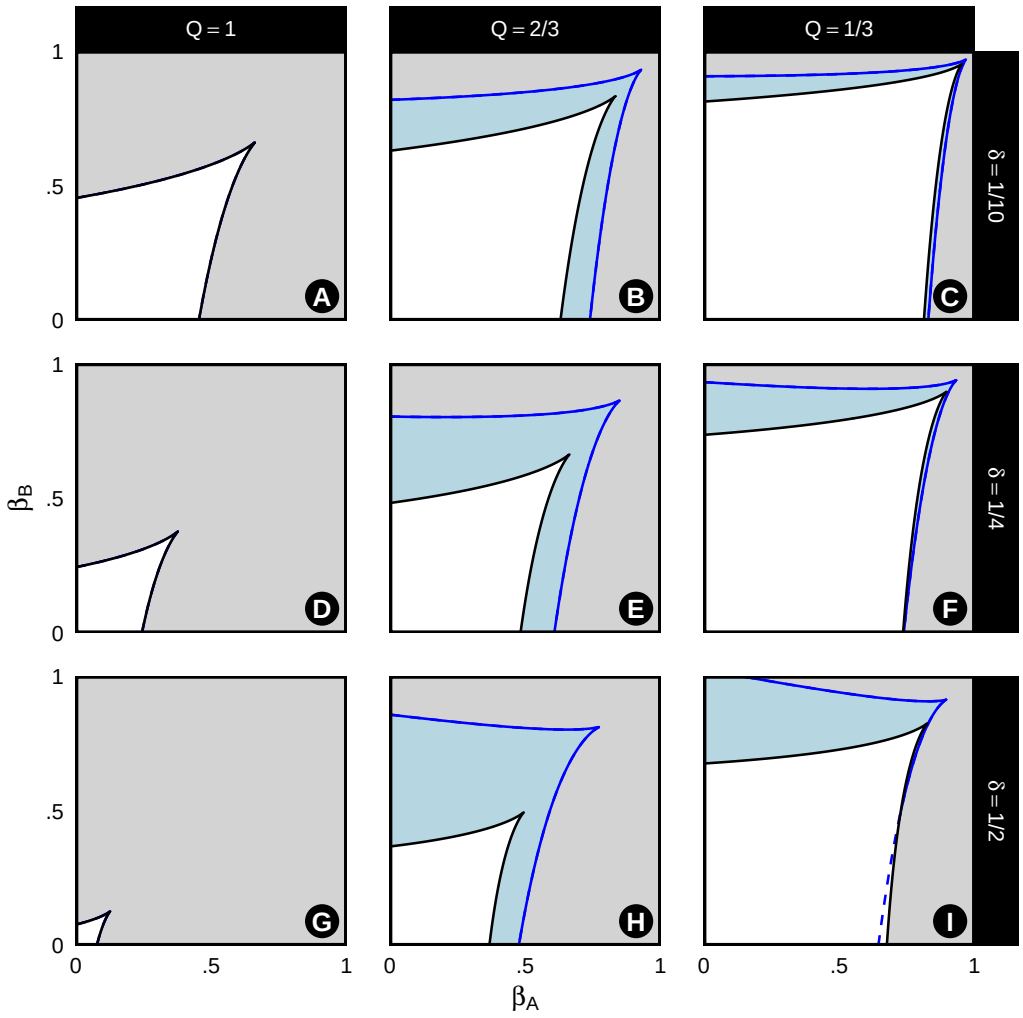



Figure 2.2: Plots showing how the boundaries of coexistence change as a function of the strength of larval competition suffered by species $A$ ($\beta_A$) and $B$ ($\beta_B$). Panel rows show different levels of reproductive interference for both species $\delta$ ($\delta_A = \delta_B = \{\frac{1}{10}, \frac{1}{4}, \frac{1}{2}\}$), while panel columns show different shared host availability ($Q = \{1, \frac{2}{3}, \frac{1}{3}\}$). The black line and white regions denote the boundary for a scenario where both species have a linear behavioural response (both type I, $\lambda_i = 1$ and $\mu_i = 1$) and the blue line and shading for a scenario where species $A$ is highly anthropophilic (type II, $\lambda_A = 4$ and $\mu_A = \frac{1}{4}$) and $B$ highly zoophilic (type IV, $\lambda_B = \frac{1}{4}$ and $\mu_B = 4$). Both cases show that coexistence is possible for greater levels of larval competition when reproductive interference is lower. However, when behavioural responses differ between species (blue regions), the species which is disinclined to use the shared host will be able to experience higher levels of larval competition as it suffers a reduced cost from reproductive interference. This is most noticeable in panels H and I, where the cost of reproductive interference is highest. Overall, there is a greater potential for coexistence when behavioural responses differ.

Figure 2.3 shows the zero-net-growth isoclines derived from equations 2.5 and 2.6 for different levels of female sterilisation of species $A$ ($\epsilon_A$) in the rows and $B$ ($\epsilon_B$) in the columns. Each panel gives the isoclines for a scenario where larval competition is limited by conspecifics ($\alpha > \alpha\beta$, solid lines) and heterospecifics ($\alpha < \alpha\beta$, dotted lines). In panel A, coexistence is not possible as the aggregate costs of reproductive interference and larval competition are greater than the strength of within-species competition. In panels along the diagonal (where $\epsilon_A = \epsilon_B$), as fewer females of both species contribute eggs, the effects of intraspecific larval competition are diminished to the point where coexistence is possible (panels A, E, I). However, this is only the case when the system is limited by intraspecific larval competition (solid lines). Off-diagonal, coexistence is not possible when discrepancy between $\epsilon_A$ and $\epsilon_B$ is greatest (panels C and G). However, for the intermediate differences in sterilisation shown in panels F and H, coexistence is possible. Counter-intuitively, in panels F and H the species with *more* sterilised females has a higher predicted coexistence density. This only occurs when larval competition is self-limiting (solid lines), suggesting that this counter-intuitive benefit to the sterilised species is unique to these circumstances.

### Epidemiology

In the previous section, we demonstrated that the position and stability of stable-state vector populations is, in part, determined by the process of reproductive interference and host availability (through $\delta_i$ and $f_i(Q)$). Notably, we have shown that the system could yield either coexistence or single-species dominant states. It is therefore necessary to examine how vector population size affects disease spread so that this can be related to the different configurations of the vector populations. Moreover, the behavioural responses to hosts will also alter the biting rate on human hosts (Yakob, 2016), suggesting that the alternate-stable states could be epidemiologically non-equivalent. The vector dynamics in this section are described by equations 2.3 and 2.4; we do not include examples where vector population dynamics are described by equations 2.5 and 2.6. This is because equations 2.5 and 2.6 do not include behavioural responses to hosts, only female sterilisation. In the absence of behavioural responses, there is no feedback between the process of host selection, reproductive interference and epidemiology.

In Figure 2.4, the panel backgrounds show how the potential for a disease outbreak ($R$) changes with vector abundance. Overlaid are the zero-net-growth isoclines corresponding to the behavioural response combinations and host availability for each panel. In the baseline case (the first column), humans are the only hosts, which means it does not matter which behavioural response the vectors exhibit. In panels A-C, both species have linear behavioural responses, so $R$ is diminished symmetrically as as human hosts become rarer. In panels E, F, H, I, K and L, the species do not share the same behavioural responses and humans are not the only hosts ($Q < 1$). This leads to asymmetric values of $R$ depending on which vector is most abundant. This is expected, given that a zoophilic vector will contribute less to human disease than an anthropophilic one. What has not yet been appreciated is that this same process – mediated by reproductive interference – will additionally determine the location of the stable and unstable vector states. For instance, in panels K and L,

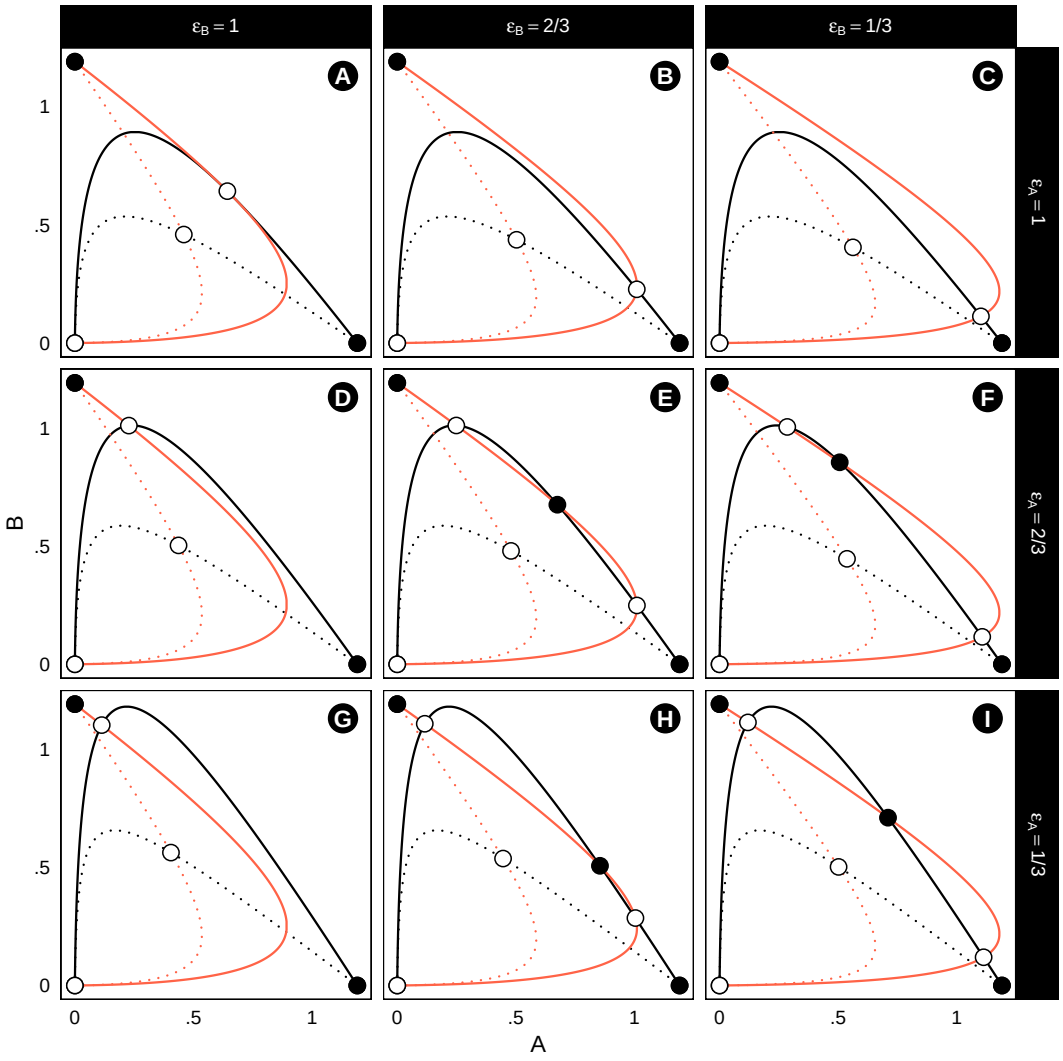



Figure 2.3: Zero-net-growth isoclines for species *A* (black) and *B* (red) derived from equations 2.5 and 2.6. Solid black points denote stable equilibria, and open circles unstable equilibria. Facets correspond to proportions of females of species *A* in the columns $(\epsilon_A = \{1, \frac{2}{3}, \frac{1}{3}\})$ and *B* along the rows $(\epsilon_B = \{1, \frac{2}{3}, \frac{1}{3}\})$ going on to contribute eggs (and therefore larvae) to the process of density-dependence after heterospecific matings. The strength of larval competition is varied within each panel (with $\beta_A = \beta_B$). The solid line shows results for self-limiting ($\alpha > \alpha\beta$) larval competition and the dotted lines shows a case limited by heterospecific competition ($\alpha < \alpha\beta$). Along the diagonal the proportion of sterilised females is increased for both species symmetrically, introducing the prospect of coexistence (it is not possible in the initial case with no sterilisation). Off-diagonal, coexistence is possible when intraspecific competition is limiting (solid lines), but the coexistence state is biased toward the species experiencing *more* sterilisation (panels H and F). Unvaried parameter values are given in Table 2.2, otherwise $\delta = \frac{1}{10}$, $\beta_A = \beta_B = \frac{2}{3}$ (solid line) or $\beta_A = \beta_B = \frac{4}{3}$ (dotted line).

a stable coexistence point is introduced which falls within the disease outbreak range. A coexistence point would not be introduced if there was no feedback between host-availability and reproductive interference.

We were motivated to use stochastic simulations of our differential equations to gain a more nuanced understanding of how behavioural responses to hosts affect the *realised* stability of the vector system, as well as the consequences of multi-stable population dynamics for disease spread. However, exploratory simulations indicated that for all but very small time delays ($\tau$), cyclic or chaotic dynamics would occur. Indeed this was the case when using a time delay informed by empirical observations of *Aedes* development times. For this reason, we assume $\tau = 0$, as highly non-linear dynamics are not the focus of the current study. We suspect that these non-linear dynamics occur because of the linear form of density-dependence in our model; other delay-differential equation models of *Aedes* population dynamics (e.g. Dye (1984b)) which use more complex forms of density-dependence do not yield cyclic or chaotic dynamics so readily. They do, however, sacrifice analytic tractability with regards to multi-species modelling.

Figure 2.5, depicts scenarios with linear/linear (panels A-C) and anthropophilic/zoophilic (panels D-F) combinations of behavioural responses to hosts. The availability of hosts is changed across columns. The system is simulated to give both the ecological (main plot) and epidemiological (sub-plot) stochastic dynamics. The parametrisation of these scenarios is the same as panels A-C and J-L in Figure 2.4, where the deterministic isoclines are shown. The local asymptotic stability used to determine the nature of single- and multi-species states identified in Figure 2.4 is insufficient to describe the full system dynamics. While the states found by the isocline analysis in Figure 2.4 can be visually identified, there are different probabilities of each state being occupied. The state where the anthropophilic species is dominant is rarely occupied in panels E and F, reflective of the fact that it incurs a greater cost of reproductive interference and is unlikely to out-compete a zoophilic competitor. In the sub plot of panel E, epidemiological dynamics (disease extinction versus disease outbreak) are bimodal, reflecting the transition in the vector state-space. Coexistence with an anthropophilic vector has more severe epidemiological consequences than the single-species dominant state of the zoophilic host, as anthropophilic vectors will seek out rare humans and increase disease transmission.

Figure 2.6 shows how the distribution of infected hosts (across many stochastic simulations) changes as humans become rarer (i.e $Q$ is reduced). Across columns the strength of reproductive interference is increased, while rows denote different combinations of behavioural responses. In all panels, when only human hosts are available ($Q = 1$), the distribution of infected humans is the same as behavioural responses cannot alter biting rates. In panels A-C, where both vectors have a linear behavioural response to hosts, the number of infected hosts declines with host availability, doing so more steeply when reproductive inference is stronger (panels B and C). This outcome is intuitive; as hosts become rarer, the vector will bite human hosts less and there will be fewer infections. When behavioural responses are not the same (panels D-L), there is a non-linear relationship between host availability and the distribution of infections. The combination of reproductive interference and host selection lead to a concomitant relationship between ecology and epidemiology. As humans become rarer, the costs from reproductive interference are reduced and the biting rate on

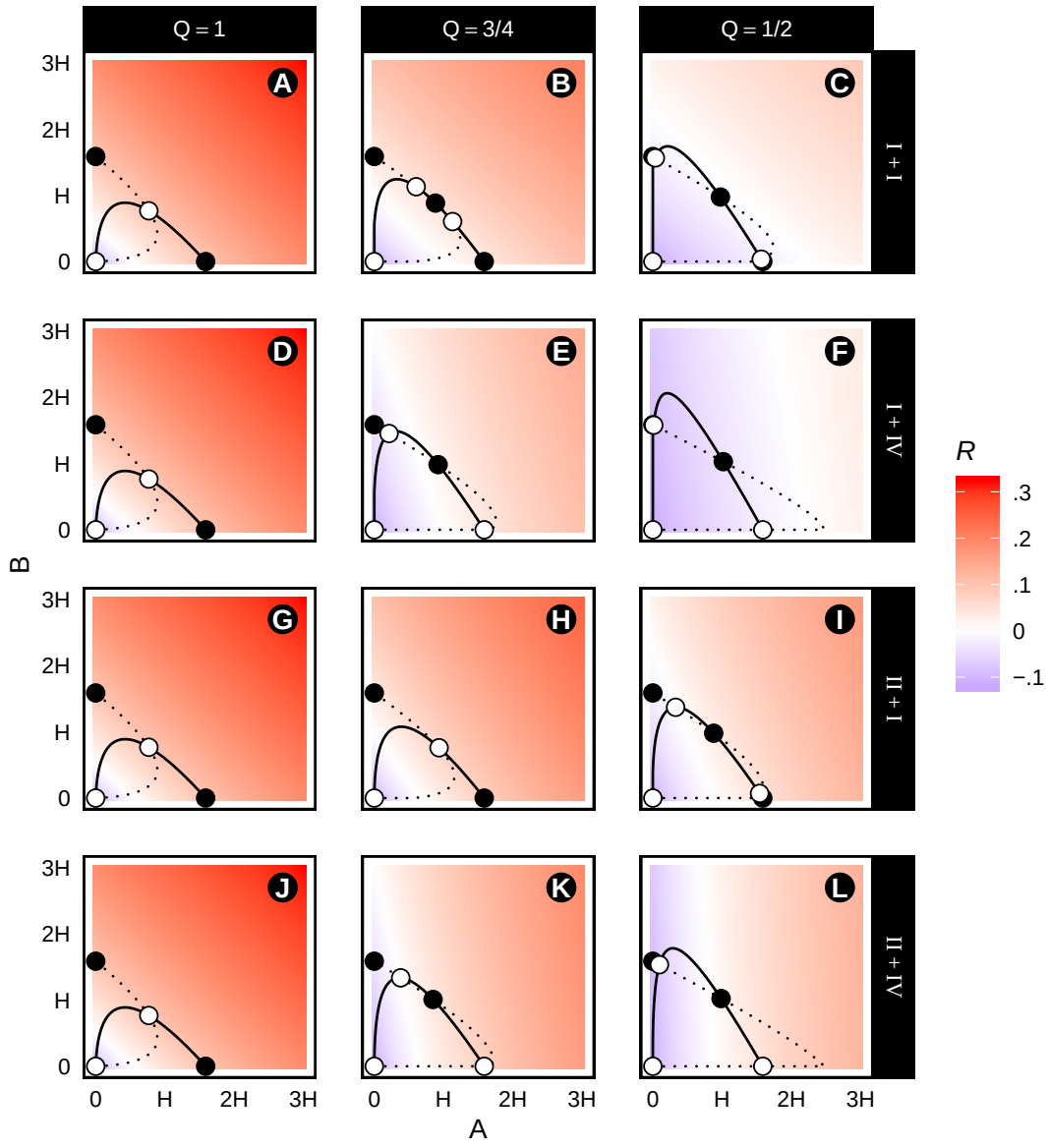



Figure 2.4: Surfaces exploring the effect of behavioural responses to hosts on the disease outbreak potential of a two-vector system. The x-axis shows the equilibrum population size of species *A*, and the *y*-axis species *B*. Axes are given as multiples of the human host population, up to a 3:1 ratio of vectors to hosts. Whether the disease-free equilibrium is stable ($R < 0$) or unstable ($R > 0$) across the vector state-space is given by the background colour (blue disease would die out, red it would take-off). Columns denote changes in the availability of hosts $\left(Q = \{1, \frac{3}{4}, \frac{1}{2}\}\right)$ and rows different combinations of linear (type I, $\lambda_i = 1$ and $\mu_i = 1$), highly anthropophilic (type II, $\lambda_i = \frac{1}{4}$ and $\mu_i = 4$) and highly zoophilic (type IV, $\lambda_i = 4$ and $\mu_i = \frac{1}{4}$) behavioural responses (first giving the response of *A*, then *B*). Overlaid are the zero-net-growth isoclines (from equations 2.3 and 2.4) for the corresponding vector system, with solid lines those of *A* and dotted lines for *B*. Stable-states are denoted with black points, unstable with white. In the first row, where both species respond linearly to host availability, the region over which $R > 0$ diminishes symmetrically. When the species have have different behavioural responses and humans are not the only available hosts (panels E, F, H, I, K and L), *R* will be lower when the system is biased towards the zoophilic vector and vice-versa. The isoclines (from equations 2.3 and 2.4) show the feedback between the behavioural responses and reproductive interference; changes in host availability can change the location of stable-states, which in turn fall on different values of *R* (panels K and L). Unvaried parameter values are given Table 2.2, otherwise $\beta_A = \beta_B = \frac{1}{2}$, $\delta_A = \delta_B = \frac{1}{3}$ and $H = \frac{3}{4}$

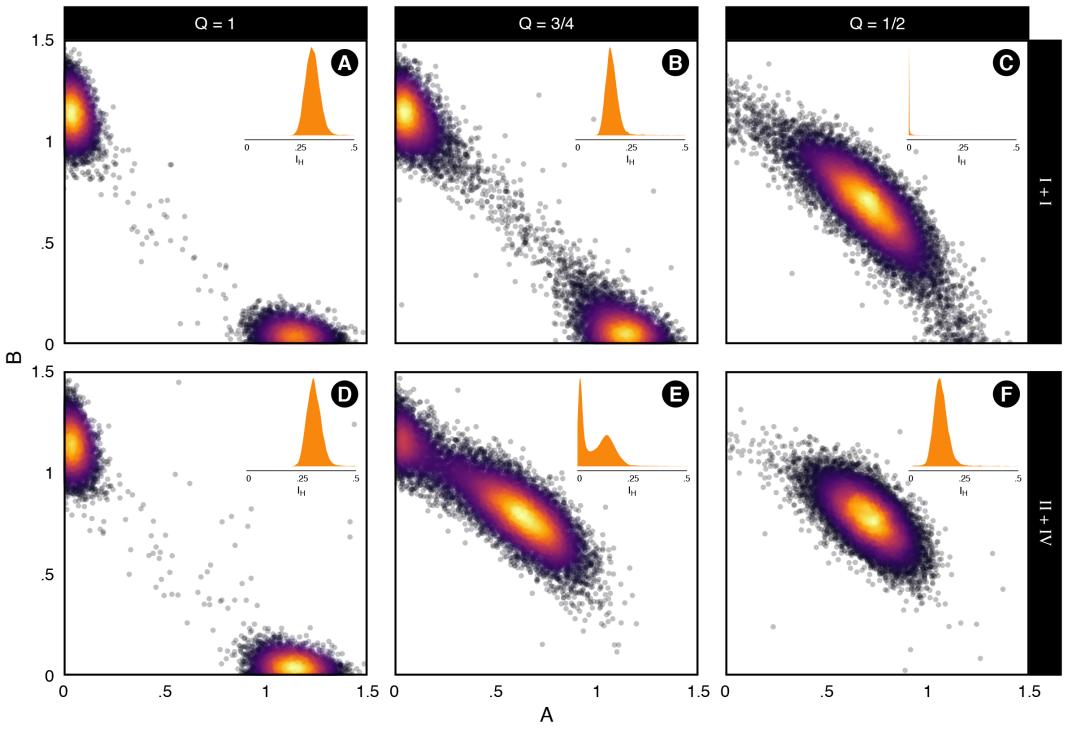



Figure 2.5: Aggregated results of 100, 1000-iteration stochastic simulations of the multi-vector system with a step-size ($dt$) of $1 \times 10^{-3}$. Scatter-plots of the vector state-space (hot colours indicate higher frequency of occurrence) are shown with density plots of the number of infected humans ($I_H$) shown in the upper right of each facet. We examine are two behavioural response scenarios. Panels A-C show a "null" case where both have linear (type I, $\lambda_i = 1$ and $\mu_i = 1$) responses. Panels D-F show a case where $A$ is highly anthropophilic (type II, $\lambda_A = 4$ and $\mu_A = \frac{1}{4}$) and $B$ is highly zoophilic (type IV, $\lambda_B = \frac{1}{4}$ and $\mu_B = 4$). Parameter values are the same as the first and fourth rows in Figure 2.4, so the deterministic dynamics would be those given by the isoclines in this plot. Observable are the discrepancies between the possible stable states that *could* be occupied and the *realised* states in the stochastic simulations. In panel E, there are frequent state transitions between the $B$-dominant and coexistence states. This corresponds to a diffuse pattern in the number of infected humans, which show a range of values tracking the abundance of the anthropophilic host (sub-plot, panel E). It is notable that the $A$-dominant state is never occupied in this panel. In the final column, the coexistence state becomes the most likely state to be occupied (single-species states are rarely visited), however this corresponds to drastically different epidemiological dynamics. As $A$ is anthropophilic in panel F, a coexistence state with this species will allow for disease transmission, whereas it will not for the linear case in panel C. Unvaried parameter values are given in Table 2.2, otherwise $\beta_A = \beta_B = \frac{1}{2}$, $\delta_A = \delta_B = \frac{1}{3}$ and $H = \frac{3}{4}$, $\{\psi_A, \psi_B, \psi_{I_A}, \psi_{I_B}, \psi_{I_H}\} = 6 \times 10^{-2}$, $\{\chi_A, \chi_B\} = 6 \times 10^{-2}$ and $\{\chi_{I_A}, \chi_{I_B}, \chi_{I_H}\} = 0$.

hosts lessened. This reduced competitive cost can facilitate the coexistence of vectors in circumstances where the zoophilic vector would have otherwise dominated, leading to a higher $R$ than the linear/linear case. This non-linearity is most clear in panels H and L. In panels H, I and L, bimodal distributions of infected humans are observed as the system transitions between single-species dominant and coexistence states (the same dynamics are observed in Figure 2.5, panel E). The state where the more anthropophilic species is dominant is rarely occupied as it suffers a greater cost from reproductive interference, suggesting that it is very unlikely that the zoophilic species will be outcompeted.

## Discussion

We present a theoretical framework for examining the roles of two mechanisms of competition for *Aedes* population dynamics and epidemiology. Our model employs a generalised parameterisation of *Ae. aegypti* and *Ae. albopictus* reproductive rate, death rate and density-dependence to test if reproductive interference and larval competition can explain observed patterns of co-occurrence and competitive exclusion in the wild. These mechanisms were embellished with *Aedes*-bespoke features relating to these forms of competition: functional-response mediated encounter rates and sterilisation of females by copulation with heterospecific males. A generalised model of *Aedes* epidemiology was then used to examine the feedback between the concomitant process of host selection, reproductive interference and biting rate.

### Ecological insights

Our findings suggest that population coexistence and competitive exclusion could be driven by differences in the availability of a shared host, provided competitors suffer from reproductive interference and have divergent behavioural responses to hosts. This is because *Aedes* use hosts to find mates (Nelson, 1986; Yuval, 2006), suggesting that *Ae. aegypti* and *Ae. albopictus* will only encounter heterospecifics (and incur the cost of reproductive interference) at shared hosts. We show that when the behavioural responses of both species are linear the effects of reproductive interference are symmetrically scaled and the possibility of coexistence is increased – even when the associated costs are high. This is due to the encounter rate with heterospecifics being reduced in tandem with humans becoming rarer. More interesting are cases where the vectors have *different* behavioural responses. In these cases, as host availability is reduced, the possibility of coexistence varies asymmetrically with the costs associated with reproductive interference; the species with the more zoophilic behavioural response can suffer higher costs of reproductive interference while still coexisting with the anthropophilic species. This is intuitive, as a smaller proportion of the zoophilic population will be exposed to heterospecifics and incur the associated costs.

Also notable is the indirect effect of reproductive interference on larval competition. While the behavioural responses do not *directly* affect the process of reproductive interference, it will still influence the costs associated with larval competition. With linear behavioural responses, reducing human host availability increased the strength of larval competition ($\beta_i$) that can be suffered while still permitting the species to co-

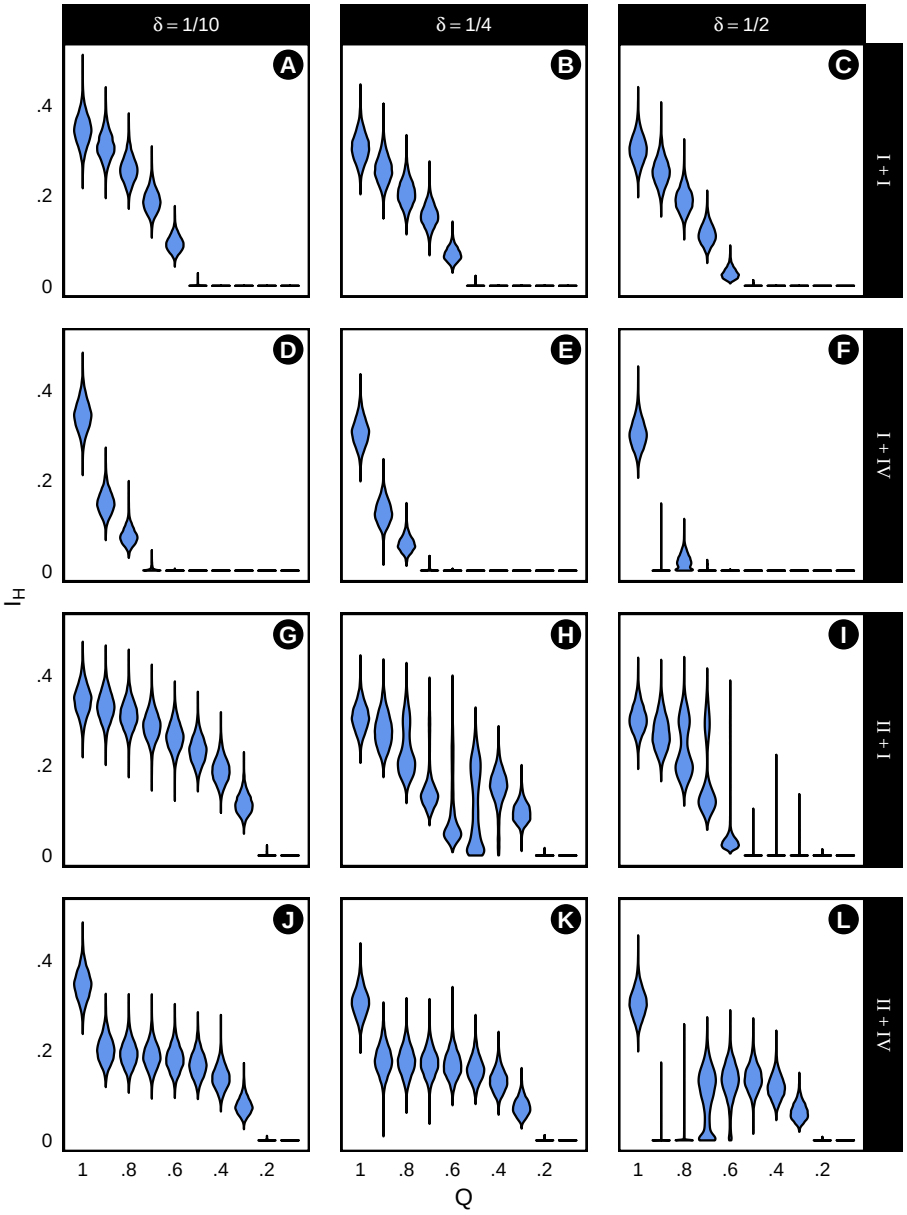



Figure 2.6: Violin plots demonstrating how changes in host availability ($Q$, from 1 to 0.1 in increments of 0.1) affect the distribution of infected humans ($I_H$). Each violin is a summary of 100, 1000-iteration stochastic simulations of the multi-vector system with a step-size ($dt$) of $1 \times 10^{-3}$. Behavioural responses are varied in the rows, with scenarios a combination of linear (type I, $\lambda_i = 1$ and $\mu_i = 1$), highly anthropophilic (type II, $\lambda_A = 4$ and $\mu_A = \frac{1}{4}$) and highly zoophilic (type IV, $\lambda_B = \frac{1}{4}$ and $\mu_B = 4$) behavioural responses. The response of species $A$ is given first, then $B$. Columns show different strengths of reproductive interference, where the costs are the same for both species $\left(\delta_A = \delta_B = \{\frac{1}{10}, \frac{1}{4}, \frac{1}{2}\}\right)$. In the first row, the number of infected humans decreases with host availability (both vectors have linear responses). When behavioural responses are not same, dynamics can be highly non-linear. Panels H and L show an initial reduction in the number of infected humans before infections counter-intuitively begin to increase with decreasing host availability. In panels H, I, and L, human infections are bimodally distributed for some values of $Q$. This is indicative of shifts between single-species dominant and coexistence states. The epidemiology of these dynamics are contingent on which species is dominant (coexistence with an anthropophilic will result in a greater transmission potential than a zoophilic dominant state). Effects are most severe when the cost of reproductive interference is larger (i.e. across rows). Unvaried parameter values are given Table 2.2, otherwise $\beta_A = \beta_B = \frac{1}{2}$, $\delta_A = \delta_B = \frac{1}{3}$, $H = \frac{3}{4}$, $\{\psi_A, \psi_B, \psi_{I_A}, \psi_{I_B}, \psi_{I_H}\} = 6 \times 10^{-2}$, $\{\chi_A, \chi_B\} = 6 \times 10^{-2}$ and $\{\chi_{I_A}, \chi_{I_B}, \chi_{I_H}\} = 0$.

exist. However, we show that when behavioural responses differ between species a zoophilic mosquito can suffer higher levels of larval competition while still coexisting with the anthropophilic one. Overall, we find that higher costs of reproductive interference reduce the possibility of coexistence for high coefficients of larval competition.

Kishi and Nakazawa (2013) provided a rigorous analysis of Kuno's (1992) model, and gave valuable insights into the processes of reproductive interference and how it might interact with Lotka-Volterra competition. When behavioural responses are linear, our results corroborate this finding as the function describing reproductive interference will linearly scale with the exposure to heterospecific mosquitoes. Our work has expanded this to investigate non-linear behavioural responses, demonstrating that behavioural responses can drive significant asymmetries in the levels of competition experienced by each species, leading to different patterns of coexistence and exclusion, even when the strength of reproductive interference and larval competition are the same. This is contingent on the shared host not being the only available host. For instance, if a lab- or field-study determined the same coefficients of larval competition and reproductive interference for both *Ae. aegypti* and *Ae. albopictus*, then our model predicts that, in practice, the availability of the hosts could result in these costs manifesting in different competitive outcomes if the species have different behavioural responses. These discrepancies between the measured costs of competition and the *realised* costs under different host regimes is crucially important for those studying, analysing and reviewing the competitive effects found in *Aedes* lab, semi-field and field studies. In order to correctly interpret study findings (e.g. which competitor is superior) the environmental context must also be accounted for. This is in addition to already understood dependencies, such as resource (Reiskind et al., 2012), population (Leisnham and Juliano, 2009), habitat (Rey et al., 2006) and climatic (Camara et al., 2016; Costanzo et al., 2005) mediated differences in competitive outcome. Indeed further complications are likely to include strain-specific responses to host availability (it is unlikely that all *Ae. aegypti* and *Ae. albopictus* populations will share the same host preferences).

### Sterilised females

Our model also explored the effect of sterilisation of female mosquitoes from matings with heterospecific males (Tripet et al., 2011) on patterns of coexistence and exclusion. This is an another indirect effect of reproductive interference on larval competition; when both species become sterilised, we find that coexistence is promoted as larval density-dependent competition is alleviated. When the levels of sterilisation in the two species differ, outcomes depend on whether the system is limited by interspecific or intraspecific larval competition. Counter-intuitively, we find that the sterilisation of females by heterospecific matings lead to *higher* equilibrium densities of the species experiencing *higher* levels of sterilisation (where coexistence was possible). However, this occurs only when the population is limited by intraspecific larval competition. A comparable phenomena is observed with the superior efficacy of late-acting lethal control strategies (e.g. GM mosquitoes) compared with early-acting sterilising strategies (e.g. sterile insect technique) (Phuc et al.,

2007). Theory suggests that removing the density-dependent competition by "skimming-off" excess individuals will increase the reproductive rate of the species. In the *Aedes* case, alleviating the larval competition in the shared pools would increase survivorship and lead to an increased reproductive rate for the sterilised population (relative to the reproductive interference free situation). Similar models, such as those for tsetse fly control (Rogers and Randolph, 1984) suggest a similar increase in the equilibrium populations sizes would be observed under sterile insect releases. The unifying assumption is that populations are density-limited.

The counter-intuitive increase in equilibrium population density arising when mortality (or in our case sterility) is also increased is termed a "hydra-effect". Abrams (2009) outlined three candidate mechanisms which could cause this, with one particularly relevant for our model; "the temporal separation of mortality and density-dependence". While the process of sterilisation in our second model (equations 2.5 and 2.6) does not describe an increase in mortality *per se*, the outcome is the same in that larvae experience reduced density-dependent regulation. Abrams (2009) also identify that in order for this mechanism to produce a hydra-effect, then there must be over-compensatory density-dependence which is absent from our model as our within-species competition is only compensatory. McIntire and Juliano (2018) provided empirical support for Abrams's (2009) temporally-separated mortality hypothesis by rearing cohorts of *Ae. albopictus* in the lab and exposing them to a regime of either early and late-acting mortality. They found that early-acting mortality resulted in higher adult densities. This suggests that the predictions of models in the vector-control literature are correct in cautioning against sterile insect techniques when species are limited by strong over-compensatory density-dependent processes, and gives real-world context to the predictions of our model.

The sensitivity of these conclusions to the system being limited by within or between-species competition is clear; if conspecifics exert a greater cost in terms of within-species larval survivorship, then fewer conspecifics will allow them to do better. However, if the sterilised species suffers a greater cost from heterospecific larvae than conspecific larvae, this process will not confer the same benefit.

### Epidemiological consequences

This study advances our understanding of the epidemiological consequences of host selection and availability (as described by Yakob (2016)) in two ways. First, the same framework can be applied to multi-vector systems with different host preferences. Second, host selection has *ecological* consequences for *Aedes*. Indeed, we have shown the ecological and epidemiological processes to be inextricably linked with regards to reproductive interference. These effects can be both detrimental and beneficial for vector-borne disease transmission. Our exploration of the disease potential of the multi-vector state-space showed that the potential for outbreaks varies drastically with different population sizes of zoophilic and anthropophilic vectors. The process of reproductive interference determines the region of this state-space likely to be occupied by vector populations, leading to a complex feedback of the two processes; an anthropophilic vector is more competent at transmitting disease, but will be more likely to be excluded by reproductive interference. The reverse may

also be true however, as reducing human host availability may, through diminished reproductive interference, balance other costs (such as differential costs of larval competition) and promote coexistence between zoophilic and anthropophilic species.

Our stochastic simulations tie-in with our deterministic findings by describing the *realised* stability of the system, not solely the asymptotic stability precisely at the equilibrium. Evident from our simulations is that the deterministic predictions do not fully demonstrate dynamical differences between the scenarios. In our example, the multi-stable states are not equivalently likely, with some states more likely to precipitate a state-change than others. Stochastic processes will more easily shift the system between states of comparable stability and may prohibit the occupation of some states as they are simply too unlikely. Our simulations also show that changes in host availability and behavioural responses can alter system stability and promote the occupation of certain states. In the example, we show that different behavioural responses can result in drastically different dynamics, which correspond to very different epidemiological outcomes; as states transition from single-species dominant to multi-vector states the system can fall in a region of the state-space where an outbreak is possible. In short, selecting which host to bite determines the level of reproductive interference suffered, as well as the outbreak potential in humans. This leads to a highly non-linear relationship between host availability and the outbreak of infection when the species have different behavioural responses.

### Insights, assumptions and extensions

*Ae. aegypti* and *Ae. albopictus* can occur as segregated populations across landscapes (Rey et al., 2006), potentially due to the outcomes of competition being mediated by climate (Costanzo et al., 2005) or larval resource type (Reiskind et al., 2012). On a finer spatial scale, differences in resting behaviour could mean that the species have access to different hosts (Takken and Verhulst, 2012), with *Ae. aegypti* often resting indoors (Kohn, 1990) and *Ae. albopictus* outdoors (Delatte et al., 2010). In our model, we assume that host availability is the same for both species, but differences in the availability of hosts at the local and landscape scale will be critical in determining the costs of reproductive interference, as any species-level host preferences will play out heterogeneously across space. An extension to our work could consider how the overlap in host availability could diminish or enhance the effects of reproductive interference.

We use a frequency-dependent function to describe the process of reproductive interference; increasing the relative frequency of heterospecifics to conspecifics scales the reproductive rate. Kyogoku and Sota (2017) present a model of reproductive interference where heterospecific encounters are governed by a density - dependent function (rather than the frequency dependent function used here and by Kuno (1992)). Their model is noteworthy in that it can produce a more diverse range of patterns of coexistence and exclusion because reproductive interference is a product of both frequency and density. For instance, in their model invasions from rare are possible if the *density* of heterospecifics is sufficiently low that the costs of reproductive interference is negligible. We elected not to use this model as a our frequency-dependent function is recovered

when the population densities are very high.

While the density of *mosquitoes* could affect the outcomes of reproductive interference, so too could the density of *hosts*. We assume that hosts will be used in proportion to their availability. However, should all hosts be at low density – and host encounters are overall very rare – then it is possible that preference would yield to necessity and host choice would break-down (Takken and Verhulst, 2012). With hosts at a low density, reproductive interference would still occur as rare hosts would be used by both species out of necessity. However, the asymmetric differences in the cost of reproductive interference may not manifest, as there would be no differential host-use. Our model also assumes that there is no additional cost to using specific hosts; for instance, a human host may exhibit anti-biting responses or use a repellent, but we assume they are as easy as any other host to access. This would mean that choosing a host could incur different costs (e.g. energetic) or expose the mosquito to hazards (e.g. swatting) that could potentially affect reproduction and longevity.

Fitting appropriate mathematical functions to the processes of density-dependent intra- and interspecific larval competition is challenging for *Aedes*, particularly for wild populations (Legros et al., 2009). Here we have assumed that a linear function is an adequate description of the process (i.e. the logistic-assumption holds, with each larvae contributing equally to the process of competition). Examining the interaction between non-linear forms of population regulation and the process of reproductive interference outlined in this research is a logical and worthwhile extension. Given the links between over-compensatory density-dependence and the Hydra effect (Abrams, 2009; McIntire and Juliano, 2018), exploring different forms of population feedback will be valuable in elucidating the role of population regulation in increasing equilibrium densities of sterilised species with competitive interactions.

Bonsall et al. (2010) analysed a model of *Aedes* larval competition without the process of reproductive interference, instead including the effect of sterile or GM (late-acting lethal) mosquito releases targeted at one of the species. They derived non-linear isoclines, driven by one species experiencing population control. Our work raises an important question with regards to population control; if both species experience reproductive interference, then releases targeted at one species will almost certainly affect the non-target population. We advocate the exploration of the interaction between reproductive interference and targeted-population suppression techniques, as the effects on predicted coexistence and exclusion could be profound.

## Conclusion

Kuno's (1992) model of reproductive interference and Yakob's (2016) study of vector behavioural responses provide independent insights into two crucial processes. The models presented in this paper are unique in uniting these insights into a model of *Aedes* competition. We embellished a general model of *Aedes* ecology and epidemiology to allow us to isolate the effect of reproductive interference – mediated by host choice – on population and disease dynamics. This allowed us to elucidate the relative roles of reproductive interference and larval competition, demonstrating that host selection can allow these processes to be "traded-off", facilitating coexistence where it would be difficult to predict from practical studies. We demonstrated that the

ecological process of competition is inextricably linked with epidemiology, as host selection determines the costs of reproductive interference (potentially leading to vector coexistence) and also mediates biting rate. In doing so, we have added to the complex range of candidate mechanisms which could explain variable patterns of exclusion and coexistence between *Aedes* mosquitoes.

# 3 | DIFFERENTIAL EFFECTS OF CONSPECIFIC AND HETEROSPECIFIC DENSITY ON THE DEVELOPMENT OF *AEDES AEGYPTI* AND *AEDES ALBOPICTUS* LARVAE

Between-species competition shapes the distribution and abundance of populations. *Aedes aegypti* and *Aedes albopictus* are vectors of pathogens such as dengue and are known to compete at the larval stage. The outcome of this inter-species competition has been found to be context-dependent, with the strength and direction changing with resource availability and type. We were motivated by this uncertainty and aimed to elucidate the magnitude and mechanism of competition. In this study we manipulated the density of single- and mixed-species cohorts of larvae, measuring the effects on survivorship and development time. Unlike other related studies, we adjusted the feeding regime so that the per-capita resource availability was kept constant across all density treatments, at a level sufficient for successful development. This ensured that each larva at least had the *opportunity* to gain the requisite resources for pupation. Our analysis found that *Ae. aegypti* suffered notably less mortality due to intra- and interspecific competition. For both species, intra- and interspecific competition led to the survival of faster-developing individuals, with the exception that slower developing *Ae. albopictus* larvae survived when exposed to a combination of both high con- and heterospecific densities. These results show that the competition between *Ae. aegypti* and *Ae. albopictus* can still occur even when resources are theoretically adequate for development. This suggests that larvae can alter resource seeking and consumption parameters when exposed to high densities of conspecifics and heterospecifics, leading to contest competition. Evidence for resource-independent mechanisms of competition – such as crowding – are also found, as is evidence for the importance of demographic stochasticity in population processes.

**Contributing authors**: Paton R.S., Heath K., Wilson, A.J. and Bonsall, M.B.

## Introduction

Studying the processes driving the occurrence and persistence of populations is central to the field of ecology (Morin, 2011). Species with overlapping niches will compete for resources and space, just as they do with conspecifics. These interactions between individuals of the same species (intraspecific) and different species (interspecific) are crucial in shaping ecological communities and can help explain the abundance and distribution of populations (Chesson, 2000; Morin, 2011). Theory predicts that species suffering a greater cost from within-species competition can co-occur, whereas the opposite (between-species > within-species) will lead to competitive exclusion (Armstrong and McGehee, 1980). The extent of intra- and interspecific interactions can change across gradients of biotic (e.g. predator abundance) and abiotic (e.g. resource availability, climactic) variables, meaning both competitive exclusion and coexistence can occur in heterogeneous environments or across landscapes and regions (Amarasekare, 2003; Chamberlain et al., 2014). For two species competing for the same resource, competition can be for the resource directly and/or indirectly through interference. The former is simply the effect one species will have on the other if it depletes an essential common resource. In the second case, one species inhibits the competitor by using mechanical, signalling or chemical interference (Chesson, 2000). The effects of competition manifest as penalties in life history traits, such as survival and development. Quantifying the direction, magnitude and mechanism of intra- and interspecific competition has been the objective of a plethora of empirical and theoretical studies (see Chesson (2000) and the references therein). Some opt to take a phenomenological approach, describing the "net-outcomes" of competition, while others focus on finding mechanistic explanations. Here, we are interested in a specific instance of inter-species competition; that between *Aedes* mosquitoes.

Mosquito-borne viruses are a significant cause of mortality and morbidity particularly in the developing world (Bhatt et al., 2013). The recent Zika outbreak in Brazil and an estimated 390 million annual dengue infections motivates the need for a concerted effort to curtail disease transmission (Bhatt et al., 2013; Yakob and Walker, 2016). With the notable exception of yellow fever, vaccine efficacy is poor, and availability and coverage continue to be a problem (Bhatt et al., 2013). This has led to a focus on controlling the *Aedes* vectors of these diseases, with emphasis on releases of sterile, genetically-modified or *Wolbachia*-infected male mosquitoes designed to suppress wild populations. The effectiveness of these strategies is contingent on a robust understanding of the ecology of the principal disease vectors, *Aedes aegypti* and *Aedes albopictus*. Experimental (Hancock et al., 2016) and theoretical (Yakob et al., 2008) work has highlighted the importance of ecological processes – such as density-dependent competition – in determining the efficacy of control.

*Aedes aegypti* originated in Africa, but has now become established in Asia and the Americas (Brown et al., 2014; Kraemer et al., 2015). It is a primary vector of many arboviral diseases, such as dengue, chikungunya and Zika (Black et al., 2002; Chouin-Carneiro et al., 2016). Female *Ae. aegypti* bite during the day and are highly anthropophilic (Scott and Takken, 2012). This means that the bed-net based biting-prevention strategies employed against malarial mosquitoes are ineffective against *Ae. aegypti*.

*Aedes albopictus* is a secondary vector of arboviruses originating from south-east Asia (Gratz, 2004). Invasive in much of its range, *Ae. albopictus* is capable of occupying more temperate environments, with a range extending northward to the USA and southern Europe (Kraemer et al., 2015). The range expansion of *Ae. albopictus* was facilitated by international shipping, where its dormant eggs can survive in transit, often in second-hand tyres (Delatte et al., 2009; Simard et al., 2005). *Ae. albopictus* is generally considered to have a preference for biting outdoors, only feeding opportunistically on humans (Paupy et al., 2009; Richards et al., 2006) (though see Ponlawat and Harrington (2005) and Delatte et al. (2010) for examples of *Ae. albopictus* anthropophily). Despite its more general host preferences, *Ae. albopictus* has still been implicated in several outbreaks, such as in Hawaii, China and Japan (Paupy et al., 2009). Particularly relevant to this study is the finding that female *Ae. albopictus* were more likely to become infected with dengue when they had experienced increased levels of intra- and interspecific larval competition (Alto et al., 2008). This highlights its potential as a disease transmitter, and has led to increasing concern that it could act as a maintenance or primary vector (Gratz, 2004; Paupy et al., 2010).

### Competing vectors

*Ae. aegypti* and *Ae. albopictus* are successful invasive species, both having established persistent populations on new continents (Brady et al., 2014). The two species have increasingly come into contact as *Ae. albopictus* expanded its range throughout the $20^{th}$ century. These species are known to share larval habitats of ephemeral freshwater pools. This direct niche overlap makes larval pools a forum for inter-species competition. It should be noted that the two species also compete through asymmetric mating interference (see Tripet et al. (2011)), that we do not examine here.

Historically, *Ae. aegypti* displaced *Ae. albopictus* from urban areas in Asia (Macdonald, 1956), such as in Calcutta (Gilotra et al., 1967). Braks et al. (2003) and Simard et al. (2005) document spatially segregated co-occurrence in Brazil and Cameroon respectively. The same segregation is documented on some islands, such as in Hawaii (Winchester and Kapan, 2013) and Reunion (Bagny et al., 2009), though declines (but not extinctions) of *Ae. aegypti* were also noted. More recent introductions of *Ae. albopictus* into *Ae. aegypti* occupied areas has resulted in a rapid displacement of *Ae. aegypti*. In the mid-1980s, the introduction of *Ae. albopictus* in Texas resulted in a rapid displacement of *Ae. aegypti* across the Southern States, with it persisting only in urban environments (O'Meara et al., 1995). Indeed, habitat preference studies suggest that *Ae. aegypti* more frequently occupies urban environments, while *Ae. albopictus* has a preference for more vegetated areas (Rey et al., 2006).

Several studies have attempted to determine which vector is the superior larval-stage competitor (reviewed in Juliano (2009)). Results are mixed, with some studies finding *Ae. aegypti* to be the superior competitor (Moore and Fisher, 1969; Moore and Whitacre, 1972) and other studies *Ae. albopictus* (Braks et al., 2004; Juliano et al., 2004; Reiskin and Lounibos, 2009). In general, there is a larger body of evidence (and field data) to

suggest that *Ae. albopictus* is a better larval-stage competitor (Lounibos and Juliano, 2018). Most crucial is evidence that the strength and directions of inter-species competition can be context-dependent. For instance, competitive outcomes have been found to change in response to different resource types (Barrera, 1996; Murrell and Juliano, 2008), temperatures (Farjana et al., 2012) and seasonality (Camara et al., 2016). Moreover it has also been shown that sympatric and allopatric populations of *Ae. aegypti* and *Ae. albopictus* can suffer from and exert different levels of interspecific competition (Leisnham et al., 2009). Context-dependent variation in the outcome of *Aedes* competition was corroborated by Juliano's 2010 meta-analysis of larval competition studies. He concluded that *Ae. albopictus* suffered less interspecies competition than *Ae. aegypti* in habitats with high-quality food, but that they were competitively equivalent in resource poor habitats. The fact that *Aedes* mosquitoes compete across heterogeneous, fragmented habitats, further complicate findings. Across a heterogeneous landscape, differences in competitive outcomes could allow for persistence in some areas but not others (Amarasekare, 2003; Juliano, 2009).

### Mechanisms of larval competition

Resource competition has long been considered the primary driver of intra- and interspecific larval competition between *Aedes* mosquitoes (Dye, 1984a). Indeed this mechanism has been represented as density-dependent competition in models of mosquito population dynamics (Dye, 1984b), including those aiming to inform optimal disease interventions (Bonsall et al., 2010; Yakob et al., 2008). The functions describing intra- and interspecific competition in such models can be parametrized by studies where single and mixed species cohorts are reared in different densities and measure the effects on life history parameters.

However, Heath et al. (*In review*) highlight that many mosquitoes-focused empiricists conflate the effects of larval resource availability with *all* density-dependant processes. That is to say that many studies hold feeding regimes constant across density treatments (e.g. Reiskin and Lounibos (2009)), reducing the per-captia resource availability (same resources, more individuals). The subsequent effects measured on survival/growth rates/fecundity are all then treated as the result of resource-mediated competition, aggregating other mechanism with it. This is important, as there are there are other mechanisms by which competition could occur. For instance, evidence from Moore and Fisher (1969) and Moore and Whitacre (1972) demonstrated that the development times of *Ae. albopictus* larvae in high-density mixed-species cohorts were significantly lengthened by increased densities of *Ae. aegypti*. As the larvae were not resource-limited, the authors attribute this to the production of a chemical compound termed a growth retardant factor, thought to be produced by *Ae. aegypti* at high larval densities (though this result could not be repeated by Dye (1982)). Alternatively, evidence from Dye (1984a) suggests that differences in development time could be attributed to the volume the larvae were reared in. This could be due to mechanical interference reducing feeding efficiency, or by jostling to reach the surface to breath.

We are motivated by the degree of uncertainty around the outcome of larval competition between *Ae. aegypti* and *Ae. albopictus*, and the mechanism by which this competition occurs. In this study, we manipulated

the conspecifc and heterospecific larval densities of *Ae. aegypti* and *Ae. albopictus*, and recorded the effect this had on larval survivorship and development time. Crucially, unlike many *Aedes*-focused competition studies, we adjusted the feeding regime so that the per-capita resource availability was kept constant across all density treatments. We specifically chose a feeding regime under which each larva *theoretically* had the necessary resources to successfully develop. This allowed us to comment on mechanistic aspects of larval competition, and better observe what components of competition were attributed to direct resource-mediated or interference- mediated competition.

## Methods

### Routine colony maintenance

Colony mosquitoes were kept at the Pirbright Institute in Surrey, UK. Rearing rooms were maintained at 25 ± 1 with a 16:8 light:dark cycle. Pirbright's *Ae. aegypti* colony was established from a line at the Liverpool School of Tropical Medicine, which was originally from West Africa (Macdonald, 1962). Eggs were placed in 150ml of reverse-osmosis water and vacuum hatched for at least one hour. First instar larvae were then transferred into bowls filled with approximately 1 litre of tap water, in densities of around 450 - 600 larvae per bowl. Larvae were fed 0.15–0.2g desiccated beef liver powder (NOW Foods, Bloomingdale, IL, USA) every two days, when the water was also changed. Pupated larvae were decanted into small 100ml tubs of water and placed inside 40cm$^3$ Bugdorm insect cages (MegaView Science, Taichung, Taiwan). Adults were maintained on room temperature 10% sugar solution on a cotton disk, and females fed defibrinated horse blood (TCS Biosciences, Buckingham, UK) using a Hemotek membrane feeding system (Hemotek Ltd., Great Harwood, Lancashire, UK). Tubs lined with damp filter paper were put in each cage after blood feeding for egg-laying.

The *Ae. albopictus* line was Italian, and founded from the Rimini strain described in Dritsou et al. (2015). The maintenance protocol was similar to the above, with the exception that *Ae. albopictus* eggs were hatched in a medium of water and 0.3% dried active yeast (Young's Home Brew Ltd., Bilston, West Midlands, UK).

### Experimental protocols

Single and mixed species cohorts of *Ae. albopictus* and *Ae. aegypti* larvae were reared under different density conditions. *Ae. aegypti* and *Ae. albopictus* from the colonies described above were used in the experiments. However, instead of hatching *Ae. albopictus* using yeast as per the routine protocol, they were hatched in the same way as *Ae. aegypti*. This kept the procedure consistent between species and ensured that the yeast did not supplement the resources available to *Ae. albopictus*. As this method differed from the standard hatching procedure for *Ae. albopictus*, the larvae of both species were left in the vacuum overnight to ensure there was a sufficient yield for the experiments.

Hatched first instar larvae were counted into 50ml Falcon conical centrifuge tubes (Corning, New York, USA) tubes filled to 49ml with water (1ml of food solution made this up to 50ml). The number of larvae in each tube corresponded to the density combinations given in Table 3.1. The density scale was chosen to give

roughly an even number of larvae per treatment while also covering a biologically relevant range. Density was manipulated by changing the number of individuals per tube while holding the volume of the tube constant (See Figure 3.1). Tubes for low density treatments therefore contained fewer individuals than for high density treatments, reducing the sample size of larvae. The lower-density tubes were therefore repeated so that the overall number of larvae experiencing each density condition was around 50 (the number in the highest density treatment). The densities given in the Table 3.1 were explored for each species in isolation (1:0), equal ratios of each species (1:1) and biased ratios (2:1 and 1:2, 1:3 and 3:1). The procedure described in Figure 3.1 was repeated twice for each ratio. For low-density, mixed-species treatments, some ratios could not be achieved with number of individuals in the tube (e.g. 4:3 can not be configured from 6 larvae). The density of these treatments was therefore increased slightly in order to allow for these configurations.

| | **density treatment** | | | | |
|---|---|---|---|---|---|
| | T1 | T2 | T3 | T4 | T5 |
| **Larvae per tube** | 6 | 16 | 28 | 38 | 50 |
| **Density** (larvae/ml) | 0.12 | 0.32 | 0.56 | 0.76 | 1 |
| **Volume** (ml) | 50 | 50 | 50 | 50 | 50 |
| **Number of tubes** | 10 | 3 | 2 | 2 | 1 |
| **Food per larva** (mg/larva/feed) | 0.55 | 0.55 | 0.55 | 0.55 | 0.55 |
| **Food per tube** (mg/tube/feed) | 3.3 | 8.8 | 15.4 | 19.8 | 27.5 |
| **Ratios** | 1:0, 0:1, 1:1, 2:1, 1:2, 3:4, 4:3, 3:1, 1:3 | | | | |

Table 3.1: A description of the density conditions (in larvae per millilitre) explored in each treatment (T1 - 5). The quoted ratios are those of *Ae. aegypti* to *Ae. albopictus*. Each condition/ratio combination was repeated twice. Tubes are repeated so that there were approximately 50 larvae subjected to each of the density treatments. Food treatments are scaled to the number of larvae in each pot (milligrams per pot, mg/pot) from the amount decided on in the pilot study. In low-density treatments, 6 individuals were insufficient to achieve the required ratios. We therefore increased the number of larvae to the minimum amount needed to make the ratio, and adjusted the feeding regime accordingly.

A pilot study (see the appendix) demonstrated that 0.55 mg of liver powder delivered on day 0, 2 and 4 post-hatching supported the successful development of an individual larva of either species in isolation. Liver powder was delivered as a dilution, mixed so that 1ml of food solution contained the correct concentration of food per-capita for each density treatment. When a larva pupated, it was decanted to a separate container with a small amount of water until emergence. We recorded the number of survivors and the development time of these survivors. The species and sex of the emerged adult was then determined. We took the development time of a larva to be from hatching to pupation. A summary of the experimental procedure is given in Figure 3.1.

### Analysis

We analysed the survival and development time data using Bayesian generalized additive (GAM) and generalized linear models (GLM). A total of 2435 larvae were analysed in the survival analysis, and 1489 larvae for

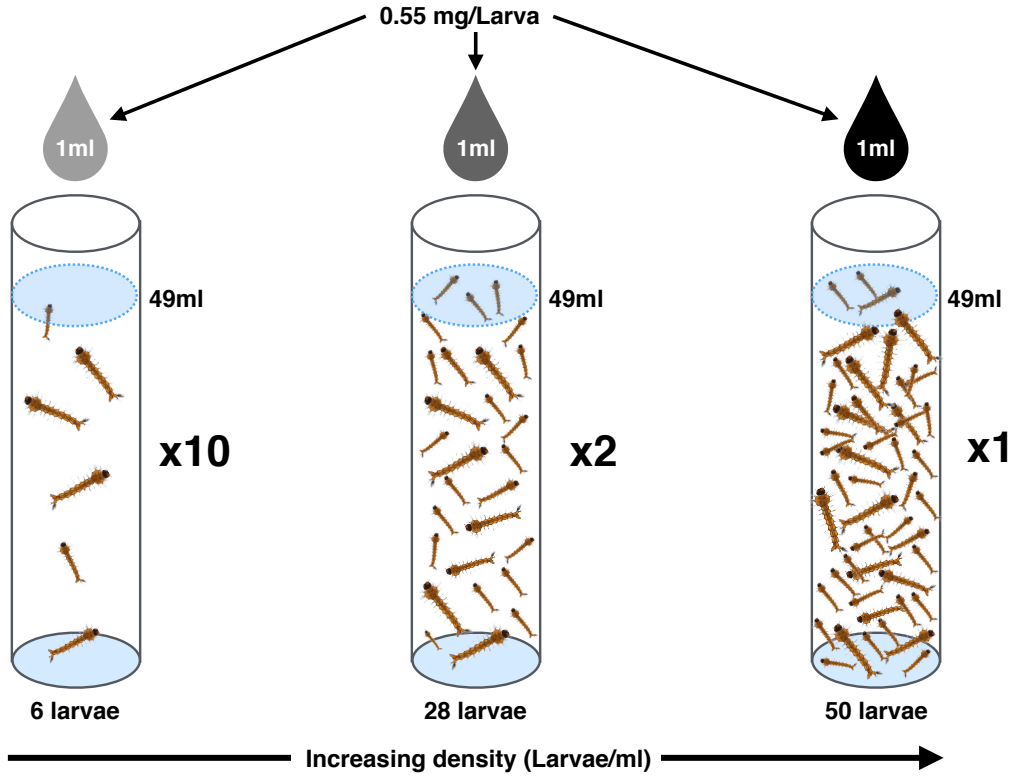



Figure 3.1: Summary schematic of the experimental design and procedure, shown for a 1:0 species ratio and 3 of the 5 density treatments tested. Falcon tubes were filled with reverse-osmosis water to 49ml, then made up with a final 1ml of a food dilution. Food dilutions were mixed so that 1ml held 0.55mg per larva in suspension for each treatment (therefore a higher concentration was needed to cater for more larvae in higher density treatments). A further 1ml was added on day 2 and 4 of development. A number of larvae corresponding to one of the densities (6, 16, 28, 38 and 50 larvae for 0.12, 0.32, 0.56, 0.76 and 1 larvae per ml) were hatched and added to the falcons using a pipette. As the low density treatment contained only 6 larvae and the high density 50, it was necessary to repeat these tubes 10 times to achieve a similar sample size. All density treatments were repeated so that there were around 50 individuals experiencing each treatment. Pupated larvae were counted every day, and were removed and decanted to a small water filled tube until emergence. The emerged adults were sexed and identified to species level (for mixed species experiments). This procedure was repeated twice for each of the species ratios in Table 3.1.

development time (as only surviving larvae could be analyzed). These statistical models were written and fit in JAGS (v4.3) (Plummer, 2003), a Bayesian inference package for the statistical software R (v3.4.2) (R Core Team, 2019). All models mentioned hereafter were run across four chains for a minimum of $2x10^5$ iterations, with every second sample discarded to reduce autocorrelation. Chains were continued for additional iterations if they had not yet converged (until the potential scale reduction factor was $< 1.02$). For all models, parameters were given appropriately diffuse priors centred on zero, unless the pilot studies could be in some way informative (see appendix Table B.1).

### Survival

The survival data were modelled as either a binomial distribution or hierarchical beta-binomial distribution. The latter was included after initial inspection of the data showed that the proportions of larvae surviving in tubes undergoing the same density treatment varied. A beta distribution accounts for this variance, and could better explain the data. A binomial regression would model the number of survivors ($S$) from the total

number ($N$) in the $i^{th}$ tube as the outcome of a binomial distribution with a probability $p$:

$$S_i \sim Binomial(p, N_i)$$

The probability $p$ is written as a function of explanatory variables (say a vector of predictors $X$) ($p = f(X)$). A logit-link was used to bound $p$ between zero and one ($logit(M) = f(X)$).

In the case of the beta-binomial distribution, the probability is given by a beta distribution with with two shape parameters, $s_1$ and $s_2$:

$$p \sim Beta(s_1, s_2)$$

This beta distribution is re-parametrized in terms of the mode of the distribution, for the following two reasons. First, neither $s_1$ or $s_2$ describe a useful property of the beta distribution (e.g. mean, standard deviation) to write as a function of covariates. Second, the mode is a far better description of skewed distributions than other statistics such as the mean, which can be heavily influenced by "long tails". The re-parametrization is as follows, with the mode $M$ and a certainty parameter $\theta$ (Kruschke, 2015):

$$s_1 = M(\theta - 2) + 1$$

$$s_2 = (1 - M)(\theta - 2) + 1$$

In this case the mode $M$ is written as as a function of the covariates ($M = f(X)$). A logit-link was used to bound the mode between zero and one ($logit(M) = f(X)$).

Exploration of the survival data showed some evidence that the survival probability might vary as a non-linear function of *Ae. aegypti* and *Ae. albopictus* density. Generalized additive models (GAMs) use data-derived splines to fit smoothed non-linear responses to continuous explanatory variables (Wood, 2006). As they are derived from the data, these splines are not constrained in the same way higher order (e.g. quadratic) interaction terms in GLMs. We therefore included smoothed responses in both the binomial and beta-binomial models in addition to the linear terms. GAM terms can be estimated in a Bayesian framework by modelling the smoothing parameters as random effects, where each smoothing parameter comes from a the same normal distribution with an estimated standard deviation (Crainiceanu et al., 2005). We used 5 knots for our splines, one per sampled point on the density scale.

### Development time

We modelled the development times as a gamma distribution (positive continuous values). As with the beta distribution, the shape and rate parameters of the gamma distribution do not describe any useful property to model as a function of the covariates. Additionally, when close to zero, the gamma distribution can be skewed. We therefore re-expressed the shape ($k$) and rate ($r$) parameters of the gamma distribution in terms of the mode, $M$, and standard deviation, $\sigma$ (Kruschke, 2015)

$$r = \frac{M + \sqrt{(M^2 + 4\sigma^2)}}{2\sigma^2}$$

$$k = 1 + Mr$$

where the mode is written as a function of explanatory variables with a log-link, to ensure the mode is positive ($log(M) = f(X)$). The form of $f(X)$ was assumed to be a standard linear model, as there was no evidence of non-linearity beyond that afforded by the link function.

## Selecting predictors and model structures

### Gibbs variable selection

Thoroughly exploring all biologically relevant combinations of predictors can be extremely time consuming, particularly when dealing with multiple categorical interactions. For instance, development time can be explained by two categorical variables, species and sex, and two continuous variables, *Ae. aegypti* and *Ae. albopictus* density. To test the full model space, it would be necessary to explore all second and third order interactions between these terms (this is similarly the case for survival, less the sex variable). We therefore opted to use Gibbs variable selection (GVS), which combines model estimation and variable selection into the same step (Tenan et al., 2014).

In brief, GVS adds a set of binary variables to the model, which are capable of turning individual parameters on and off during optimisation. As an example, we could write a generic response variable $y$ as being predicted by $p$ predictors. This model could be written in matrix form, using a vector of parameters $\beta$ (length $N$) and a design matrix, $\mathbf{X}$

$$y = \sum_{j=1}^{N} \beta_j \mathbf{X_j}$$

In the case of GVS, a column vector of binary indicator variables, $\gamma$ is added, where $\gamma \in \{0, 1\}$. Each element of $\gamma$ corresponds to a parameter in $\beta$.

$$y = \sum_{j=1}^{N} \gamma_j \beta_\mathbf{j} \mathbf{X_j}$$

The state of each element of $\gamma$ denotes whether a predictor should be included in the model (1), or excluded (0). Each element of $\gamma$ is assigned an unbiased 50:50 *Bernoulli* prior (i.e. there is a prior probability of 0.5 of any one parameter being included). The frequency with which combinations of model variables are activated can then interpreted as the preference for including predictors.

In our case, this procedure is complicated by the inclusion of two and three way categorical interactions with hereditary constraints (the constituent, lower-order terms of an interaction must also be included in the model). The priors for the $\gamma$ terms corresponding to the interactions were therefore written as the multiple of the states of the lower order terms ($\gamma_i \sim Bernoulli(\gamma_j \pi_i)$, where $j$ denoted a lower order term on which

the higher order term, $i$, depends). This ensured that the state of the interaction indicator could only be one ($\gamma_i = 1$) if the lower order terms were also active ($\gamma_j = 1$). This does however make higher order interactions inherently less likely to be included (Kruschke, 2015), though this is not necessarily undesirable for high order interactions terms should only be included with strong support.

Our implementation of GVS also makes use of pseudo-priors, as suggested by Dellaportas et al. (2000). Pseudo-priors are priors which are do not affect the posterior distribution of the estimated parameters, instead they are designed to improve the performance of the MCMC sampler itself. Pseudo priors were taken from an initial model run where all indicator variables were set to 1. This model was therefore the "full model", with a posterior estimates obtained for each parameter. These posteriors are then used as pseudo-priors, where they are only active when $\gamma_j = 0$. Otherwise (i.e. when the parameter is active and being optimised) the standard prior is used. This can be written, for a normally distributed parameter, with the mean and standard deviation either given as pseudo-priors from an initial model run ($\overline{\mu}$ and $\overline{\sigma}$) or as the actual priors ($\mu$ and $\sigma$) depending on the state of $\gamma$

$$Pr(\beta_j \mid \gamma_j) \sim \mathcal{N}(\gamma_j\overline{\mu}_j + (1-\gamma_j)\mu_j, \gamma_j\overline{\sigma}_j + (1-\gamma_j)\sigma_j)$$

Where $\beta_j$ is an element of the parameter vector, and $\gamma_j$ the corresponding element of the vector of binary variables. The motivation for using pseudo-priors is to encourage the sampler to frequently turn model parameters on and off in order to thoroughly explore the model space. This is desirable as certain parameter combinations may be sampled less solely because the likelihood surface is very uneven, not because the model is not a good fit to the data. Pseudo-priors prevent this by sampling from the posterior estimate of the a parameter (the pseudo prior) when it is inactive and encourage it to switch the parameter on (the posterior will clearly be more likely than the uninformed prior). Turning the parameter back on, the prior returns to the "true" value and the model is estimated as normal.

### Product space method

GVS is useful for selecting predictors as the full model space does not need to be *explicitly* specified, saving time and effort. It is however not suited to the comparison of different model *structures* and *distributions* (such as the binomial and beta-binomial being compared for the survival data). Bayes factor can be used to compare the likelihood of the data under two statistical models, even when they are not nested. Models are assessed on the prior-weighted average of how well they fit the data, over the whole parameter space (Lodewyckx et al., 2011). Complexity is implicitly penalised by this averaging, as models with many poorly fitting parameters will perform worse in aggregate than a model with a few well fitting parameters. The product space method (PSM) is a way of obtaining a Bayes factor to compare between model structures.

Lodewyckx et al. (2011) explain how the PSM can yield the Bayes factor for multiple models. They suggest that all models should be fit simultaneously as part of an aggregate model, with a stochastic categorical

distribution coded to select which model is active. The frequencies with which each model is selected to explain the data is then a measure of the Bayes factor. The use of pseudo priors is suggested in order to promote switching, and they operate in the same way as those in GVS. Pseudo priors are obtained by optimizing each model separately, obtaining posteriors for each. As before, the pseudo priors do not affect the likelihood, and there therefore do not influence the posterior directly. They are included solely to improve the performance of the sampler itself, and promote frequent switches. Other checks recommended in Lodewyckx et al. (2011) were also carried out to ensure that Bayes factor estimates were robust. A preferred model was chosen based on the thresholds given in Raftery (1995).

All parameter estimates and predictions are presented as medians, with 95% highest density intervals (HDI's) as a measure of uncertainly. We elected to use HDI's as they are less misleading than symmetric quantiles when describing skewed sample distributions, as can be produced by MCMC methods (Kruschke, 2015). HDI's correspond to a range across which 95% of the probability mass of a sample falls, and is therefore an intuitive metric of uncertainty.

## Results

### Survival

GVS yielded optimal predictor combinations for the two candidate model structures (the binomial and the beta-binomial). These GVS results are reported in full in appendix Tables B.2 and B.3. The two best models from the GVS were then compared using the product space method. This yielded a log Bayes factor strongly in favour of the beta-binomial model ($log(BF_{12}) = -36.54$). The hierarchical beta-binomial structure was therefore selected as the best model.

This model included a species-specific intercept, a species-specific response to *Ae. aegypti* density and a species-agnostic response to *Ae. albopictus* density. Notably, none of the non-linear (GAM-type) responses were included in the final model, implying that the process could adequately be captured by a linear response. This combination of predictors was selected in 33.51% of $4x10^6$ iterations, with the next nearest parameter combination at 24.20% (see Table B.3 for full GVS results). Parameter estimates for this model are given in Table 3.2 and shown in appendix Figure B.3.

In the lowest density single-species treatments, *Ae. aegypti* was 6.58% [0.76, 15.89] more likely to survive than *Ae. albopictus*. *Ae. albopictus* survivorship declined in response to *Ae. aegypti* density, and did so more severely than *Ae. aegypti* in response to conspecific density. Across the density range, the estimated intraspecifc response of *Ae. aegypti* was a reduction in survival probability of 17.36% [5.69, 29.33], while the interspecifc response of *Ae. albopictus* was a reduction of 37.99% [21.67, 52.01]. The species did not differ in how they responded to *Ae. albopictus* density, with the intraspecific response of *Ae. albopictus* and interspecific response of *Ae. aegypti* being a 22.81% [10.98, 34.65] reduction in survival probability. Figure 3.2 shows the effect of conspecific density on the survival probability of both species (intraspecific competition), while Figure 3.3 shows the effect of both conspecific and heterospecific density (intraspecific *and* intraspecific).

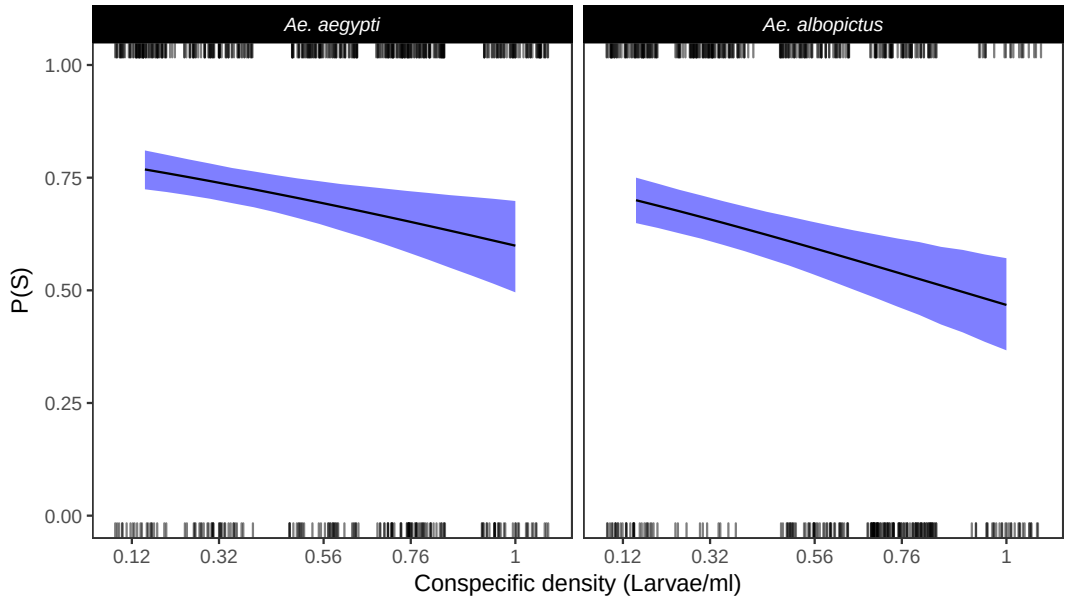



Figure 3.2: Model fit for the beta-binomial model of the survival data. Data are shown as jittered tick marks on the floor (deaths) and ceiling (survivors). Both species respond linearly to conspecific density (as no non-linear generalized additive model terms were retained through GVS). *Ae. albopictus* responds more strongly to conspecific density than *Ae. aegypti* (17.36% [5.69, 29.33] reduction versus 22.81% [10.98, 34.65]).

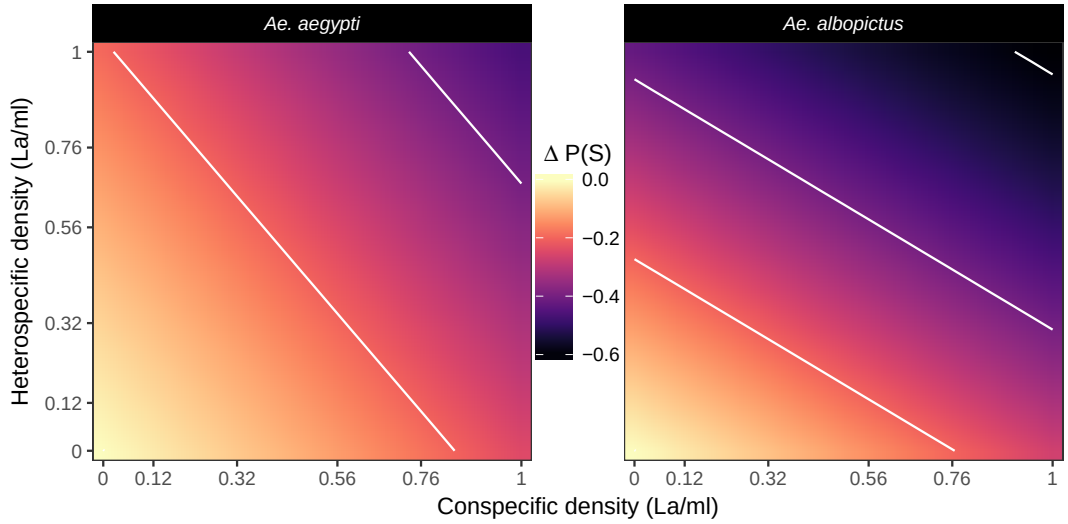



Figure 3.3: Changes in the survivorship predicted by the beta-binomial survival model across the combinations of density conditions outlined in Table 3.1. The intraspecific responses run along the x-axis and the interspecifc response along the y-axis. Off-axis values are the additive combinations of inter- and intraspecific competition. Values are expressed as the difference from the baseline survival probability (Δ P(S)), which is the probability associated with the bottom left hand corner in each panel. Contour lines delineate 20% decreases in survival probability, with colder colours indicating decreases in survival.

| parameter | median | lower 95% - upper 95% |
|---|---|---|
| ***Ae. aegypti*** | | |
| Intercept | 1.34 | 1.04 to 1.65 |
| Intraspecific | -0.94 | -1.55 to -0.33 |
| ***Ae. albopictus*** | | |
| Intercept | 1.02 | 0.73 to 1.31 |
| Interspecific | -1.83 | -2.71 to -0.96 |
| **Both species** | | |
| *Ae. albopictus* density | -1.15 | -1.70 to -0.60 |
| $\theta$ (certainty parameter) | 22.94 | 16.57 to 30.86 |

Table 3.2: Parameter estimates for the beta-binomial model of the survival data, after GVS. Values are quoted as the medians, with the 95% highest density intervals also given. Values are given for each species if there was species specific response included in the final model. Note these values are on a logit scale. Note that the value for *Ae. albopictus* density is the intraspecific density for *Ae. albopictus* and interspecific competition for *Ae. aegypti*.

### Development Time

The most frequently selected model during GVS was one including a species- and sex-specific adjustment to the intercept as well as species-specific response to *Ae. aegypti* density, *Ae. albopictus* density and the *interaction* between these two densities. This model was selected in 22.92% of $4x10^6$ iterations, with the next nearest model at 21.95% (8.70% after that). The full GVS results are given in appendix Table B.4. This next nearest model excluded the interaction term and the species-specific response to either density, meaning it was nested in the former. As these two models were selected with a comparable frequency and therefore had similar support, we compared these two models using the product space method to further assess the performance of each model. The Bayes factor supported the more complex model ($log(BF_{12}) = -0.795$), which included the species specific effects and interaction.

Parameter estimates are given in Table 3.3 (and shown in appendix Figure B.4). The development times of surviving *Ae. aegypti* in the lowest density treatment were 15.52% [11.84, 19.30] faster than those of *Ae. albopictus*. Surviving females of both species took 7.85% [5.86, 10.01] longer to develop than males. Increasing densities of conspecifics led to faster development times for both species, but far less so for *Ae. aegypti*. Across the density range intraspecific competition reduced development times by 8.37 % [4.00, 12.61] for *Ae. aegypti* and 16.14 % [11.19, 20.72] for *Ae. albopictus*. Interspecific competition resulted in the survival of faster developing larvae; pupation occurred 10.86% [0.53, 20.30] faster for *Ae. aegypti* and 25.39% [14.98, 34.92] for *Ae. albopictus*. The intraspecific effects are illustrated in Figure 3.4, and the combined intra- and interspecific effects in Figure 3.5.

Interestingly, the interactive effect of density for *Ae. aegypti* was estimated as being tightly centred on

| parameter | median | lower 95% - upper 95% |
|---|---|---|
| ***Ae. aegypti* males** | | |
| Intercept | 2.01 | 1.98 to 2.04 |
| Intraspecific density | -0.10 | -0.15 to -0.05 |
| Interspecific density † | -0.12 | -0.29 to 0.05 |
| Density interaction † | -0.01 | -0.06 to 0.03 |
| ***Ae. albopictus* males** | | |
| Intercept | 2.17 | 2.14 to 2.20 |
| Intraspecific density | -0.20 | -0.27 to -0.14 |
| Interspecific density | -0.47 | -0.68 to -0.26 |
| Density interaction | 0.11 | 0.06 to 0.16 |
| **Both species** | | |
| Sex (female) | 0.08 | 0.06 to 0.10 |
| $\sigma$ (standard deviation) | 1.48 | 1.42 to 1.53 |

Table 3.3: Parameter estimates for the gamma-distributed GLM for development time, following GVS and comparison by the PSM. Values are quoted as the medians, with the 95% highest density intervals also given. Values are given for each species where there are species specific responses. All values are on a log scale. The predictor for the interaction term was multiplied by 10 to keep it on the same scale as the two independent densities, so the effect size is directly comparable. † symbols denote parameters with intervals that cross zero. These have been retained due to hereditary constraints in predictor selection.

zero (-0.01 [-0.06, 0.03], log scale), meaning that it did not respond differently to combined higher densities of both species. In contrast, the interactive response of *Ae. albopictus* was strongly positive (0.11 [0.06, 0.16], log scale). Extrapolating the model, it predicts that at the maximum *combined* densities of both species, surviving *Ae. albopictus* would take 59.11 % [11.03, 109.54] *longer* to develop compared to the lowest density treatment. This is contrary to the faster development time observed when responding to conspecific and heterospecific density in isolation. The interactive effect is observable in Figure 3.5, towards the back right corner of the *Ae. albopictus* panels.

## Discussion

As vectors of diseases such as dengue and Zika, the ecology of *Aedes* mosquitoes is of the utmost importance for predicting vector occurrence, disease incidence and the efficacy of interventions. Our study aimed to quantify the effects of inter- and intraspecifc competition on the survivorship and development time of larvae under a particular per-capita feeding regime. We find that *Ae. aegypti* suffered intra- and interspecific competition to a lesser extent than *Ae. albopictus*. Indeed, effect sizes were very small for *Ae. aegypti* (particularly for development time) whereas *Ae. albopictus* suffered higher mortality and took longer to develop when in high conspecific and heterospecific densities. However, the fact we observe any effect is of note, as the larvae were fed per-capita, and at a level which *could* have supported the successful development of *all* larvae. The higher

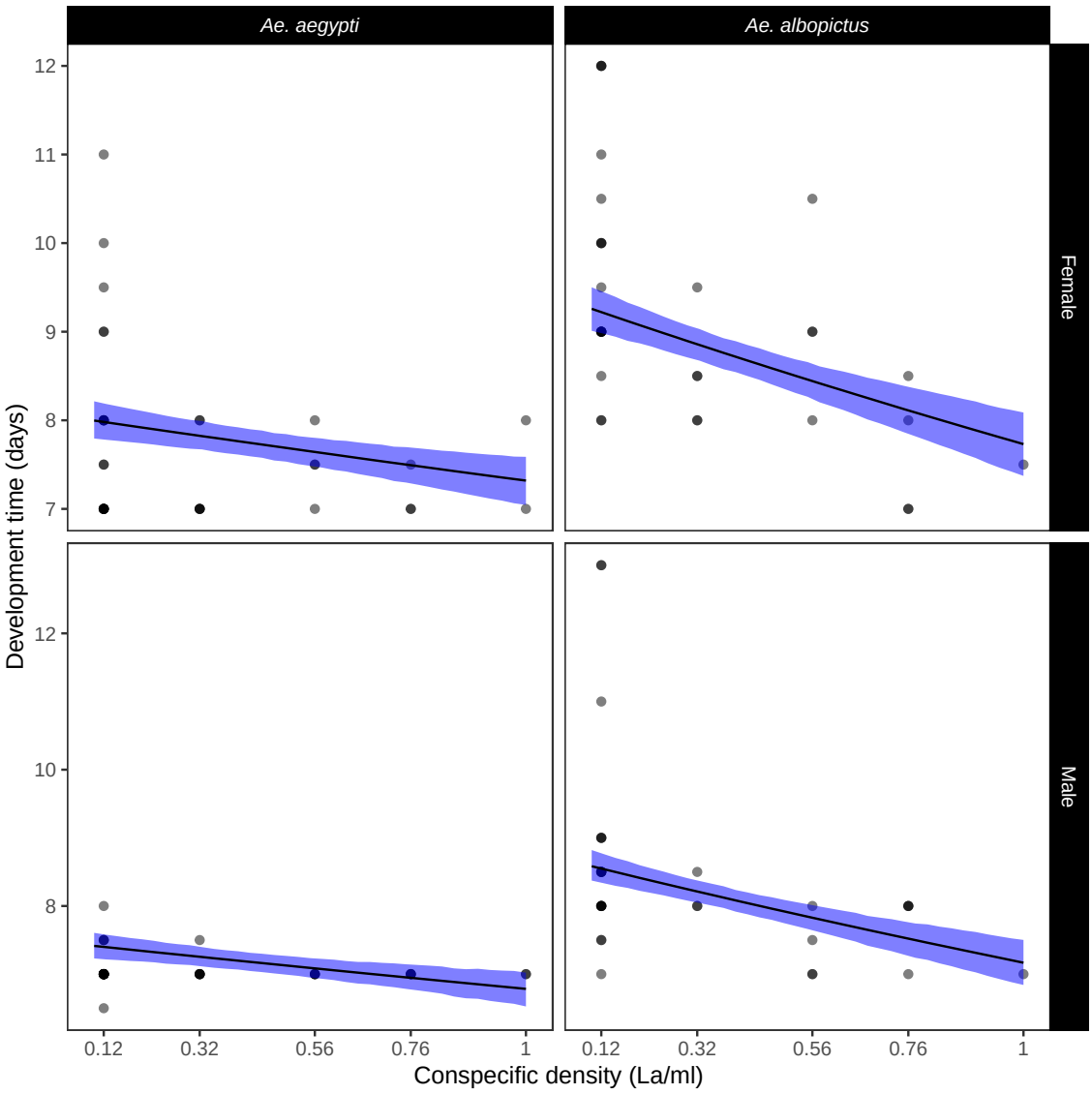



Figure 3.4: Model fit for the gamma-distributed model of the development time data. This figure shows intraspecific competition for both species. Evident is the slower baseline development time of *Ae. albopictus* (15.52 % [11.84, 19.30] slower), and marginally slower development of females for both species (7.86 % [5.86, 10.01]). Note that there is no sex-specific gradient, only an adjustment to the intercept. Across the range of densities, development times are reduced by 8.37 % [4.00, 12.61] for *Ae. aegypti* and by 16.14 % [11.19, 20.72] for *Ae. albopictus*.

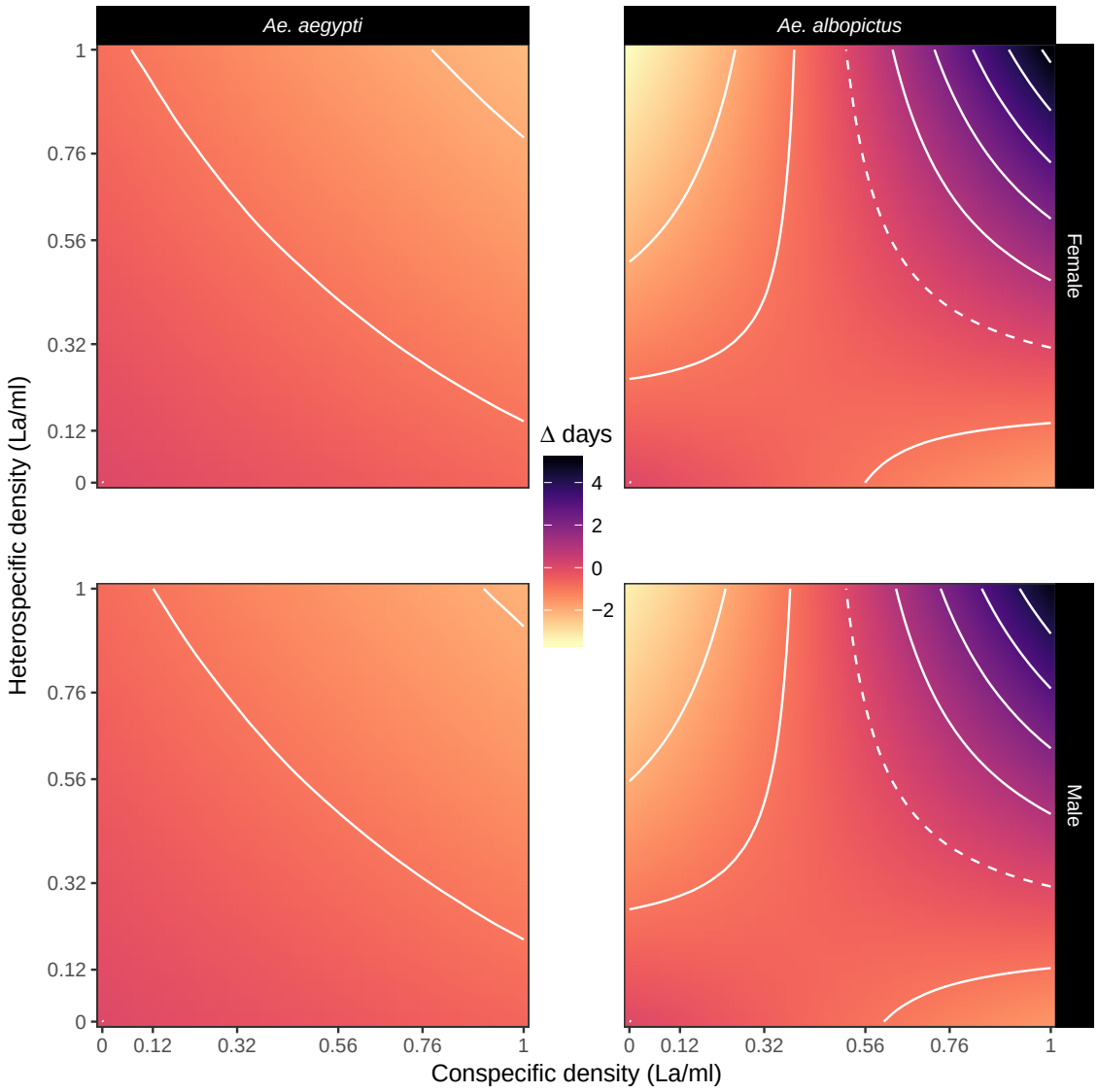



Figure 3.5: Changes in the predicted development time (Δ days) across the combinations of density conditions outlined in Table 3.1. Within-species competition is shown along the x-axis and between-species on the y-axis. Values are expressed as the differences from the intercept development time in each panel (the development time associated with the bottom left hand corner of each panel). Colours warmer than the zero mark in the legend indicate decreases in development time, while colder colours indicate increases in development time (compared to the bottom left-hand value). Contour lines delineate changes of 2 days, with the dashed contour the zero mark. There is notably little change in the development time of *Ae. aegypti* across the surface (smaller effect sizes), with no interactive effects of density. In contrast, surviving *Ae. albopictus* larvae were those who developed faster in response to hetero- and conspecific density, albeit to a greater extent for heterospecifics. However, the positive interactive effects of density on *Ae. albopictus* development time mean the model predicts slower development when densities of conspecifics *and* heterospecifics are high. Differences between males and females are minor, and determined only by the shift in the intercept (there were no sex-specific responses to density).

baseline survivorship of *Ae. aegypti* is consistent with historic lab studies (Macdonald, 1962) and studies using a similar food resource (Barrera, 1996), but not other studies using other food types (Juliano et al., 2004). There was no support for a species-specific response of survivorship to *Ae. albopictus* density, indicating that the strength of intraspecific competition in *Ae. albopictus* is equal to the effect of interspecific competition on *Ae. aegypti*. The same is not true for the response to *Ae. aegypti* density, where there is a greater effect of interspecific competition on *Ae. albopictus* than intraspecific competition on *Ae. aegypti*. The findings for survivorship run somewhat contrary to other competition studies, where the effects of interspecific competition are usually greater for *Ae. aegypti* (Juliano et al., 2004; Reiskin and Lounibos, 2009) or neutral (Black et al., 1989). This could be explained by the use of liver powder as our choice of larval resource, as this has been known to favour *Ae. aegypti* (Barrera, 1996). Alternatively, this could be the result of strain-specific properties (Dye, 1984a).

The superiority of the beta-binomial model structure in explaining the survivorship data tells us that an additional second-level process was required to account for the variance in larval survival between tube replicates. This variance could either be "true" demographic variance in survival or "error" variance caused by our experimental setup across tubes and replicates (miscounts of larvae, food dilutions). Should it be the former, this is indicative of interesting features of larval demographic variation. In low-density treatments there were fewer individuals, a difference which we accounted for by repeating these tubes (so that the numbers per treatment were the same). However, we could not control for the demographic make-up of mosquitoes in each tubes, and therefore the dynamics in low-density tubes will be affected by the range of larval phenotypes expressed in this relatively small sample of individuals. For instance, if each larva has a certain capacity to respond to conspecifc and heterospecifc density (e.g. increased resource uptake), then in a small cohort a *single* larva capable of outperforming the others would have a profound effect on the density effects observed in the tube. Individual phenotypes are known to generate the population dynamics we observe (Sumpter and Broomhead, 2001), and it is of note that in smaller cohorts of mosquitoes variation in processes such as survival could shape the observed patterns of persistence and abundance. This evidence suggests that demographic processes could be important in the overall dynamics of mosquito populations at low larval densities.

Across the combinations of densities, surviving *Ae. aegypti* larvae developed more quickly than *Ae. albopictus*. For both species, the surviving larvae were those that developed most quickly. This suggests that the surviving larvae either accrued the necessary resources to pupate faster than competitors, or had a lower resource threshold for pupation. *Ae. aegypti* development times changed only marginally, whereas *Ae. albopictus* did so to a far greater extent.

Of most interest is the observation that *Ae. albopictus* larvae which survived in treatments with high densities of conspecifics *and* heterospecifics developed more slowly. This is the opposite of its response to intraspecific competition, where faster-developing larvae were those that survived. It could be the case that slowly developing individuals are able to cannibalise deceased larvae which break down over time (dead larvae were not removed during counts). It is known that invertebrate carcasses can be a food source for larvae

(Daugherty et al., 2000), so perhaps some *Ae. albopictus* larvae are "playing the long-game", and benefiting from the delayed release of this additional resource. The longest development times for *Ae. albopictus* also occur under conditions where the mortality of both species is highest, meaning the number of carcasses would also be highest. This fits with evidence that *Ae. albopictus* is better able to survive periods of starvation (Barrera, 1996). While the chemical retardant hypothesis (Moore and Fisher, 1969; Moore and Whitacre, 1972) has received little recent attention, it is worth mentioning that this mechanism could also account for the delayed development time observed in *Ae. albopictus*.

Our study is novel in that our feeding regime was adjusted for each density treatment so that the per-capita resource availability was the same. From our pilot studies we knew that this amount was sufficient for a larva of either species to pupate. Despite the larvae of both species feasibly being able to pupate on the available resources, many did not, especially for *Ae. albopictus* at high densities. The implication is that non-pupating larvae were not getting the threshold resources required to become pupae. This could be attributed to con- and heterospecifics taking more than the "allotted" 0.55mg per larva. Interestingly, this could point to the rate and degree of resource uptake being mediated by the density of other larvae – both of the same and different species. It would seem that *Ae. aegypti* is better able to alter these resource seeking/uptake parameters than *Ae. albopictus*, as it suffers fewer deaths as a result of competition. Had our study provided even more food per-capita, it is possible that the effects of competition would have been ameliorated. This is because there may come a level of food availability where even significant changes in the rate and extent of uptake by larvae would not be sufficient to inhibit competitors. Repeating this experiment at a greater range of per-capita feeding regimes is certainly an avenue worth pursuing.

These penalties in survivorship are therefore likely to be a manifestation of contest competition, whereby the uptake of resources by the faster developing larvae results in the death of slower developing larvae who never gain the requisite resources for pupation. In contrast, if all larvae expressed the same resource seeking and accruing behaviours that they had in isolation, there would have been sufficient food for all to pupate.

It is noteworthy that in a single-species example (using only *Ae. aegypti*), Heath et al. (*In review*) did not find an effect of conspecific density on either survival and development time using this exact feeding regime. The only difference between the experiments was the type and volume of containers used to rear the larvae. This may allude to an effect of habitat volume and surface area, with individuals potentially competing for space, and access to the surface to breathe. Smaller containers with smaller surface areas may amplify the behavioural responses, leading to the outcomes described above. Such mechanisms have been suggested in the past (Dye, 1984b), and further emphasise the extent to which habitat properties can alter competitive outcomes.

## Conclusion

When seeking a consensus from competition experiments between *Ae. aegypti* and *Ae. albopictus*, Juliano (2009) and others found that competition was context dependent. Outcomes varied across gradients of habi-

tat resource availability, temperature and constancy. It was therefore never the case that any one study could *fully* explain the competition between these two species. However, our study contributes a unique insight into the consequences of competition under this specific feeding regime. The results show how these larvae could potentially alter the rate and extent of resource uptake to the detriment of their peers. We also provide evidence of an interactive effect on *Ae. albopictus* development time, which we suggest could be mediated by mechanisms other than resource uptake, such as cannibalism or chemical interference. Our model selection revealed that our survival data were over-dispersed, which highlights the importance of demographic processes in driving variation in population-level processes at low densities. We add to the broader understanding of how within and between species competition can be driven by both resource mediated and resource independent processes, and give insight into the degree to which even relatively simple organisms can display a diverse range of responses to increased densities of competitors.

# 4 | TEMPERATURE-DEPENDENT COMPETITIVE OUTCOMES DRIVE THE DISTRIBUTION AND EPIDEMIOLOGY OF THE ARBOVIRUS VECTORS *AEDES AEGYPTI* AND *AEDES ALBOPICTUS*: PREDICTIONS FROM A MATHEMATICAL MODEL

The epidemiology of arboviruses is inextricably linked to the ecology of the *Aedes* mosquitoes that transmit them. *Aedes aegypti* and *Aedes albopictus* are the principle vectors of viruses such as dengue and Zika, and their global distribution is shaped by both climate and between-species competition. Interspecific competition has resulted in displacements of these *Aedes* species in the wild, but studies aiming to identify the better competitor have found that the strength of competition is context-dependent. Many models of interspecific interactions average over species-specific responses to climate, analysing the outcomes of competition at a steady-state. We therefore create and analyse a temperature-dependent model of *Aedes* population dynamics and epidemiology, which includes interspecific interactions in the form of resource competition (as larvae) and reproductive interference (as adults). Our simulations suggest that climate drives both population dynamics and epidemiology, which interact to produce complex patterns of disease outbreaks impossible to predict with simpler models. *Ae. albopictus* was predicted to exclude *Ae. aegypti* through competition for relatively small costs to heterospecifics from larval competition. Notably, this competitive difference is exacerbated in climates where *Ae. albopictus* has previously displaced *Ae. aegypti*. The effects of reproductive interference are more complex; as more mating attempts fail due to exposure to heterospecific adults, this can lead to *increases* in adult population sizes. This is a manifestation of the so-called hydra effect, which results from alleviating strong within-species larval competition. The hydra-effect is, however, mitigated by the inclusion of interspecific larval competition. Uniquely, our model quantifies how temperature affects the outcomes of competition between *Ae. aegypti* and *Ae. albopictus* by mediating complex interactions between larval competition and reproductive interference. This work has significant implications for vector distributions and control under anthropogenic climate change.

**Contributing authors**: Paton R.S. and Bonsall, M.B.

## Introduction

Arboviruses (arthropod-borne viruses) are a tremendous public health concern. It is estimated that a staggering 96 million people present symptoms of dengue infection every year (Bhatt et al., 2013). The outbreak of Zika virus in Brazil focused global attention and stoked the appetite for cohesive and comprehensive efforts towards disease mitigation (Faria et al., 2016; Yakob and Walker, 2016). Crucially, the distribution and prevalence of these pathogens is inextricably linked to the ecology of the *Aedes* mosquitoes that transmit them (Brady et al., 2014; Kraemer et al., 2015).

Interspecific interactions are critical in determining the distribution and abundance of animals (Morin, 2011) and are known to occur between *Aedes* species (Juliano, 2009). The strength of interactions can vary across gradients of abiotic (e.g. temperature, precipitation) and biotic (e.g. predator abundance) conditions. These abiotic conditions can vary across space and through time, potentially facilitating the coexistence of ecologically similar species in a community (Chesson, 2000). As ectotherms, mosquitoes exhibit a number of species-specific temperature-dependent traits (Brady et al., 2014, 2013; Mordecai et al., 2017). These traits are ecological (such as larval survival, development time, fecundity, adult lifespan) and epidemiological (such as extrinsic incubation period, infection probability and dissemination frequency). By affecting both vector abundance and transmission dynamics, temperature is pivotal in driving the transmission of vector-borne diseases such as dengue, Zika and chikungunya (Mordecai et al., 2017). As temperatures vary through seasons and are altered by anthropogenic climate change, the question of how temperature could affect the outcomes of competition between mosquito species is paramount. In this paper, we present a mathematical model of the temperature-driven competitive dynamics between the prolific arbovirus vectors *Aedes aegypti* and *Aedes albopictus*.

### The vectors — *Ae. aegypti* and *Ae. albopictus*

*Ae. aegypti* is considered the primary vector of arboviruses, particularly in urban settings (Black et al., 2002; Chouin-Carneiro et al., 2016; Yang et al., 2014). From its home range in Africa, *Ae. aegypti* spread aboard ships and established across much of the tropical West from the fifteenth century onward (Lounibos and Juliano, 2018). Many *Ae. aegypti* populations have evolved to strongly favour human hosts, biting and resting indoors in close proximity to humans (Scott and Takken, 2012). *Ae. albopictus* spread from Asia during the $20^{th}$ century, arriving in new regions via international shipping (Lounibos and Juliano, 2018). It does not always show a strong preference for human hosts, however it has been implicated in arbovirus outbreaks (Delatte et al., 2010; Paupy et al., 2009). As ectotherms, the reproduction and survival of both species is temperature limited, with ranges largely restricted to tropical and sub-tropical regions. However, *Ae. albopictus* is better able to endure colder climates as it can enter a period of embryonic diapause (Diniz et al., 2017). The global range of the *Ae. albopictus* therefore extends into more temperate regions (Kraemer et al., 2015).

As both *Ae. aegypti* and *Ae. albopictus* have established in new regions and share an ecological niche, a range of competitive outcomes (coexistence, exclusion and habitat segregation) have been observed (Louni-

bos and Juliano, 2018). These outcomes have been reviewed in detail by Lounibos and Juliano (2018); the most common result is the decline of existing populations of *Ae. aegypti* with the arrival of *Ae. albopictus*. This frequently leads to spatially-segregated, sympatric populations of *Ae. aegypti* and *Ae. albopictus*, with the former residing within a restricted niche. For instance, existing *Ae. aegypti* populations in the Southern USA were rapidly displaced by *Ae. albopictus* when it arrived in the mid-1980s; *Ae. aegypti* is now primarily restricted to large cities (O'Meara et al., 1995). Evidence from Florida suggests that habitat preference facilitates segregated coexistence, as *Ae. aegypti* has a preference for urbanised areas while *Ae. albopictus* prefers environments with more vegetation (Lounibos et al., 2016; Rey et al., 2006).

Both mosquitoes share the same general life-history (Nelson, 1986). Females take one (or more) blood meals from a host before being inseminated by a male. Eggs are then laid in small polls or containers of water (both natural and artificial) and hatch into an aquatic larval stage that filter feed in the water column. These larvae mature into pupae that hatch into adults. In this life cycle, there are two opportunities for within- and between-species competition. As larvae, there could be competition for food and space, resulting in greater mortality and longer development times (Juliano, 2009, 2010). Adult mosquitoes, provided they visit the same hosts (Paton and Bonsall, 2019), could mis-mate with heterospecific mosquitoes and suffer the effects of reproductive interference – a diminished reproductive output from inviable inter-species matings (Ribeiro and Spielman, 1986). These forms of competition have been proposed as mechanisms for the observed competitive displacements (Lounibos and Juliano, 2018; Tripet et al., 2011).

## Competition between *Aedes* mosquitoes

### Larval competition

A large body of laboratory and field evidence supports the occurrence of inter- and intraspecific larval competition between *Aedes* mosquitoes (Juliano, 2009; Lounibos and Juliano, 2018). The costs of this competition usually manifest as longer development times and increased mortality. Such studies typically manipulate the densities of conspecifics and heterospecifics in containers and measure the associated penalties. Juliano (2010) carried out a meta-analysis of this body of research, finding support for context-dependent outcomes in competition; *Ae. albopictus* was the superior inter-species competitor when larval resource quality was poor, but the species were competitively equivalent when reared on high quality resources. Costanzo et al. (2005) showed that the desiccation resistance of *Ae. aegypti* and *Ae. albopictus* eggs could be a determinant of competitive outcomes under different climatic regimes, providing additional support to the notion of context-dependent competition. Further variation in outcomes were identified by Leisnham et al. (2009), who demonstrated that competitive interactions can vary between geographically different populations of *Aedes* and Lounibos et al. (2010), who found that different competitive outcomes could be driven by spatially heterogeneous micro-climates. Clearly, the outcomes of larval competition are not straightforward, with competitive costs varying with abiotic and biotic conditions.

### Reproductive interference

Reproductive interference – known as satyrisation (Ribeiro and Spielman, 1986) – occurs when individuals of different species mis-identify heterospecifics as viable mates. These erroneous mating attempts do not result in any offspring, reducing the rate of reproduction due to wasted courtship and handling time. Tripet et al. (2011) demonstrated that this phenomenon occurred between *Ae. aegypti* and *Ae. albopictus*; they found that heterospecific sperm was present in *Aedes* from the field, albeit at low prevalence. Lab experiments by Bargielowski et al. (2013) and Marcela et al. (2015) demonstrated that high levels of mis-mating could occur when the mosquitoes were kept together in cages, with *Ae. aegypti* more likely to cross-mate than *Ae. albopictus*. Moreover, Bargielowski et al. (2013) found evidence that populations of *Ae. aegypti* that had previously been exposed to *Ae. albopictus* were less likely to cross-mate with heterospecific males than populations that had not yet encountered *Ae. albopictus*. The authors suggest that this could imply an evolutionary pressure for more discerning females in response to the costs of reproductive interference. This evidence has elevated reproductive interference to one of the principle mechanisms considered when explaining competitive outcomes between *Ae. aegypti* and *Ae. albopictus* (Lounibos and Juliano, 2018).

### Modelling temperature-dependent traits

Given that the outcomes of interspecific competition in *Aedes* are context dependent (Juliano, 2010), it is of critical importance to explore how model-predicted outcomes of competition differ across a range of abiotic conditions. Temperature is a crucial determinant of *Aedes* presence and abundance (Brady et al., 2013; Kraemer et al., 2015), but it has not yet been included in a model of *Aedes* interspecific competition. Models incorporating temperature responses are of increased relevance and importance when the effects of anthropogenic climate change are considered; as temperatures rise and extreme weather events become more common, how might the biotic interactions within and between *Aedes* species change?

Mathematical models of competition typically assume that model parameters are time-invariant – the effect of a competitor is assessed on a system at mean-field, stable conditions. Doing so enhances analytical tractability and makes the results generalisable and intuitive. For instance, Paton and Bonsall (2019) analysed a Lotka-Volterra model of competition, considering two mechanisms of competition between *Aedes* mosquitoes; larval competition and reproductive interference. Similarly, Bonsall et al. (2010) examined a Lotka-Volterra model of larval competition, while also including genetically modified and sterile insect releases. By modelling competition with static rates, these models could average over how species-specific responses to temperature could manifest in different competitive outcomes. We are therefore motivated to extend the insights provided by simpler models by making model parameters dynamic functions of temperature. In doing so, we aim to determine if the context-dependent outcomes of competition can be, in part, accounted for by different physiological responses to temperature.

Few existing studies have incorporated temperature-dependence into models of *Aedes* population dynamics, and to our knowledge, no study has modelled *Aedes* inter-species competition *and* temperature. Er-

ickson et al. (2010b) developed a stage-structured ordinary differential equation (ODE) model of *Ae. albopictus*, using stochastic simulations to describe abundance data from Texas, USA (Erickson et al., 2010a). This model described key model parameters with temperature-dependent functions, meaning the vital rates of the mosquito (e.g. maturation rates) were dynamic through time. Jia et al. (2016) similarly used an ODE framework to model the population dynamics of *Ae. albopictus*, using this model to examine the sensitivity of populations to heat waves (Jia et al., 2019). However, both of these models describe the state durations exponentially and only as a function of the temperature at the current time-step; upon entering a compartment, individuals will immediately begin to leave at the exponential rate determined by the prevailing temperature conditions. This approximation is unrealistic for features such as extrinsic incubation period or larval development, where there is an absolute minimum amount of time before an individual can progress into the next compartment. The approximation of exponential progression between model compartments motivated Beck-Johnson et al. (2013) and Ewing et al. (2016) to use temperature-dependent delay-differential equation (DDE) models to describe the population dynamics of mosquitoes. Beck-Johnson et al. (2013) developed a variable delay model for *Anopheline* mosquitoes, which they analyse with respect to malaria risk (Beck-Johnson et al., 2017). Ewing et al. (2016) describe the response of *Culex pipiens* (a vector of West Nile Virus) to temperature cycles, using this model to describe abundance data from the field (Ewing et al., 2019). Both models build on the framework described by Nisbet and Gurney (1983); time-delays between compartments (denoted $\tau$) are modelled as continuous functions of temperature, meaning that individuals entering at compartment at time $t - \tau$ will leave the compartment at time $t$. This variable delay framework is more realistic and can give insights into the interactions between species that would be impossible to obtain from simpler frameworks (Blythe et al., 1984; de Roos and Persson, 2003; McCauley et al., 2008).

In a meta-analysis of laboratory studies, Mordecai et al. (2017) describe a range of temperature-dependent ecological and epidemiological traits for both *Ae. aegypti* and *Ae. albopictus* by fitting mechanistic responses to data collated from many experiments. These functions describe the temperature-dependent attributes of each species in terms of a minimum and maximum temperature, setting thermal limits for both ecological and epidemiological processes. Their work therefore provides a foundation on which to develop our understanding of the effects of temperature-dependence in dynamic population models of competition.

Motivated by the importance of temperature for the life history of *Aedes* mosquitoes, we present a temperature-dependent multi-species DDE model of competition between *Ae. aegypti* and *Ae. albopictus*. This model includes both larval resource competition and reproductive interference as interspecific interactions. For mosquito dynamics, stage durations are modelled as time-delays that are continuous functions of temperature, in the spirit of Nisbet and Gurney (1983). We also model pathogen transmission dynamics in these populations, for both vectors and hosts. The temperature-dependent functions parameterised by Mordecai et al. (2017) were used to describe the ecological and epidemiological rates in the model. Our model allowed us to assess the climate sensitivity of *Aedes* population dynamics and most importantly, determine the dependence of competitive outcomes to temperature.

# Methods

## Model outline

### Ecology

Here, we outline a delay-differential equation model with variable delays based on the framework given by Nisbet and Gurney (1983), where a full derivation can be found. We recapitulate important elements of the derivation in the appendix. Let $J_i(t)$ denote the juveniles (eggs, larvae and pupae) and $A_i(t)$ the adult *females* of the $i^{th}$ species ($i = \{1, 2\}$) at time $t$, where species 1 and 2 denote *Ae. aegypti* and *Ae. albopictus* respectively. We can write the following set of equations to describe the temperature-dependent recruitment ($R$), maturation ($M$), and deaths rate ($d$) in juvenile (sub-scripted $J$) and adult (sub-scripted $A$) populations:

$$\frac{dJ_i(t)}{dt} = R_{Ji}(t) - M_{Ji}(t) - \{d_{Ji}(t) + f[J_i(t), J_j(t)]\}J_i(t) \tag{4.1}$$

$$\frac{dA_i(t)}{dt} = M_{Ji}(t) - d_{Ai}(t)A_i(t). \tag{4.2}$$

Here, individuals are recruited to the juvenile class and mature to the adult class while being subjected to a background, temperature-dependent mortality rate $d_{Ji}$. Additional mortality is caused by density-dependent intra- and interspecific larval competition, given by the function $f[J_i(t), J_j(t)]$. This function describes how the density of conspecifics ($J_i$) and heterospecifics ($J_j$) increases mortality as larvae compete for resources and space:

$$f_i[J_i(t), J_j(t)] = \alpha \left[J_i(t) + \beta_i J_j(t)\right]^{\gamma}$$

and is based on the form given in Bellows (1981), modified for the multi-species case. The parameters $\alpha$ and $\gamma$ scale and shape the density-dependence, while $\beta_i$ describes the *relative* contribution of heterospecific larvae to population regulation (if $\beta_i < 1$ then conspecifics contribute more to mortality, if $\beta_i > 1$ heterospecifics contribute more). The shape of density dependence, $\gamma$, controls where density-dependence sits on the contest-scramble spectrum (Bellows, 1981). The model can describe contest competition (undercompensatory, $\gamma < 1$) to scramble competition (overcompensatory, $\gamma > 1$) density dependence. Note that we assume that the scale and type of density-dependent population regulation is the same irrespective of the species of larva ($\alpha$ and $\gamma$ are not indexed), as we assume that the same strength and form of within-species competition applies to both species.

The recruitment term, ($R$), is the number of eggs laid per female mosquito, and is given by the following equation:

$$R_{Ji} = e_i(t)C_i\left[A_i(t), A_j(t)\right]A_i(t) \tag{4.3}$$

where the temperature-dependent egg-laying rate ($e_i(t)$) is scaled by a function, $C_i[A_i(t), A_j(t)]$, that describes how exposure to heterospecific males reduces the reproductive rate. The function $C_i$ is taken from Kuno (1992) and given by:

$$C_i[A_i(t), A_j(t)] = \left[\frac{A_i(t)}{A_i(t) + \delta_i A_j(t)}\right].$$

The frequency-dependent reduction due to conspecific mosquitoes is captured in the denominator; the parameter $\delta_i$ applies a penalty to mosquito fecundity as the density of heterospecifics increases.

Maturation into the adult class is described by the equation:

$$M_{Ji} = \frac{1}{2} R_{Ji}(t - \tau_{Ji}) S_{Ji}(t) \frac{g_i(t)}{g_i(t - \tau_{Ji})} \tag{4.4}$$

where $M_{Ji}$, is determined by the recruitment at $t-\tau_{Ji}$ (to account for the development time of juveniles) scaled by the proportion of the population surviving to adulthood during this period ($S_{Ji}$). Only half of this population is tracked through to adulthood as we are only concerned with adult female mosquitoes (we assume a 50:50 sex ratio). The fraction $(g_i(t)/g_i(t - \tau_i))$ denotes how the temperature-dependent mortality rate (given by the function $g_i(t)$) has changed between the present time and the time when the juveniles were recruited.

The proportion of juveniles surviving to adults ($S_{Ji}$) is modelled by the equation:

$$\frac{dS_{Ji}(t)}{dt} = S_{Ji}(t)\left[\{d_{Ji}(t - \tau_{Ji}) + f_i[J_i(t - \tau_{Ji}), J_j(t - \tau_{Ji})]\}\frac{g_i(t)}{g_i(t - \tau_{Ji})} - \{d_{Ji}(t) + f_i[J_i(t), J_j(t)]\}\right] \tag{4.5}$$

where the combined mortality rates from background ($d_{Ji}$) and density-dependent competition ($f_i[J_i, J_j]$) at $t - \tau_{Ji}$ are scaled by the change in development rate $(g_i(t)/g_i(t - \tau_{Ji}))$. The difference between this scaled past mortality and the present mortality gives the rate of change in the proportion of larvae surviving at the current time-step.

Finally, we track how the duration of time spent in the juvenile stage, $\tau_i$, changes with the temperature-dependent development rate function $g_i(t)$:

$$\frac{d\tau_{Ji}(t)}{dt} = 1 - \frac{g_i(t)}{g_i(t - \tau_{Ji})}. \tag{4.6}$$

Here, the rate of change is a function of the ratio between the past (at $t$ minus the development time, $\tau_{Ji}$) and present development rates.

### Epidemiology

Mosquito infections were modelled in an SEI framework. As the extrinsic incubation rate (the rate at which exposed mosquitoes become infectious) is temperature-dependent, we modelled this stage using a variable delay, as we did for juvenile mosquitoes. The adult female class was sub-divided into susceptible ($A_{Si}$), exposed ($A_{Ei}$) and infectious ($A_{Ii}$) individuals (where $A_i = A_{Si} + A_{Ei} + A_{Ii}$). The rates of change in these classes is given by equations 4.7 - 4.9, and the recruitment and maturation terms defined by equations 4.10 and 4.11:

$$\frac{dA_{Si}}{dt} = M_{Ji}(t) - R_{Ei}(t) - d_{Ai}(t)A_{Si}(t) \tag{4.7}$$

$$\frac{dA_{Ei}}{dt} = R_{Ei}(t) - M_{Ei}(t) - d_{Ai}(t)A_{Ei}(t) \tag{4.8}$$

$$\frac{dA_{Ii}}{dt} = M_{Ei}(t) - d_{Ai}(t)A_{Ii}(t) \tag{4.9}$$

$$R_{Ei}(t) = b_i(t)p_i(t)\frac{H_I(t)}{H(t)} \tag{4.10}$$

$$M_{Ei}(t) = R_{Ei}(t-\tau_{Ei})S_{Ei}(t)\frac{h_i(t)}{h_i(t-\tau_{Ei})} \tag{4.11}$$

Susceptible mosquitoes of the $i^{th}$ species bite hosts at rate $b_i$ and become infected with probability $p_i$. A background death rate ($d_{Ai}$) acts on susceptible, infected and exposed individuals. The rate at which mosquitoes leave the exposed class and become infected is given by $M_{Ei}(t)$, and varies according to a temperature-dependent extrinsic incubation rate, given by the function $h_i$. The number of exposed individuals to survive the intrinsic incubation period and advance to the infected stage is determined by survival of exposed individuals ($S_{Ei}$) and is scaled by the change in the length of the extrinsic incubation period (EIP, $\tau_{Ei}$). The rate of change in the EIP is given by the following equation:

$$\frac{d\tau_{Ei}(t)}{dt} = 1 - \frac{h_i(t)}{h_i(t-\tau_{Ei})}. \tag{4.12}$$

The change in the proportion of exposed individuals surviving to become infected is denoted by $S_{Ei}$, and the rate of change described by equation 4.13:

$$\frac{dS_{Ei}(t)}{dt} = S_{Ei}(t)\left[d_{Ai}(t-\tau_{Ei})\frac{h_i(t)}{h_i(t-\tau_{Ei})} - d_{Ai}(t)\right] \tag{4.13}$$

where the death rate at time $t - \tau_{Ei}$ is scaled by the change the extrinsic incubation rate governed by the function $h_i(t)$.

Human infections were modelled in a simple SEIR framework, using the following set of ordinary differential equations:

$$\frac{dH_S(t)}{dt} = \lambda_S H_R(t) - \left[b_1(t)\rho_1(t)A_{I1}(t) + b_2(t)\rho_2(t)A_{I2}(t)\right]\frac{H_S(t)}{H(t)} \tag{4.14}$$

$$\frac{dH_E(t)}{dt} = \left[b_1(t)\rho_1(t)A_{I1}(t) + b_2(t)\rho_2(t)A_{I2}(t)\right]\frac{H_S(t)}{H(t)} - \lambda_I H_E(t) \tag{4.15}$$

$$\frac{dH_I(t)}{dt} = \lambda_I H_E(t) - \lambda_R H_I(t) \tag{4.16}$$

$$\frac{dH_R(t)}{dt} = \lambda_R H_I(t) - \lambda_S H_R. \tag{4.17}$$

Note that we consider the human population size ($H$, where $H = H_S + H_E + H_I + H_R$) to be a closed system with no births, deaths, immigration or emigration. There are no variable delays in host model compartments; it is assumed that the rates for transitioning are exponential and not influenced by temperature. However, temperature-dependent mosquito parameters are accounted for (biting rates, $b_i$, and transmission probability, $\rho_i$) and the ratio of vectors to hosts will be contingent on mosquito population dynamics. Susceptible humans are bitten by and become infected from infected mosquitoes of species 1 and 2. Exposed hosts ($H_E$) become infected at rate $\lambda_I$, while infected hosts ($H_I$) recover at rate $\lambda_R$. Recovered hosts ($H_R$) are assumed to be resistant to infection for a period, before re-joining the susceptible class at rate $\lambda_S$. These rates ($\lambda_I$, $\lambda_R$ and $\lambda_S$) were taken to be approximately those for dengue, given by Gubler (1998b) and given in Table 4.1.

## Temperature-dependence

### Temperature responses

Mordecai et al. (2017) collated and analysed a substantial body of data from laboratory studies examining *Ae. aegypti* and *Ae. albopictus* temperature-sensitive traits. They extracted key epidemiological and life history parameters by fitting one of two temperature-dependent functions to the data. These took the form of either a quadratic ($r_i[T - T_{mi}][T - T_{Mi}]$) or Brieré ($r_i T[T - T_{mi}][T - T_{Mi}]^{\frac{1}{2}}$) function. Both are described in detail by Brieré et al. (1999). The functions describe the species-specific response in terms of a rate constant $r_i$, minimum temperature $T_{mi}$ and maximum temperature $T_{Mi}$. The difference is that the Brieré form skews the peak of the function to the right (i.e. the maximum rate is skewed towards higher temperatures). The functions used for *Ae. aegypti* and *Ae. albopictus* are summarised in Table 4.1 and include the egg-laying rate, juvenile development time, egg-to-adult survival, adult mosquito lifespan, biting rate, extrinsic incubation rate, probability of infection and the probability of transmission. Illustrations of how these functions operate (and the parameters used) are given in Mordecai et al. (2017), and are recapitulated in the appendix (see appendix Figure C.1 and appendix Table C.1).

### Describing temperature changes

To test the sensitivity of their *Culex* population dynamics model to temperature, Ewing et al. (2016) present a flexible function capable of describing a diversity of annual temperature cycles:

$$T(t) = \left(\overline{T} - \Delta T\right) + 2\Delta T\left[\frac{1}{2} + \frac{1}{2}cos\left(\frac{2\pi[t - P \times 365]}{365}\right)\right]^S. \tag{4.18}$$

Here, the temperature at time ($T(t)$) is a function of the average temperature across the year ($\overline{T}$) and the amplitude of the yearly temperature fluctuation from this mean ($\Delta T$). The timing of the peak is given as a proportion of the number of days in a typical year ($P$, where $P \in [0, 1]$) and $S$ is the sharpness with which the

| function | description | form |
|---|---|---|
| *ecological functions* | | |
| $g_i$ | the development rate of juvenile mosquitoes (inclusive of pupae, larvae and eggs) | Brieré |
| $c_i$ | egg-to-adult survival probability | Quadratic |
| $e_i$ | egg-laying rate | Brieré |
| $d_{Ai}$ | adult mosquito death rate (equal to the inverse of the adult lifespan) | Quadratic |
| $d_{Ji}$ | juvenile death rate, equal to $\frac{-log(c_i(t))}{\tau_{Ji}(t)}$ | - |
| *epidemiological functions* | | |
| $h_i$ | the extrinsic incubation rate (the time taken for a mosquito to become infectious) | Brieré |
| $p_i$ | probability of a mosquito becoming infected after a blood meal from an infected host | Brieré |
| $\rho_i$ | probability of a bite from an infected mosquito transmitting the infection to the host | Brieré |
| $b_i$ | the mosquito biting rate | Brieré |

| parameter | description | value |
|---|---|---|
| *temperature-invariant ecological parameters* | | |
| $\alpha$ | scaling of density dependence | $1 \times 10^{-6}$ |
| $\gamma$ | shape of the density dependence, ranging from undercompensatory ($\gamma < 1$) to overcompensatory ($\gamma > 1$) | 1 by default, varied to 1.25 |
| *temperature-invariant epidemiological parameters* | | |
| $\lambda_I$ | the rate at which exposed hosts become infectious | $\frac{1}{10}$ |
| $\lambda_R$ | the rate at which human hosts recover | $\frac{1}{5}$ |
| $\lambda_S$ | the rate at which previously infected human hosts become susceptible again (we assume that immunity is life-long) | 0 |

Table 4.1: Table of the temperature-dependent functions (taken from Mordecai et al. (2017)) and temperature invariant ecological and epidemiological parameters (taken from Gubler (1998b)) used to describe the population and epidemiological dynamics in our model. Temperature responses are visualised in appendix Figure C.1 and the parameters used in these functions given in appendix Table C.1.

| state variable | definition | initial value |
|---|---|---|
| *ecological variables* | | |
| $J_i$ | the density of juvenile mosquitoes (both sexes, eggs through to pupae) | 0 |
| $A_{Si}$ | the density of susceptible adult female mosquitoes | 1000 |
| $S_{Ji}$ | the proportion of larvae to survive into the susceptible adult female class | $c_i(0)$ |
| $\tau_{Ji}$ | the development time of larvae at time $t$ | $g_i(0)^{-1}$ |
| *epidemiological – mosquitoes* | | |
| $A_{Ei}$ | the density of exposed female mosquitoes | 0 |
| $A_{Ii}$ | the density of infected female mosquitoes | 0 |
| $S_{Ei}$ | the proportion of exposed female mosquitoes that survive the EIP to become infectious | $e^{[-d_{Ai}(0)h_i(0)^{-1}]}$ |
| $\tau_{Ei}$ | the length of the extrinsic incubation period | $h_i(0)^{-1}$ |
| *epidemiological – hosts* | | |
| $H_S$ | the density of susceptible hosts | 49,999 |
| $H_E$ | the density of exposed hosts | 0 |
| $H_I$ | the density of infectious hosts | 0 (+1 after 5 years) |
| $H_R$ | the density of recovered hosts | 0 |

Table 4.2: Table of state-variables for equations 4.1 to 4.17, along with the initial values used for the simulations. The juvenile survivorship was initialised from the function $c_i$ evaluated for the temperature at initial time-step. Initial values for both dynamic time lags – the juvenile development time and the extrinsic incubation period – can be set from the inverse of the rate functions ($g_i$ and $h_i$). Initial survival of exposed individuals ($S_{Ei}$) was set using the adult death rate ($d_{Ai}$) and the inverse of the intrinsic incubation rate, $h_i$, both evaluated at the initial temperature.

temperature cycle reaches and leaves the maximal and minimal values. We use this function to describe the temperature cycles in this paper, examining the sensitivity of model outcomes to these parameters.

## Simulations

All simulations were conducted in the statistical programming software R version 3.5.3 (R Core Team, 2019), using the numerical simulation package deSolve (Soetaert et al., 2010). Initial conditions were set according the values in Table 4.2. Simulations were initialised with 1000 adult mosquitoes for each species, with no juveniles. The initial (and past) values of all of the temperature-dependent traits in Table 4.1 can be calculated by using the past temperature calculated from equation 4.18. Other initial conditions require the manipulation of some of the temperature-dependent functions and are given in Table 4.2. Susceptible hosts were initialised at 49,999 with no infecteds in any class. This number of hosts was chosen as exploratory simulations showed that adult female *Ae. aegypti* and *Ae. albopictus* populations reached a maximum combined size of approximately double this value, giving a peak 2:1 ratio of vectors to hosts. A single infected host was introduced after five years of simulation burn-in, and the subsequent three years analysed. This was to ensure that the epidemiology of the system was not influenced by interim vector dynamics caused by a particular set of initial conditions.

We began by assessing the responses of *Ae. aegypti* and *Ae. albopictus* to the parameters of equation 4.18,

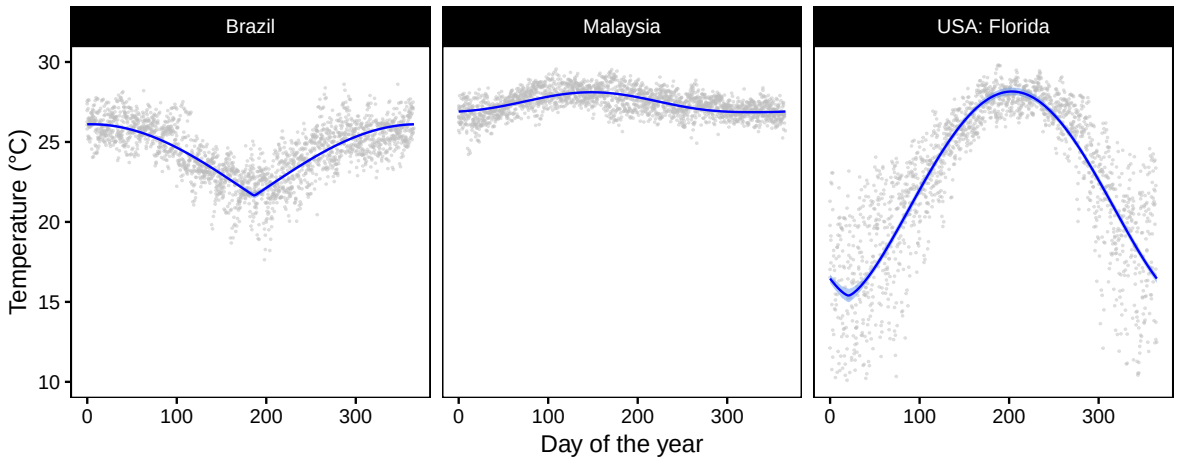



Figure 4.1: Model fits (shown in blue with 95% HDIs) for the yearly temperature responses of Brazil, Malaysia and Florida. Weather station data is shown as grey points (taken for the five years from 2013 to 2018). Differences in temperature cycles are immediately apparent, most notably that as Brazil is in the Southern hemisphere, meaning the peak is early in the year (this is unlikely to change model predicted outcomes, just the timing of events). Other differences are in the amplitude of fluctuation (the temperature cycle is largest in Florida and minimal in Malaysia) and average temperature (highest in Malaysia). Parameter values and associated uncertainties are given in appendix Table C.2.

in the absence of competition ($\beta_1 = \beta_2 = 0$ and $\delta_1 = \delta_2 = 0$). Simulations were run across different combinations of mean temperature ($\overline{T}$), amplitude of temperature fluctuation ($\Delta T$) and severity of temperature change ($S$). The timing of the temperature peak ($P$) was set at 0.5 (exactly the middle of the year), as this parameter only changed the timing of events, rather than altering the fundamental responses to climate.

This high-dimensional climatic parameter space (i.e. the combinations of parameters in equation 4.18) could not be fully explored for all types and strengths of between-species competition as it was prohibitively large. Therefore, in our analysis of competition, we explored three climatic scenarios relevant to both species. We used the Bayesian analysis software JAGS (Plummer, 2003) to fit equation 4.18 to temperature observations from locations where both species have been recorded; Brazil, Malaysia and the state of Florida in the USA. Temperature data from 2013 to 2018 were downloaded using the GSODR (global summary of the day) package in R (Sparks et al., 2017) for all weather stations in each country. This allowed us to fit a representative yearly temperature cycle for each location. Model fits are shown in Figure 4.1, and parameter estimates given in the appendix Table C.2. By restricting our analysis of the effects of competition to these three climatic scenarios, we ground our conclusions in circumstances where these mosquitoes have actually been observed.

From our simulations, were also able to calculate the vectorial capacity for each species. Vectorial capacity is an aggregate metric derived from transmission models to describe the proficiency of a vector in spreading disease (Brady et al., 2016; Dye, 1992). For our model, the vectorial capacity at time $t$ for the $i^{th}$ species is given by $V_i(t)$:

$$V_i(t) = \frac{A_i(t)}{H}\left[\frac{b_i(t)^2 p_i(t) \rho_i(t) L_i(t)^{E_i(t)}}{-ln(L_i(t))}\right] \tag{4.19}$$

where $L_i(i)$ is daily adult mosquito survival probability $\left(e^{-d_{Ai}(t)}\right)$, $E_i(t)$ is the extrinsic incubation period $\tau_{Ei}$, and the term $\frac{A_i(t)}{H}$ gives the ratio of vectors to hosts (we assume that the number of hosts is time invariant in our

model). Other parameters are given by the functions in Table 4.1. Our model is well placed to examine vectorial capacity, as our temperature-dependent extrinsic incubation period and adult death rates will impact the metric directly, while other functions (e.g. larval development time) will indirectly influence the metric by determining the number of adult females, $A_i$.

Finally, we conducted a sensitivity analysis of the model-predicted vectorial capacity of both species under different parameterisations of the functions described in appendix Table C.1. Specifically, we tested the sensitivity of vectorial capacity to the species-specific thermal limits described for each function. We did so by expanding the temperature niche by 10% ($T_{mi}$ and $T_{Mi}$ were decreased and increased by 5% respectively) and contracting the temperature niche by 10% ($T_{mi}$ and $T_{Mi}$ were increased and decreased by 5% respectively). We calculated the percentage change in the mean vectorial capacity for each species relative to the vectorial capacity under the standard values.

## Results

### Species-specific responses to temperature

Figure 4.2 shows the average, maximum and minimum adult female and juvenile population sizes for *Ae. aegypti* and *Ae. albopictus*. Values are taken from the final three years of numeric simulations across different combinations of average temperature and amplitude of temperature fluctuation. For populations of adult females, *Ae. aegypti* shows greater variation in population sizes compared to *Ae. albopictus*. The largest average *Ae. aegypti* adult populations are reached when temperature cycles are small and average temperatures high, while the largest maximum population sizes are reached when the amplitude of cycles are high (though this is accompanied by very low minimum sizes).

The average and maximum *Ae. albopictus* population sizes are more conserved across the parameter space. The minimum adult population size of *Ae. albopictus* drops very low when the average temperature is low and the amplitude of temperature fluctuations were high (bottom right). This is intuitive, as these large amplitude cycles will take temperatures to low values which are unsuitable for adult and juvenile mosquito survival. Less expected is the severe drop-off in minimum population size at high average temperatures with large amplitudes (top right); these minima are actually reached in the *summer* months, when temperatures are highest. This occurs because temperatures become too hot for *Ae. albopictus* survival; the peak of the population therefore shifts from the summer to the winter. The *timing* of peak population sizes in relation to climate are shown in appendix Figure C.4, and illustrate how thermal limits can lead to shifts in where maximal population sizes are achieved. Of note is the higher abundance of *Ae. albopictus* juvenile populations across almost all climates, which is the opposite of what is observed for adult female densities. This is important, as fewer *Ae. albopictus* adults emerge (due to density-dependent competition and a lower egg-to-adult survival than *Ae. aegypti*; see the temperature-dependent relationships in appendix Figure C.1).

With respect to the climatic scenarios referenced in the next section (marked on the surface plot by the first letter of the location name), *Ae. aegypti* has larger adult female population sizes in Malaysia and Brazil,

while *Ae. albopictus* populations are larger in Florida. The minimum population size of *Ae. aegypti* becomes very small in Florida, as the cold season is more severe than the other climates. *Ae. albopictus* larval populations are predicted to be greater than *Ae. aegypti* in all countries; this proves critical in our analysis of competition.

The sensitivity of disease transmission to climate is shown in Figure 4.3. Vectorial capacity was shown to be substantially higher for *Ae. albopictus* than *Ae. aegypti*; maximum, minimum and average values were larger across the parameter space. *Ae. aegypti* is predicted to have its highest vectorial capacity in Malaysia, where all values are non-zero. However, in Brazil and Florida, the vectorial capacity of *Ae. aegypti* reaches a minimum around zero. Inter-species differences in vectorial capacity are likely driven by the longer lifespan of *Ae. albopictus* (see appendix Figure C.1); in order for disease transmission to occur, adult females must live long enough to become infectious and take further blood meals (reflected in equation 4.19). *Ae. albopictus* had a non-zero maximum and average vectorial capacity in all climates, but the minimum dropped to zero in Florida, suggesting that even for the more competent vector, Floridian winters are too cold for transmission. In panel B, as expected, disease transmission is lessened at low temperatures (with almost no infection), while warmer temperatures generally result in larger peak outbreaks. Less expected are the wave-like transitions moving from cold to hot average temperatures and small to large cycles. The epidemiology of this system is driven by multiple vector species, whose abundance, biting rates, infection, extrinsic incubation rate and dissemination probabilities are temperature dependent (reflected in vectorial capacity). A complex feedback between vector abundance and the temperature-dependent epidemiological rates combine to give non-linear patterns of disease outbreak, and abrupt changes can occur across the climatic parameter space.

### Interactions between larval competition and climate

In Figure 4.4, we demonstrate the sensitivity of the outcomes of larval competition to both climate (Malaysia, Brazil and Florida) and the strength of density-dependent larval competition ($\gamma$). The coefficients of larval competition describe whether a heterospecific larva contributes less ($\beta_i < 1$) the same ($\beta_i = 1$) or a greater ($\beta_i > 1$) cost than a conspecific larva to density-dependent larval competition. In these simulations, there was no reproductive interference ($\delta_i = \delta_2 = 0$). The colour indicates the average proportion of the population that is *Ae. aegypti*, with red indicating majority *Ae. aegypti* and blue majority *Ae. albopictus*. Evident are the differences in outcomes between the two-species. In the competition free scenarios (bottom left corner in all plots), *Ae. aegypti* populations were larger in Brazil and Malaysia, while *Ae. albopictus* populations were larger in Florida. In all three climates, *Ae. albopictus* larvae do not need to be competitively equivalent to *Ae. aegypti* larvae to cause competitive exclusion. For much of the parameter space *Ae. albopictus* dominates, with the largest advantage in Florida. Overcompensatory (scramble, $\gamma = 1.25$) density-dependence benefits *Ae. aegypti* in all three climates; it persists in more of the parameter space. The benefit is not, however, sufficient to mitigate the competitive advantage of *Ae. albopictus*; *Ae. aegypti* is only predicted to out-compete *Ae. albopictus* if its larvae impose a far higher costs of competition (top left of plots in Malaysia and Brazil). From an

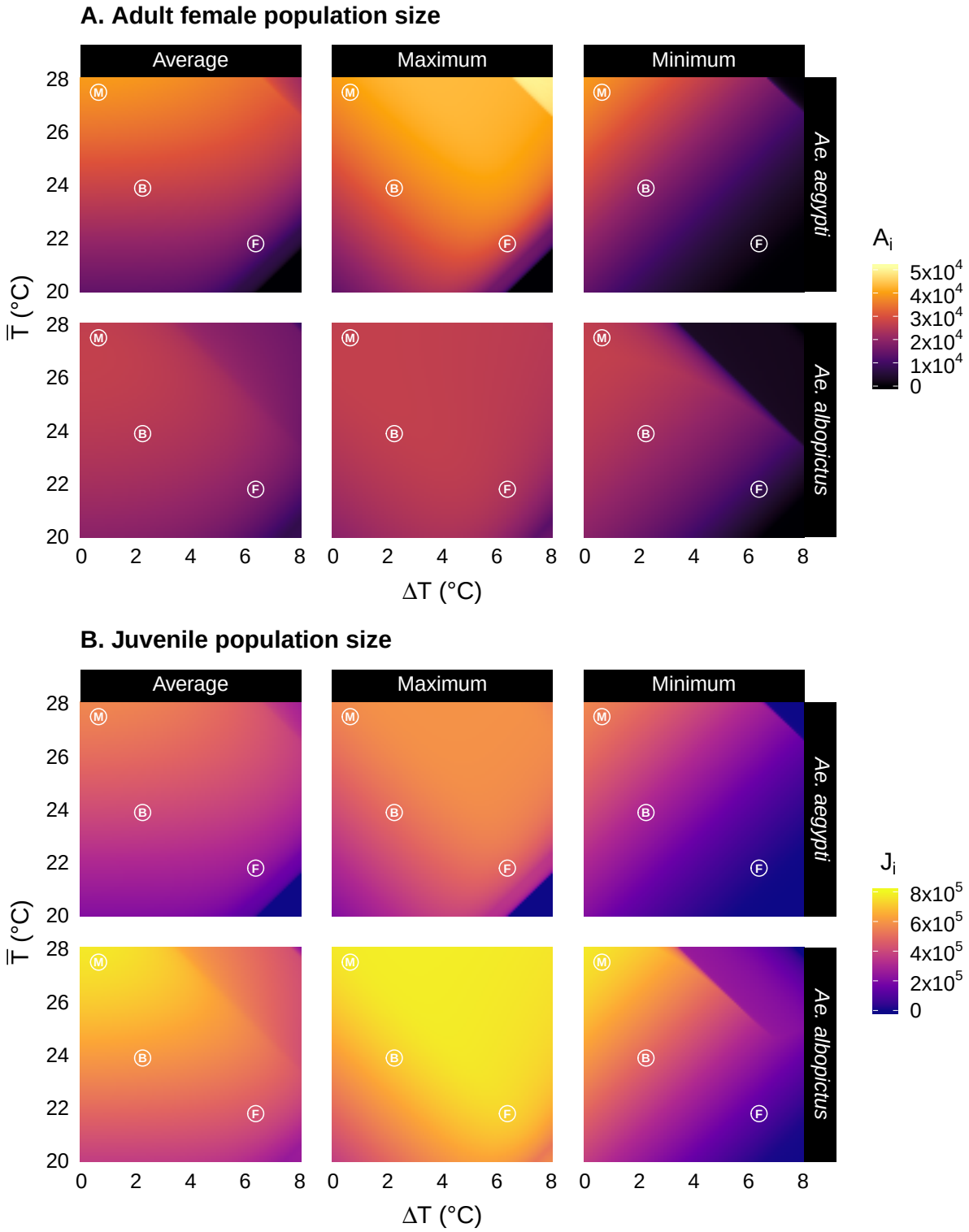



Figure 4.2: Surfaces showing how the population sizes (indicated by colour) of *Ae. aegypti* and *Ae. albopictus* responded to average temperature ($\overline{T}$) and the amplitude of annual temperature fluctuations ($\Delta T$). The first set of plots (A) give the adult female population, while the bottom set (B) shows the juvenile population. In the first column, population sizes are averaged across the final three years of simulations, with maximum and minimum population sizes given in columns two and three. The letters M, B and F denote where the climates of Malaysia, Brazil and Florida sit within this parameter space. The effect size of sharpness, $S$, is not as substantial and does not change the overall trends, but are shown in appendix Figures C.2 and C.3 for completeness. In this plot, $\alpha = 1 \times 10^{-6}$, $\gamma = 1$, $P = 0.5$, $S = 1$.

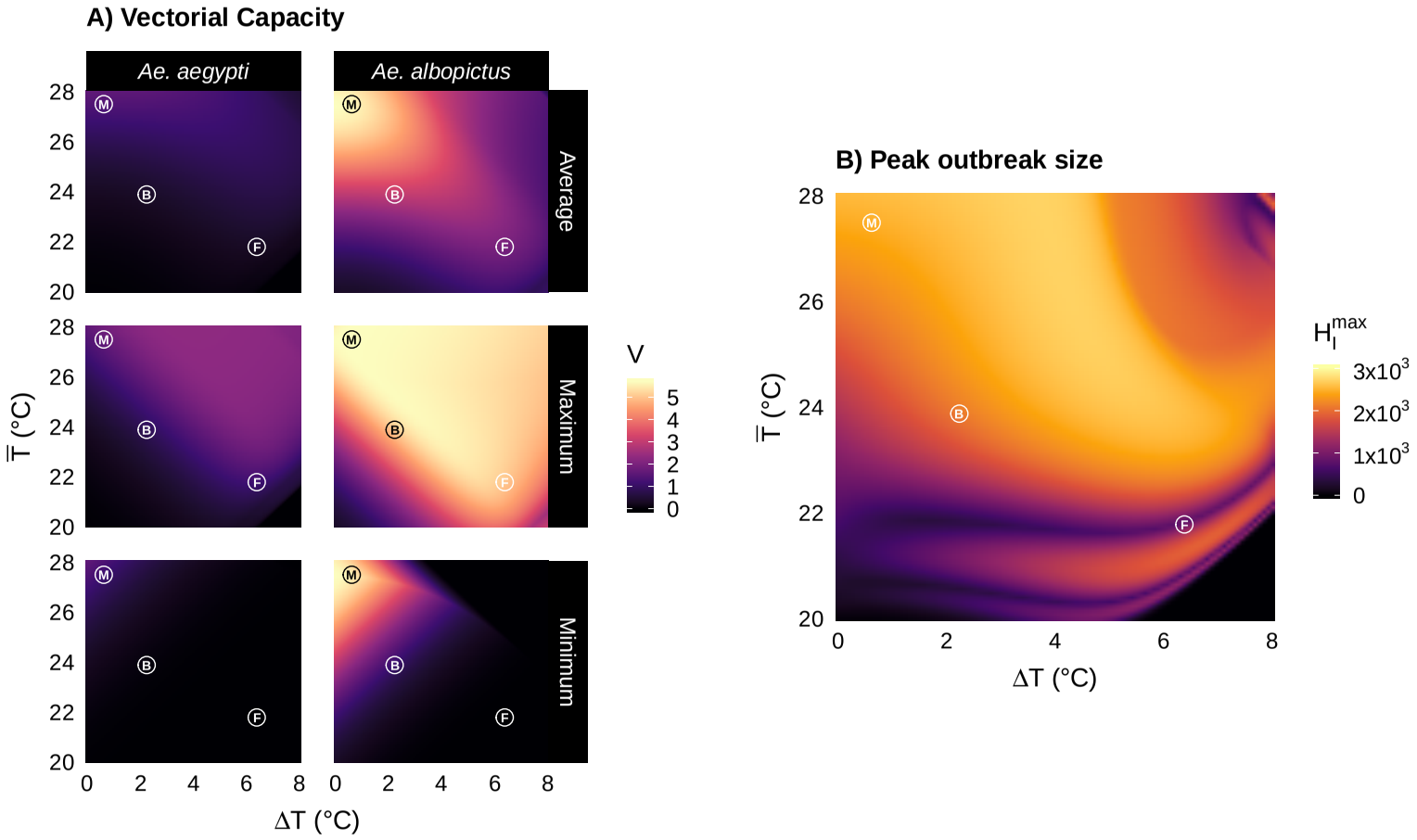



Figure 4.3: Surfaces showing how the amplitude of temperature fluctuations ($\Delta T$) and mean temperature ($\overline{T}$) change vectorial capacity and peak outbreak size. Panel A shows the average, minimum and maximum values of vectorial capacity ($V$, given by equation 4.19) for *Ae. aegypti* and *Ae. albopictus* across simulations. Panel B shows how the combined impact of the vectorial capacities in panel A combine to produce outbreaks. Here, the maximum outbreak size ($H_l^{max}$) for different climatic scenarios is denoted by colour temperature.

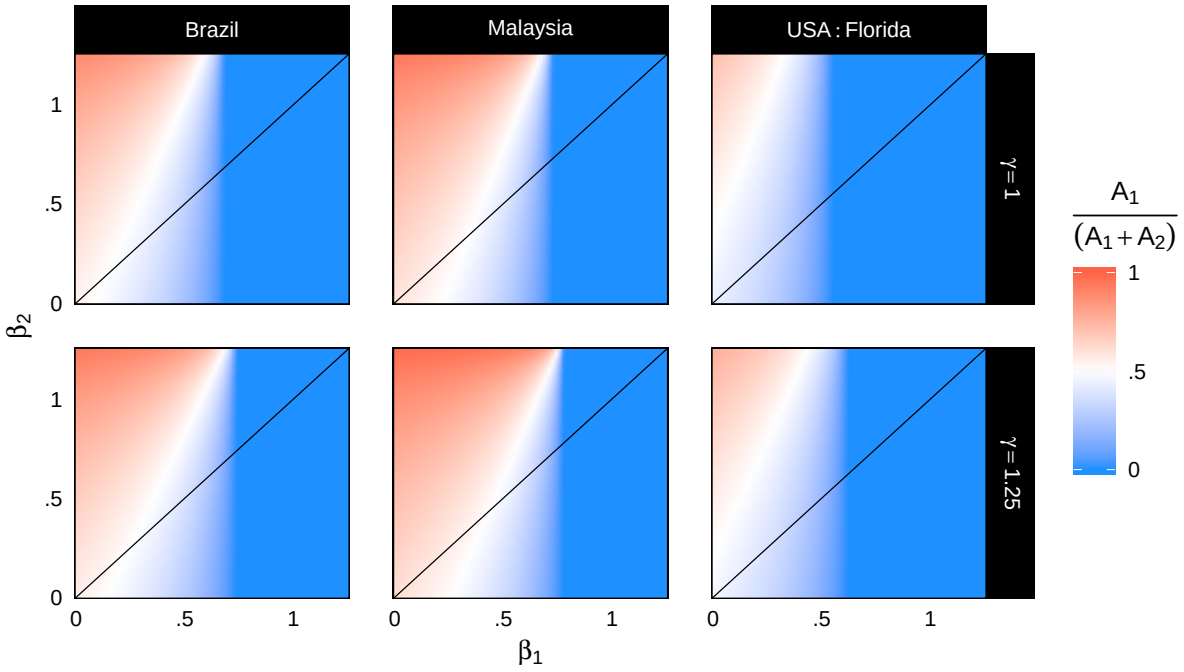



Figure 4.4: Surfaces showing how the composition of adult female *Aedes* populations changes with the strength of interspecific larval competition. Values of $\beta_i < 1$ mean that heterospecifics contribute less than conspecifics to density-dependent competition, while values $> 1$ mean they contribute more. Costs of *Ae. albopictus* on *Ae. aegypti* are given by $\beta_1$ on the x-axis, and the opposite by $\beta_2$ on the y-axis. Columns give different climates, while rows give different shapes of density-dependence. Colour indicates the proportion of the combined populations composed of *Ae. aegypti* adults; white denotes populations *Ae. aegypti* and *Ae. albopictus* are of equal size, red indicates that the *Ae. aegypti* population is larger and blue that the *Ae. albopictus* population is larger. The diagonal line indicates where the coefficients of competition are equal.

epidemiological standpoint, larval competition will only ever lead to reductions in outbreak severity, as competition will reduce combined mosquito densities relative to the competition-free scenario (see appendix Figure C.5). The decline in peak outbreaks size is shown in appendix Figure C.6.

### Interactions between reproductive interference and climate

The effects of reproductive interference and climate on the composition of *Aedes* populations is summarised in Figure 4.5. Results are shown in the absence of larval interspecific competition (i.e. $\beta_1 = 0$ and $\beta_2 = 0$). Trends are the opposite of those described for larval competition in Figure 4.4; increasing the cost of reproductive interference confers a competitive advantage to the species suffering increased costs. In Malaysia, *Ae. aegypti* is competitively superior, increasing its share of the total population for much of the parameter space. In Brazil, the competitive ability of both species is more comparable, with a slight advantage to *Ae. aegypti*. However, in Florida, *Ae. albopictus* dominates. This is consistent with model-predicted outcomes of larval competition in Florida, where the costs of larval competition strongly favoured *Ae. albopictus*. The shape of larval competition has a smaller effect on reproductive interference than larval competition, which is unsurprising as it affects only intraspecific competition in this example. However, a slight benefit for *Ae. aegypti* is conferred in the $\gamma = 1.25$ scenario. It is important to note that reproductive interference does not lead to competitive exclusion (at least in this parameter space). Unlike larval competition, which only reduces population sizes relative to the competition-free scenario, reproductive interference can actually lead to higher

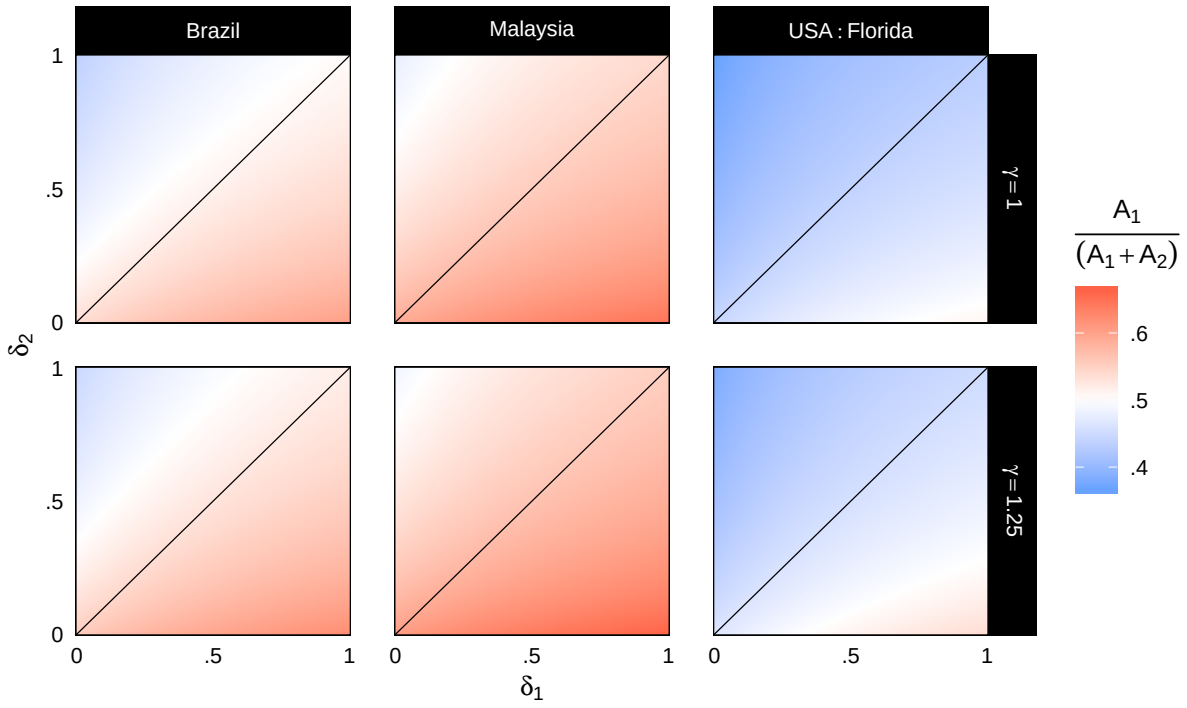



Figure 4.5: Surfaces showing how the composition of simulated *Aedes* populations changes in response to the strength of reproductive interference; $\delta_1$ gives the strength acting on *Ae. aegypti* and $\delta_2$ the strength acting on *Ae. albopictus*. Population composition is defined as the average proportion of the population that is *Ae. aegypti* (the mean of $\frac{A_1}{(A_1+A_2)}$). Red indicates that there are on average more *Ae. aegypti*, blue denotes that there are more *Ae. albopictus*. Note that the colour scale does not go from 0 to 1 as it does in Figure 4.4, as neither species is fully excluded in this $\delta$ parameter space. These simulations were conducted without larval interspecific competition ($\beta_1 = 0$ and $\beta_2 = 0$). Columns show different climates, while rows show different strengths of larval *intraspecific* competition ($\gamma$). The diagonal black line denotes where the strength of reproductive interference is equal for both species.

densities of mosquitoes (shown in appendix Figure C.7). This can lead to higher peak outbreak sizes in climates such as Malaysia (shown in appendix Figure C.8).

### Interactions between larval competition and reproductive interference

In Figure 4.6, we show the larval competition parameter space under different strengths of reproductive interference. These simulations show that the advantage conferred to *Ae. aegypti* by reproductive interference does not mitigate the high costs it suffers from larval competition. When *Ae. aegypti* experiences reproductive interference and *Ae. albopictus* does not ($\delta_1 = 0.5$ and $\delta_2 = 0$), the shift to *Ae. albopictus* dominance becomes more severe (particularly in Florida). This implies that while the cost of reproductive interference results in an increased population share for *Ae. aegypti* in the *absence* of larval competition, it does not confer the same magnitude of benefit when larval competition is present. When *Ae. albopictus* also suffers from reproductive interference ($\delta_2 = 0.5$), then *Ae. aegypti* can competitively exclude *Ae. albopictus*, but only if the costs of larval competition strongly favour *Ae. aegypti* (this is most pronounced in Malaysia).

### The sensitivity of vectorial capacity to thermal limits

We analysed the sensitivity of vectorial capacity to expansions and contractions of the thermal maxima ($T_{Mi}$) and minima ($T_{mi}$) for each of the temperature-dependent functions described in Table 4.1. Figure 4.7 shows the interaction between changes in thermal tolerances with both larval competition and climate. While there

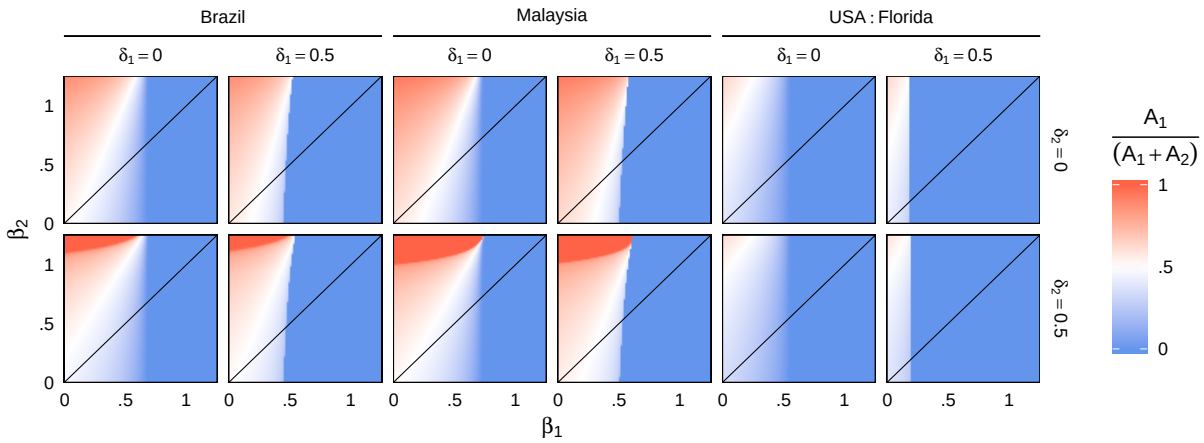



Figure 4.6: Surfaces showing the interactive effects of larval competition ($\beta$, shown on the axes) and reproductive inference (shown in the $\delta$ facets). Red denotes a majority *Ae. aegypti* population and blue a majority *Ae. albopictus* population (given as the average of $\frac{A_1}{(A_1+A_2)}$ across the simulation).

are some inter-climate differences in the competition free-scenarios (bars with no outlines), there are significant differences in the presence of larval competition (outlined bars), particularly for *Ae. aegypti*. In the absence of larval competition, narrowing the thermal niche of the functions reduces the vectorial capacity, with the exception of the egg-laying rate, $e_i$ (though the increase in minimal). Unsurprisingly, broadening the thermal niche increases the vectorial capacity; the adult lifespan ($d_i^{-1}$) consistently has a large effect for both species and all climates (just under a 50% increase for *Ae. aegypti* and just over for *Ae. albopictus*). For *Ae. aegypti*, competition greatly increases the importance of larval development time, $g_1$, for vectorial capacity. In Florida, where differences in vectorial capacity are largest, narrowing the thermal niche for larval development rate results in a 100% reduction in vectorial capacity, while broadening the niche increases vectorial capacity by more than 300%. Competition also increases the importance of egg-to-adult survival probability ($c_i$), especially in Florida. What is notable is that these parameters are only indirectly related to the calculation of vectorial capacity we use; for *Ae. aegypti* in particular, changes in vectorial capacity are driven by ecological parameters under interspecies larval competition. Changes in the vectorial capacity of *Ae. albopictus* are relatively conserved across climates and between competitive scenarios.

In Figure 4.8, the interaction between shifts in thermal niche and reproductive interference are depicted. Changes for *Ae. albopictus* are robust to climate and the level of reproductive interference (outlined bars); in all cases, adult lifespan is the most important determinant of vectorial capacity. For *Ae. aegypti* in the Brazilian and Malaysian climates, effect sizes are quite close in magnitude for development rate, adult lifespan, biting rate and transmission probability. In a Floridian climate, the importance of larval development rate is increased. Most functions are robust to reproductive interference, with the exception of egg-to-adult survival and egg-laying rate for *Ae. aegypti* in the Floridian climate. Decreases in the thermal niche of both functions results in a 100% reduction in vectorial capacity for *Ae. aegypti*. However, increasing the niche leads to only small increases in vectorial capacity.

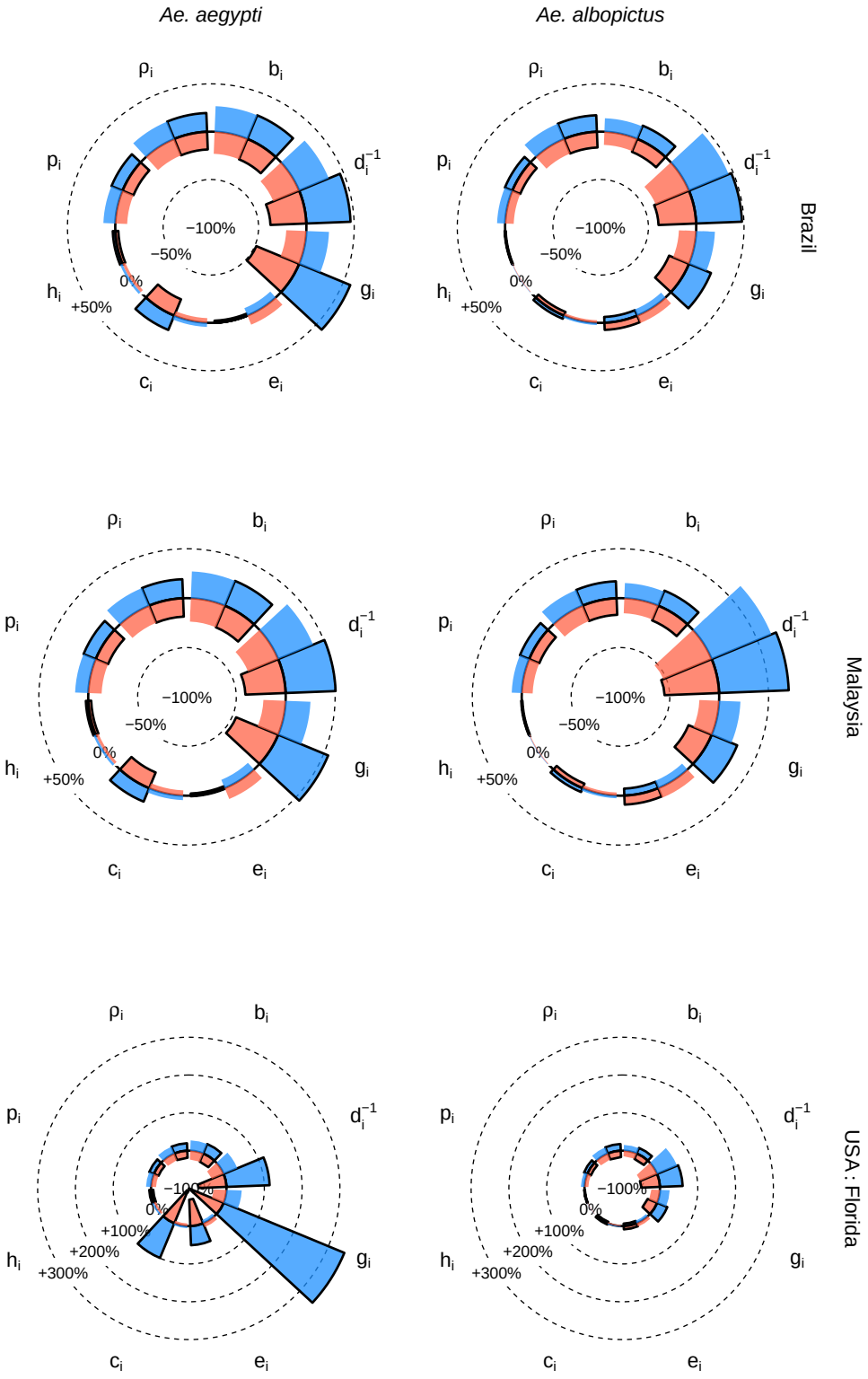



Figure 4.7: Barplots showing how model-predicted vectorial capacity changes in response to a reduced and expanded thermal niches and larval competition. The thermal limits are expanded (indicated in blue) and contracted (indicated in red) for each of the temperature-dependent functions in our model (definitions of functions are given in Table 4.1). The analysis is shown across different climates (rows), for each species (columns). Bars without outlines denote competition free scenarios, while outlined bars denote $\beta_1 = \beta_2 = 0.5$. Contours give the percentage change from the default parameterisation (0% therefore denotes no change from the baseline value). Other parameters were set as follows: $\gamma = 1$ and $\delta_1 = \delta_2 = 0$.

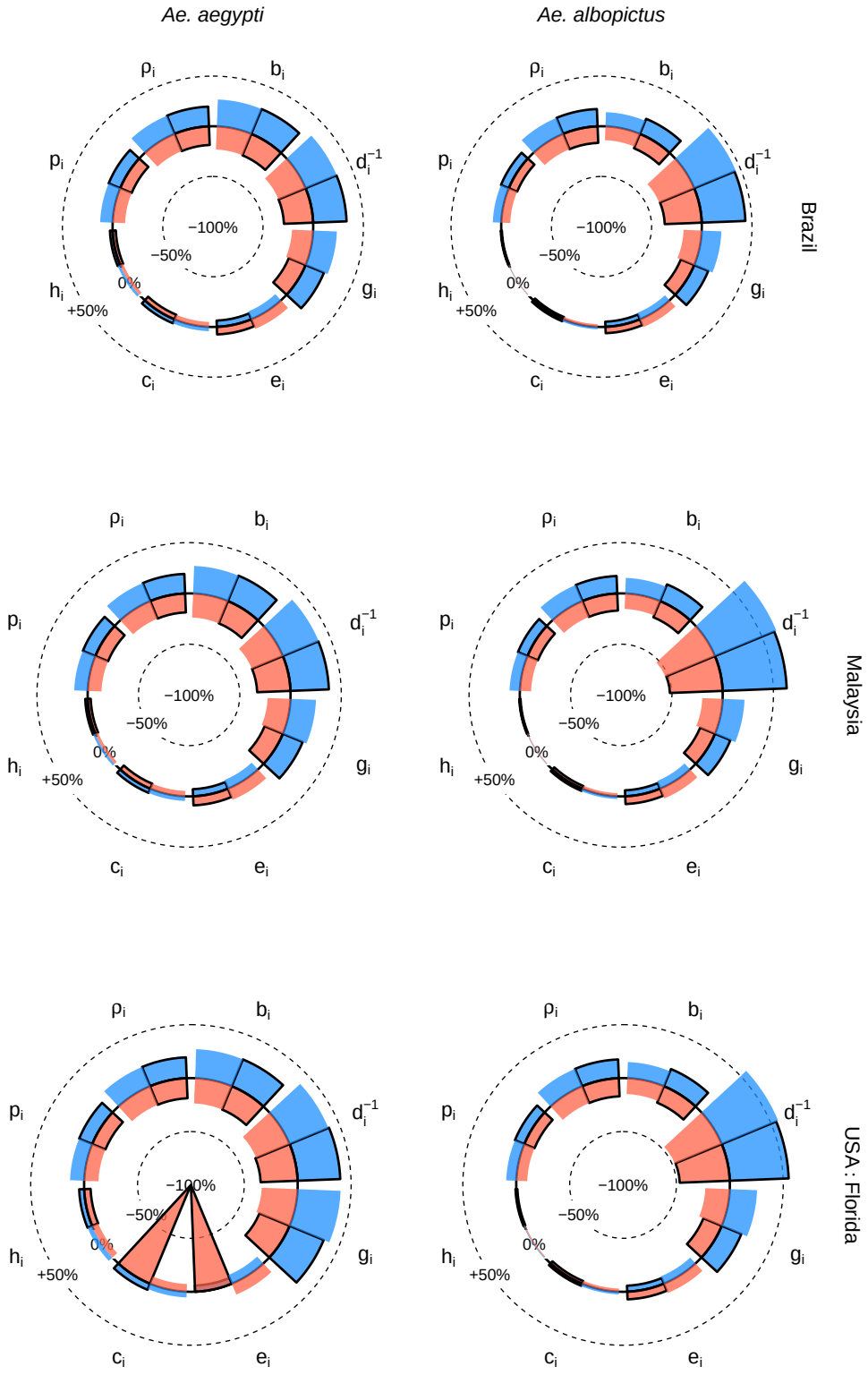



Figure 4.8: Barplots showing how model-predicted vectorial capacity changes in response to a reduced and expanded thermal niches and reproductive interference. The thermal limits are expanded (indicated in blue) and contracted (indicated in red) for each of the temperature-dependent functions in our model (definitions of functions are given in Table 4.1). The analysis is shown across different climates (rows), for each species (columns). Bars without outlines denote competition free scenarios, while outlined bars denote $\delta_1 = \delta_2 = 0.5$. Contours give the percentage change from the default parameterisation (0% therefore denotes no change from the baseline value). Other parameters were set as follows: $\gamma = 1$ and $\beta_1 = \beta_2 = 0$.

## Discussion

Both temperature and interspecific interactions are fundamental in shaping the distribution of *Aedes* mosquitoes, with a myriad of downstream consequences for epidemiology and population control. Here, we have explored the interaction between temperature and competition, observing climate-dependent outcomes that could – at least in part – account for the distributions of *Aedes* in the field. Our research is unique in the *Aedes* literature and rare in the mosquito literature (Beck-Johnson et al., 2013; Ewing et al., 2016) in modelling temperature responses using a variable delay model, as opposed to temperature-forced exponential rates between compartments (as in Erickson et al. (2010b); Jia et al. (2016)). This makes the competition in our model more representative than the idealised Lotka-Volterra models (with constant rates) that have been used to examine *Aedes* competition in the past (e.g. Bonsall et al. (2010); Paton and Bonsall (2019)).

### Insights into the ecological and epidemiological climatic niches of *Ae. aegypti* and *Ae. albopictus*

Our model found that simulated *Aedes* population dynamics are highly climate-sensitive. *Ae. aegypti*, as expected from field observations, shows strong seasonality with winter troughs and summer peaks. For much of the climatic parameter space, our model predicts that – at least for this parameterisation of the temperature-dependent functions – *Ae. aegypti* will typically reach larger adult female population sizes than *Ae. albopictus*. Dynamics for *Ae. albopictus* are more complex. Specifically, we document that *Ae. albopictus* is less limited in colder temperatures than *Ae. aegypti*, but is severely limited by high temperatures. This has implications for populations under anthropogenic climate change; if summer temperatures become too high, then populations of *Ae. albopictus* are predicted to be smaller in summer months, with population peaks shifting to winter. This is, of course, contingent on larval habitat availability; if there is insufficient precipitation in winter months, then populations will not persist as our model predicts. However, in human-modified landscapes, larval habitats are often created by waste water and artificial pools, providing populations with breeding sites in winter months, even if precipitation is low (Juliano, 2009; Messina et al., 2015).

In terms of epidemiology, our model predicts that outbreaks are highly sensitive to temperature for this multi-vector system. The complexity of the interactions influencing infection and dissemination probabilities, biting rates and population sizes mediate an extremely complex pattern of outbreak severity. While intuitive patterns exist in hotter climates, it is at the extremes of the climates we explore that outbreaks become highly variable. We explored vectorial capacity as a metric to elucidate these outbreak patterns. To our surprise, *Ae. aegypti* was predicted to have a substantially smaller impact than *Ae. albopictus* on disease transmission. This occurs despite *Ae. aegypti* having higher predicted adult population sizes throughout much of the climate parameter space.

The greater vectorial capacity of *Ae. albopictus* is of interest for two reasons. First, it warns that *Ae. albopictus* has the capacity to transmit in the absence of *Ae. aegypti*; this is supported by evidence suggesting it can singularly support pathogen transmission in places such as Gabon and Madagascar (Delatte et al., 2010;

Paupy et al., 2010). However, we know that in many locations *Ae. albopictus* is *not* the principle vector of disease, with *Ae. aegypti* the primary vector (Scott and Takken, 2012). One assumption our model makes is that all blood meals are taken from human hosts. With a propensity to bite and rest outdoors (Paupy et al., 2009; Richards et al., 2006), the biting rate of *Ae. albopictus* on humans is likely to be lessened through the process of host selection, both by host availability and preference (Paton and Bonsall, 2019; Yakob and Walker, 2016). Human biting rates could be reduced further by the habitat preference of *Ae. albopictus*; it favours peri-urban environments where humans are present at lower densities and other hosts are available. These are likely explanations for the mis-match between the epidemiological contribution predicted by our model and the realised vectorial capacity of *Ae. albopictus* in many field situations. In modern interpretations of the vectorial capacity equation, a term Q is added to denote the proportion of blood meals taken from a human host, scaling the biting rate (Brady et al., 2016). As Q is included with the biting rate – a squared term in the equation – vectorial capacity decline non-linearly with reductions in human host use. Moreover, the process of host choice could be critical both for epidemiological and *ecological* processes; differences in host choice across both species and populations of mosquitoes will clearly be of importance (Paton and Bonsall, 2019).

### Climate interacts with larval competition – to the benefit of *Ae. albopictus*

Our simulations reveal that species-specific temperature responses can mediate the outcomes of larval competition. Specifically, we find that that *Ae. albopictus* larvae do not need to be competitively equivalent to *Ae. aegypti* larvae to cause competitive exclusion. Our model demonstrated that *Ae. albopictus* larvae existed at higher densities in the three climates we examined. This was likely driven by faster egg laying rates relative to *Ae. aegypti* (see appendix Figure C.1). Even though *Ae. albopictus* larvae had a smaller egg-to-adult survival probability, it seems likely that the higher larval densities of *Ae. albopictus* result in increased density-dependent interspecific costs for *Ae. aegypti*. The superiority of *Ae. albopictus* was consistent across all three climates, but its advantage was greatest in Florida. It is likely that the much higher larval densities predicted for *Ae. albopictus* in each of these climates drives greater costs of larval competition for *Ae. aegypti*.

It is notable that the competitive advantage of *Ae. albopictus* was greatest in Florida, one of the states in the USA where it successfully invaded and displaced many *Ae. aegypti* populations (Lounibos and Juliano, 2018; O'Meara et al., 1995). In Florida, *Ae. aegypti* continues to persist in urban areas; this might be due to documented between-species differences in habitat preference, with *Ae. aegypti* preferring urban and *Ae. albopictus* peri-urban environments (Lounibos et al., 2016; Rey et al., 2006). However, cities often contain micro-climates – particularly at scales relevant to arthropods. If cities generally have micro-climates that better suit *Ae. aegypti* than *Ae. albopictus*, then this could account for spatially heterogeneous patterns of competitive outcomes. Indeed, Lounibos et al. (2010) found that differences in egg desiccation rates across micro-climates could account for differential patterns in coexistence and exclusion across cemeteries in Florida. As our model aggregates eggs, larvae and pupae into one juvenile age class, we miss differences in the species-specific egg survivorship; this could be important if differences in micro-climate result in differential egg hatching

success, and therefore differences in larval density. Our aggregation of the juvenile class was motivated by the fact that many studies report egg-to-adult survivorship, not stage-specific survivorship (Mordecai et al., 2017). A worthwhile extension to this work would be to sub-divide the juvenile class (as in Ewing et al. (2016)) and include egg-specific mortality. This may change the outcomes of competition, as the larval density of the species suffering from a greater egg mortality will contribute less to within- and between-species competition at the larval stage.

### Reproductive interference counter-intuitively *increases* population size, and varies with climate

Results for reproductive interference are more complex. Our model predicts an unexpected pattern of *increased* population sizes as the strength of reproductive interference increases, the opposite to larval competition. This is counter-intuitive, as reproductive interference is suggested as a mechanism of competitive displacement, rather than facilitation (Tripet et al., 2011). However, there is a logical cause. By reducing the number of viable matings, reproductive interference will reduce the number of eggs laid and therefore reduce larval-stage competition (Abrams, 2009). The hydra-effect has been documented in experiments on *Ae. albopictus* (McIntire and Juliano, 2018) and previous models of *Aedes* competition (Paton and Bonsall, 2019). These experiments from McIntire and Juliano (2018) demonstrated that strong, over-compensatory larval competition means that when adults are removed from the system, subsequent generations reach larger population sizes. From an epidemiological standpoint, the hydra-effects caused by reproductive interference are vitally important. A similar effect was forewarned by models of sterile mosquito releases – if release ratios were not sufficiently high, then it is possible for releases to increase population sizes by ameliorating within-species competition (Phuc et al., 2007; Rogers and Randolph, 1984). Most crucial for this study is that the outcomes of reproductive interference were shown to be highly climate-dependent; when larval competition was absent, the hotter and more stable climates of Brazil and Malaysia led to increases in the relative abundance of *Ae. aegypti* to *Ae. albopictus* for much of the parameter space. In Florida, only *Ae. albopictus* was predicted to increase its population size across almost all of the parameter space. Again, in the Floridian climate, *Ae. albopictus* seems to demonstrate a competitive advantage, at least for the parameter space explored here. It is notable that, unlike larval competition, reproductive interference is unable to lead to the complete exclusion of the other species. Indeed our simulations show that the competitive advantage gained by *Ae. aegypti* in Brazil and Malaysia through reproductive interference is almost completely negated by larval competition.

### Changes to thermal limits: interactions between competition and climate

Our sensitivity analysis demonstrated that the vectorial capacity of *Ae. aegypti* was highly sensitive to changes to the thermal limits of its temperature-dependent traits, principally when it experienced larval competition. Notably, it was changes to thermal limits of the larval development rate that resulted in the largest

changes in vectorial capacity, even though it is not *directly* involved in the calculation. This is intuitive, as larval development time is likely to be a key determinant of the outcome of competition, and therefore reductions/expansions in the thermal limits will lead to decreases/increases in adult females. This was most pronounced in Florida, where the costs of larval competition were highest; clearly, when competition is strong, relatively small shifts in the thermal niche of a species can have large effects on epidemiological dynamics by mediating species coexistence.

For reproductive interference, *Ae. aegypti* showed a high sensitivity to reductions (not increases) in its thermal limits for egg-to-adult survival and egg laying rate. As reproductive interference induces some level of sterility in the competition species, this result is not unexpected. In the other climates, competition did not have a significant impact on changes to vectorial capacity.

*Ae. albopictus* did not exhibit the same sensitivities to either type of competition; this is unsurprising, as it was generally the stronger competitor in our model. In all climates, the most sensitive parameter was adult lifespan; as the thermal niche for *Ae. albopictus* adult survival is narrower than that of *Ae. aegypti*, expanding its limits is likely to confer a greater vectorial capacity (see appendix Figure C.1). It seems, then, that the vectorial capacity of *Ae. albopictus* is conserved compared to *Ae. aegypti*.

### Model assumptions and potential extensions

As our climate model is deterministic, there is no inter-annual variation in temperature cycle. In reality, weather varies significantly across years (though some climates are more stable than others, see Figure 4.1). Our results show that – particularly at low temperatures – even small shifts in the amplitude of temperature fluctuation and average temperature can result in wildly different outbreak severities. Between years, the potential for outbreaks will vary drastically, particularly in climates such as Florida where there is greater intra-annual variation. As climates become hotter, and extreme weather events become more common, out model suggests that epidemiological dynamics could change abruptly. Some studies have considered the effect of the DTR (diurnal temperature range) on *Aedes* epidemiology (Liu-Helmersson et al., 2014). They do so because – even compared to the seasonal cycles of this model – day-night temperatures can change outbreak potential; large diurnal cycles will expose mosquitoes (and the viruses they carry) to rapid changes in climatic suitability. These daily cycles are averaged over by the seasonal trends we employ, and we therefore advocate the further investigation of daily in combination with seasonal cycles.

We model the effects of temperature as acting on the vital rates of the mosquitoes (e.g. egg-laying rate, survival), not directly on the parameters of competition ($\beta$ and $\delta$). Consequently, any affect temperature has on competitive outcomes are indirectly mediated by changes in other temperature-dependent life history parameters, not through changes to the competition parameters *themselves*. This is a reasonable assumption, provided that the way in which mosquito species interact competitively does not change as a function of temperature. Should coefficients of competition also be functions of temperature (i.e. $\beta(t) = f(T)$ and $\delta(t) = f(T)$), then our model could misrepresent the outcomes of competition. For example, say *Ae. aegypti*

larvae consume resources at faster than *Ae. albopictus* at high temperatures but slower at low temperatures. In this case, the coefficients $\beta_i$ would in this case need to be dynamic model variables to capture the fact that the costs associated with heterospecifics larval density would change with temperature. We felt that, at present, there is insufficient data to include these hypothetical temperature-dependent competition parameters accurately in our model, but note that they could fundamentally change model predictions.

It is possible that the functional forms and parameterisations of the temperature responses from Mordecai et al. (2017) might not be transferable between all populations and to all field settings; indeed different strains of the same mosquitoes can exhibit different vital rates (Leisnham et al., 2009). A key dependency for vectorial capacity is adult lifespan, as is highlighted by our sensitivity analysis. Senescence in mosquitoes can result in faster mortality rates for older adults, and has been explored experimentally for *Ae. aegypti* (Styer et al., 2007) and quantified for both species by Brady et al. (2013). In our model, *Ae. albopictus* adults can live far longer than *Ae. aegypti* adults (see appendix C.1), with the model assuming that even very old adults will exhibit the same vital rates as younger adults. Brady et al. (2013) analysed the thermal niche of adult survival for both *Ae. aegypti* and *Ae. albopictus*. Like Mordecai et al. (2017), their analysis also finds that *Ae. albopictus* adults have a significantly longer lifespan than *Ae. aegypti*, with a narrower thermal niche. However, they also find that a generalised additive model was required to capture nonlinearities in the thermal responses, whereas Mordecai et al. (2017) found that a quadratic function with an exponential decay was sufficient. Our model does not capture changes in mortality across the mosquito lifespan, which is likely to be very important for *Ae. albopictus*, given it can live so long. Moreover, Brady et al. (2013) reconcile their lab-based estimates with mark-release-recapture studies to correct for additional field-induced mortality, which we do not do here. Moreover, the data collated by Mordecai et al. (2017) showed considerable within- and between-study variance, which is not reflected in the temperature-dependent functions used in our simulations. Even if the *precise* parameters used in the temperature-dependent life-history functions are inaccurate in some contexts, it seems likely that the broad qualitative findings from our model are robust provided general patterns of inter-species differences in temperature response are maintained.

In our model, mosquito development and ecology are described using two competitive mechanisms (larval competition and reproductive interference). With respect to larval density-dependent competition, we describe a penalty in survivorship, not a penalty on development time (both of which occur in *Aedes* as a consequence of competition (Juliano, 2009)). This is defensible, as we are unaware of data extensive enough to parameterise a function to describe species-specific changes in development time with respect to temperature, conspecific and heterospecific densities. However, this interaction is likely to be important for competitive outcomes, as the time spent in the juvenile class will determine exposure to mortality associated with heterospecific competitors. We also neglect theoretical advancements made with respect to modelling reproductive interference; Kyogoku and Sota (2017) advanced Kuno's (1992) original formulation considerably by making the costs of reproductive interference a function of the *density* rather than just the *frequency* of heterospecifics.

Mosquito ecology is affected by a complex, multivariate function of biotic and abiotic conditions. The goal of insightful models of mosquito dynamics is to decide on an interpretable level of complexity, by selecting the most informative mechanistic drivers. We have included temperature, larval density-dependent mortality and reproductive interference as mechanisms in our model. Future models could include precipitation, host availability or density-dependent development rates as extensions; this will certainly make substantial changes to model-predicted outcomes of competition and epidemiology.

## Conclusion

Past studies that modelled inter-*Aedes* competition ignored temperature-dependent mosquito ecology and epidemiology. We reveal that patterns of disease outbreaks are highly sensitive to temperature because climate will determine both the population sizes of vector populations while also interacting with a number of temperature-sensitive epidemiological parameters (e.g. biting rates, infection probabilities). This results in patterns of outbreaks that would not be produced by temperature-invariant models. Our model shows that *Ae. albopictus* is likely to out-compete *Ae. aegypti* even when its larvae are not competitively equivalent. This advantage is reduced by reproductive interference and overcompensatory density-dependence, and is increased in colder climates with larger temperature cycles (such as Florida). Our model predicts that the hydra-effect could operate in *Aedes* populations; when larval competition is absent, equilibrium population sizes of both species can be increased by asymmetric reproductive interference. However, this effect does not occur when larval competition is high; in this case *Ae. albopictus* dominates. This work has advanced our understanding of climate-specific outcomes of competitive interaction in *Aedes* and reveals the complexities of temperature-epidemiology interactions. This information is useful for those aiming to mitigate arbovirus transmission by controlling vector populations in the field.

# 5 | DISCUSSION

I began my thesis by introducing *Ae. aegypti* and *Ae. albopictus* as arbovirus vectors with distributions that are, at least in part, shaped by interspecific competition. Determining the drivers of vector distributions is vital for the effective mitigation of vector-borne disease, motivating the work in my thesis. Using mathematical models and an empirical study, I explored the relative roles of reproductive interference and larval competition. In this discussion, I draw together the most important lessons from my work chapters.

## The interplay of ecological and epidemiological dynamics

An emergent theme of Chapters 2 and 4 is the inter-dependency of ecological and epidemiological processes. The intuition that ecology matters for vector-borne disease is not novel in itself; it was identified as far back as Finlay (Finlay, 1881). However, what *is* novel, is the finding that the interactions between mosquito species can play a pivotal role in disease transmission. This is exemplified by the model I present in my second chapter, where I was able to demonstrate that host choice and availability were important not only for transmission (Yakob, 2016), but also for determining the costs of reproductive interference. By mediating the strength of reproductive interference, host selection consequently determined mosquito presence and abundance, further affecting transmission. Moreover, in Chapter 4, an analysis of the model-derived vectorial capacity revealed that some of the most important determinants of vector competence were ecological traits (such as larval development rate) as opposed to processes that *directly* related to infection (e.g. infection probability). This emphasises the importance of mosquito ecology for the transmission of vector-borne disease.

The process of host choice and availability is important as it also provides an explanation as to why *Ae. albopictus* might not achieve the vectorial capacity predicted by my model in Chapter 4 in field settings. *Ae. albopictus* is generally considered a secondary vector of arboviruses, but it has nonetheless been implicated in arbovirus outbreaks (Delatte et al., 2010; Paupy et al., 2010). The risk of *Ae. albopictus* emerging as a principle vector of disease has long been acknowledged; its broader distribution and ability to undergo embryonic diapause (Diniz et al., 2017) could potentially bring arboviruses into more temperature climates, such as Europe and North America (Kraemer et al., 2019). *Ae. albopictus* is generally less urbanised than *Ae. aegypti* (Lounibos et al., 2016; Rey et al., 2006) and prefers to bite and rest outdoors (Paupy et al., 2009; Richards et al., 2006). These traits are likely to be inter-dependent; living in habitats with lower human densities will reduce availability, while potential preferences for other hosts could see further (even non-linear) reductions in human-host use (Paton and Bonsall, 2019). The future vectorial proficiency of *Ae. albopictus* is likely to be contingent

on future patterns of land-use (that could reduce host choice and promote anthropophily), climate change (expanding distributions) and its continued competitive interactions with *Ae. aegypti* (Messina et al., 2015).

### Climate-dependent competition

My model in Chapter 4 examined how temperature could alter the outcomes of larval and adult competition. What is clear is that temperature – even if not acting *directly* on the coefficients of competition – can have a significant impact on competitive outcomes. Most notable was that *Ae. albopictus* was found to be the superior larval stage competitor across all the climates I examined. This discrepancy was the most pronounced in a Florida-type climate; this is notable, as it rapidly displaced *Ae. aegypti* in much of the state (O'Meara et al., 1995).

Evidence presented by Camara et al. (2016) suggests that the costs of larval competition can vary across seasons in Brazil. In their experiments, they assessed seasonal penalties in survivorship and development time for *Ae. aegypti* larvae under different densities of *Ae. albopictus*; in spring, penalties for *Ae. aegypti* larval survivourship were smaller than in later seasons. The authors suggest that this processes could be maintaining species coexistence in parts of Brazil. Costanzo et al. (2005) demonstrated that *Ae. aegypti* eggs were more desiccation resistant, meaning hatching rates were higher than *Ae. albopictus*. Coming out of periods of low precipitation, *Ae. aegypti* may be at a competitive advantage because more of its larvae will successfully emerge into pools with fewer heterospecifics. Evidence therefore suggests that the costs of competition vary through time.

Seasonality could also lead to temporal variation in the costs of reproductive interference. In both of the models in Chapters 2 and 4, I use a frequency-dependent function to describe reproductive interference. Kyogoku and Sota (2017) present a more complex model of reproductive interference that accounts not only for the relative frequencies of the two species, but also the *density* of conspecifics and heterospecifics. Their model can predict very low costs of reproductive interference when adult densities are low, as heterospecific encounter rates are likely to be minimal. One can imagine a seasonal component to reproductive interference; at the start of seasons when adult population densities are low, reproductive interference will incur negligible costs. Then, when adult densities increase later in the season, costs will be far greater. Larval development times will be critical here, as the species whose larvae can emerge first will suffer less reproductive interference than a competitor which generally emerges later. That being said, the frequency-dependent approximation of reproductive interference I employ is likely to be an accurate representation of reproductive interference in more stable climates, where densities of mosquitoes remain high enough to incur the costs of reproductive interference for most of the year. Moreover, as hosts are used as beacons to find mates, even at low densities heterospecific mosquitoes could still encounter each other (Paton and Bonsall, 2019; Yuval, 2006).

Context-dependent (both seasonal and spatial) costs of competition leads to a broader point about how it makes most sense to think about mosquito population regulation. Strong (1986) proposed "density-vague"

processes as a mechanism of "liberal" population regulation. He suggests that instead of the hard limits imposed by density-dependent within- and between-species regulation (that cause populations to tend to static equilibria), regulation might instead only act when hierarchically more important abiotic processes no longer limit populations. For temperature-sensitive ectotherms in patchy environments, there may be periods where the costs from abiotic conditions on adults (e.g lifespans (Brady et al., 2013)) and sub-adults (e.g. egg desiccation (Costanzo et al., 2005)) could be more limiting than con- or heterospecific density. This is not to say that competition does not occur, just that its rank-order importance is reduced in relation to abiotic variables at some points in time. This seems a sensible way to think of *Aedes* interspecies competition; abiotic conditions may reduce the effect of competitive processes such as larval competition and reproductive interference before they "kick-in" when populations increase in size in good times.

### The spatio-temporal dynamics of larval competition

The experiments I present in Chapter 3 uniquely demonstrate that interspecific competition can occur even when larvae theoretically have the necessary resources to pupate. My experiments were not intended to reach a specific conclusion as to which mosquito was *ubiquitously* the superior larval-stage competitor; the context-dependence in larval competition renders this aim unrealistic (Juliano, 2010). Instead, I aimed to document how competition can operate under a specific resource regime. At the start of the mosquito season, *Aedes* eggs could, in some cases, hatch into resource-rich larval habitats that are yet to be exploited; my design mimics these circumstances, as larvae are theoretically not resource limited. However, I still find evidence of competition; we posit that this as due to different resource uptake rates of larvae of the same age. The extrapolation of laboratory findings to the field must be approached with an appropriate degree of scepticism; controlling for a range of abiotic variables (e.g. temperature and humidity) in the lab is both a benefit and limitation. Furthermore, the mosquito strains I used had been in captivity for different lengths of time and came from different localities; this is vitally important due to population-specific life-history traits that can influence the outcomes of competition (Leisnham et al., 2009). Moreover, in my case, I use a high-quality larval resource (liver powder) that is not available to larvae in the field. Nonetheless, the reduction approach I employ has revealed an interesting aspect of mosquito competition.

My experiments consider only a single generation; while discrete-generation experiments are useful, they do not replicate the continuous process of reproduction exhibited in wild *Aedes* populations. There are generally a spectrum of ages in larval pools, with different stages requiring different amounts of resources and driving density-dependent resource competition (Juliano, 2009). In the field, the resources in larval habitats are replenished by chance events (e.g. water run-off bringing detritus). Resource replenishment will fundamentally shape the life-chances of larvae in the pool, and determine the extent of intra- and interspecific competition.

Inter-species larval competition is one of the most important drivers of *Aedes* distributions, as evidenced by my models in Chapters 2 and 4, as well as a range of field evidence (Juliano, 2009, 2010; Lounibos and

Juliano, 2018). My – and most – models average over intra-pool differences in habitat quality; the carrying capacity is represented by a single parameter for the entire location. The size of larval pools means that at almost all scales, the distribution and conditions in larval habitats will be spatially heterogeneous. Moreover, habitat heterogeneity is likely increased in urban landscape, where man-made containers supplement natural pools (Lounibos et al., 2010). The constituent larval habitats in an environment will likely manifest different costs of larval competition in resident larvae. For instance, differences in resource replenishment rates (resource availability), exposure to sunlight and precipitation, and water volume (related to permanence) will mean that larval habitats are very different places across even a small area. Indeed, Lounibos et al. (2010) demonstrate that micro-climatic differences in habitat mediated competition in Florida. Furthermore, *Aedes* females have been documented to "skip-oviposit"; they preferentially deposit their eggs in favourable (low-density, high resource) larval habitats, provided they are accessible in space (Davis et al., 2015). This means that even the *utilisation* of habitats will be heterogeneous in space, due to adult females seeking the best conditions for offspring.

This spatial heterogeneity gives rise to a question: to what extent does averaging over differences in larval habitat mean that important dynamics are missed? Some model frameworks aim to account for this heterogeneity by simulating individual larval habitats across space. For instance, simulation models such as the container-inhabiting mosquito simulation model (CIMSiM) (Focks et al., 1993) (which was subsequently modified to become the Skeeter Buster model (Magori et al., 2009)) drill down to fine-scale differences in larval physiology and development across heterogeneous larval habitats. They have proved to be powerful predictive tools for modelling adult populations in real word settings. However, with granularity comes complexity; a multitude of (potentially very sensitive) model parameters must be determined, for which data may be unavailable or uncertain. Moreover, including additional processes in these simulation models (e.g. interspecific larval competition) is challenging, as the competitive interactions must be accurately represented across a myriad of different habitat conditions. This will require numerous parameters and a detailed mechanistic understanding of competition in a wide variety of circumstances. At the other end of the spectrum is the model I presented in Chapter 2; processes are idealised and simplified in order to describe broad-brush processes. For different model applications, objectives and questions, the importance of spatial heterogeneity could prove pivotal for conclusions.

### Lessons for vector control

The added realism of the variable delay model I present in Chapter 4 has obvious application for vector control; modelling mosquito dynamics with dynamic stage durations makes predicted seasonal population sizes more accurate. The timing of mosquito releases can be pivotal in the effectiveness of control (White et al., 2010), making temperature-driven mosquito cycles important for maximising intervention efficacy. Extending the modelling framework in Chapter 4 to include transgenic or sterile mosquito releases would be worthwhile; for instance, models typically represent fitness penalties in released males as reduced mating com-

petitiveness (e.g. White et al. (2010)). However, under varying temperatures (either diurnal (Liu, 2015) or through seasons), released males could prove less robust and have higher mortality rates. Indeed, the analysis presented by Brady et al. (2013) demonstrates that adult mosquito mortality can vary non-linearly with both temperature and adult age, raising questions for the fitness of released males in field contexts. Control methods – such as *Wolbachia*-infected mosquitoes – have already been shown to be sensitive to intraspecific larval competition (Hancock et al., 2016). Future empirical studies could consider between-species interactions also.

In Chapter 2, I mention that reproductive interference has the potential to interact with mosquito releases. Reproductive interference was modelled with a function that described the frequency-dependent reduction in the proportion of successful matings ($P_i$) for *Ae. aegypti* (species *A*) and *Ae. albopictus* (species *B*) in the presence of heterospecific adults (taken from Kuno (1992)). This is given by the equations:

$$P_A = \frac{A}{(A + \delta_A B)} \tag{5.1}$$

$$P_B = \frac{B}{(B + \delta_B A)} \tag{5.2}$$

with $\delta_i$ the cost of reproductive interference. This form is similar to the penalty applied in models of sterile and transgenic mosquito releases (Bonsall et al., 2010; White et al., 2010; Yakob et al., 2008). If we imagine that one species (say *A*) is targeted by releases of sterile males (denoted $A_S$), then equations 5.1 and 5.2 for both species would become:

$$P_A = \frac{A}{(A + A_S + \delta_A B)} \tag{5.3}$$

$$P_B = \frac{B}{(B + \delta_B [A + A_s])} \tag{5.4}$$

Note that now, species *B* will now be indirectly affected by the releases aimed at species *A*, because of reproductive interference. Given we know that *Ae. albopictus* exhibits the hydra-effect under lab-conditions (McIntire and Juliano, 2018), then the possibility clearly exists for unfavourable "spill-over" effects that would see *Ae. albopictus* populations increase due to exposure to sterile heterospecifics. More generally, the most important recommendation that emerges from my work is the development of models that explicitly model control in the presence of interspecific interactions, so that unintended consequences can be better predicted.

## Conclusions

The interactions between species are fundamental to ecology (Morin, 2011), determining the presence and abundance of species. In my thesis, I have investigated larval interspecific competition and reproductive interference as mechanisms driving the distributions of the arbovirus vectors *Ae. aegypti* and *Ae. albopictus*. My first model revealed the potential importance of the process of host choice, my empirical results highlighted

the occurrence of demographically-mediated density-dependent competition and my final model identified climate-mediated outcomes of larval competition. There are numerous ways in which my work could be expanded, the most pressing being the incorporation of vector control directly into models that include detailed representations of mosquito competition. Those planning future transgenic or sterile insect releases should carefully consider the implications of interspecific interactions for control; for instance, could the competing mosquito be facilitated through the exclusion of the other? As anthropogenic emissions alter climates, human movements transport invasive species to new regions and urban environments grow, *Aedes* distributions are almost certainly set to expand (Kraemer et al., 2019; Messina et al., 2015). The evidence in this thesis demonstrates that an understanding of the competitive interactions between *Ae. aegypti* and *Ae. albopictus* will be essential if we are to successfully control arboviruses in the future.

# BIBLIOGRAPHY

Abrams, P.A., 2009. When does greater mortality increase population size? The long history and diverse mechanisms underlying the hydra effect. Ecology Letters 12, 462–474.

Alphey, L., 2002. Re-engineering the sterile insect technique. Insect Biochemistry and Molecular Biology 32, 1243–1247.

Alphey, L., 2014. Genetic control of mosquitoes. Annu. Rev. Entomol 59, 205–224.

Alphey, L., Alphey, N., 2014. Five things to know about genetically modified (GM) insects for vector control. PLoS Pathogens 10, 3–5.

Alphey, L., Benedict, M., Bellini, R., Clark, G.G., Dame, D.A., Service, M.W., Dobson, S.L., 2010. Sterile-insect methods for control of mosquito-borne diseases: an analysis. Vector borne and zoonotic diseases (Larchmont, N.Y.) 10, 295–311.

Alphey, N., Alphey, L., Bonsall, M.B., 2011. A model framework to estimate impact and cost of genetics-based sterile insect methods for dengue vector control. PLoS ONE 6, e25384.

Alto, B.W., Lounibos, L.P., Higgs, S., Juliano, S.A., 2005. Larval competition differentially affects arbovirus infection in *Aedes* mosquitoes. Ecology 86, 3279–3288.

Alto, B.W., Lounibos, L.P., Mores, C.N., Reiskind, M.H., 2008. Larval competition alters susceptibility of adult *Aedes* mosquitoes to dengue infection. Proceedings of the Royal Society B: Biological Sciences 275, 463–471.

Amarasekare, P., 2003. Competitive coexistence in spatially structured environments: a synthesis. Ecology Letters 6, 1109–1122.

Armstrong, R.A., McGehee, R., 1980. Competitive exclusion. The American Naturalist 115, 151–170.

Bagny, L., Delatte, H., Quilici, S., Fontenille, D., Bagny, L.A., 2009. Progressive decrease in *Aedes aegypti* distribution in Reunion Island since the 1900s. Journal of medical entomology 46, 1541–1545.

Bara, J., Rapti, Z., Cáceres, C.E., Muturi, E.J., 2015. Effect of larval competition on extrinsic incubation period and vectorial capacity of *Aedes albopictus* for dengue virus. PLOS ONE 10, e0126703.

Bargielowski, I.E., Lounibos, L.P., 2016. Satyrization and satyrization-resistance in competitive displacements of invasive mosquito species. Insect Science 23, 162–174.

Bargielowski, I.E., Lounibos, L.P., Carrasquilla, M.C., 2013. Evolution of resistance to satyrization through reproductive character displacement in populations of invasive dengue vectors. Proceedings of the National Academy of Sciences 110, 2888–2892.

Barrera, R., 1996. Competition and resistance to starvation in larvae of container-inhabiting *Aedes* mosquitoes. Ecological Entomology 21, 117–127.

Beck-Johnson, L.M., Nelson, W.A., Paaijmans, K.P., Read, A., Thomas, M.B., Bjørnstad, O.N., 2017. The importance of temperature fluctuations in understanding mosquito population dynamics and malaria risk. Royal Society Open Science 4.

Beck-Johnson, L.M., Nelson, W.A., Paaijmans, K.P., Read, A.F., Thomas, M.B., Bjørnstad, O.N., 2013. The effect of temperature on *Anopheles* mosquito population dynamics and the potential for malaria transmission. PLoS ONE 8.

Bellows, T., 1981. The descriptive properties of some models for density-dependence. Journal of Animal Ecology 50, 139–156.

Bhatt, S., Gething, P.W., Brady, O.J., Messina, J.P., Farlow, A.W., Moyes, C.L., Drake, J.M., Brownstein, J.S., Hoen, A.G., Sankoh, O., Myers, M.F., George, D.B., Jaenisch, T., Wint, G.R.W., Simmons, C.P., Scott, T.W., Farrar, J.J., Hay, S.I., 2013. The global distribution and burden of dengue. Nature 496, 504–507.

Black, I.V.W.C., Rai, K.S., Turco, B.J., Arroyo, D.C., 1989. Laboratory study of competition between United States strains of *Aedes albopictus* and *Aedes aegypti* (*Diptera: Culicidae*). Journal of Medical Entomology 26, 260–271.

Black, W.C., Bennett, K.E., Gorrochótegui-Escalante, N., Barillas-Mury, C.V., Fernández-Salas, I., de Lourdes Muñoz, M., Farfán-Alé, J.A., Olson, K.E., Beaty, B.J., 2002. Flavivirus susceptibility in *Aedes aegypti*. Archives of Medical Research 33, 379–388.

Blythe, S.P., Nisbet, R.M., Gurney, W.S., 1984. The dynamics of population models with distributed maturation periods. Theoretical Population Biology 25, 289–311.

Bonizzoni, M., Gasperi, G., Chen, X., James, A.A., 2013. The invasive mosquito species *Aedes albopictus*: current knowledge and future perspectives. Trends in Parasitology 29, 460–468.

Bonsall, M.B., Hassell, M.P., 1997. Apparent competition structures ecological assemblages. Nature 388, 371–373.

Bonsall, M.B., Yakob, L., Alphey, N., Alphey, L., 2010. Transgenic control of vectors: the effects of interspecific interactions. Israel Journal of Ecology and Evolution 56, 353–370.

Brady, O.J., Godfray, H.C.J., Tatem, A.J., Gething, P.W., Cohen, J.M., Ellis McKenzie, F., Alex Perkins, T., Reiner, R.C., Tusting, L.S., Sinka, M.E., Moyes, C.L., Eckhoff, P.A., Scott, T.W., Lindsay, S.W., Hay, S.I., Smith, D.L., 2016. Vectorial capacity and vector control: reconsidering sensitivity to parameters for malaria elimination. Transactions of the Royal Society of Tropical Medicine and Hygiene 110, 107–117.

Brady, O.J., Golding, N., Pigott, D.M., Kraemer, M.U., Messina, J.P., Reiner, R.C., Scott, T.W., Smith, D.L., Gething, P.W., Hay, S.I., 2014. Global temperature constraints on *Aedes aegypti* and *Ae. albopictus* persistence and competence for dengue virus transmission. Parasites and Vectors 7, 338.

Brady, O.J., Johansson, M.A., Guerra, C.A., Bhatt, S., Golding, N., Pigott, D.M., Delatte, H., Grech, M.G., Leisnham, P.T., Maciel-de Freitas, R., Styer, L.M., Smith, D.L., Scott, T.W., Gething, P.W., Hay, S.I., 2013. Modelling adult *Aedes aegypti* and *Aedes albopictus* survival at different temperatures in laboratory and field settings. Parasites Vectors 6, 351.

Braks, M.A.H., Honório, N.A., Lounibos, L.P., Lourenço-de Oliveira, R., Juliano, S.A., 2004. Interspecific competition between two invasive species of container mosquitoes, *Aedes aegypti* and *Aedes albopictus* (*Diptera: Culicidae*), in Brazil. Annals of the Entomological Society of America 97, 130–139.

Braks, M.a.H., Honório, N.a., Lourençqo-de Oliveira, R., Juliano, S.A., Lounibos, L.P., 2003. Convergent habitat segregation of *Aedes aegypti* and *Aedes albopictus* (*Diptera: Culicidae*) in southeastern Brazil and Florida. Journal of medical entomology 40, 785–794.

Brieré, J.F., Pracros, P., Le Roux, A.Y., Pierre, J.S., 1999. A novel rate model of temperature-dependent development for arthropods. Environmental Entomology 28, 22–29.

Brown, J.E., Evans, B.R., Zheng, W., Obas, V., Barrera-Martinez, L., Egizi, A., Zhao, H., Caccone, A., Powell, J.R., 2014. Human impacts have shaped historical and recent evolution in *Aedes aegypti*, the dengue and yellow fever mosquito. Evolution 68, 514–525.

Buchman, A., Gamez, S., Li, M., Antoshechkin, I., Li, H.H., Wang, H.W., Chen, C.H., Klein, M.J., Duchemin, J.B., Paradkar, P.N., Akbari, O.S., 2019. Engineered resistance to Zika virus in transgenic *Aedes aegypti* expressing a polycistronic cluster of synthetic small RNAs. Proceedings of the National Academy of Sciences 116, 3656–3661.

Burdfield-Steel, E.R., Shuker, D.M., 2011. Reproductive interference. Current Biology 21, R450–R451.

Camara, D.C.P., Codeço, C.T., Juliano, S.A., Lounibos, L.P., Riback, T.I.S., Pereira, G.R., Honorio, N.A., 2016. Seasonal differences in density but similar competitive impact of *Aedes albopictus* (Skuse) on *Aedes aegypti* (L.) in Rio de Janeiro, Brazil. PLOS ONE 11, e0157120.

Carrasquilla, M.C., Lounibos, L.P., 2015. Satyrization without evidence of successful insemination from interspecific mating between invasive mosquitoes. Biology letters 11, 20150527.

Carvalho, D.O., McKemey, A.R., Garziera, L., Lacroix, R., Donnelly, C.A., Alphey, L., Malavasi, A., Capurro, M.L., 2015. Suppression of a field population of *Aedes aegypti* in Brazil by sustained release of transgenic male mosquitoes. PLoS neglected tropical diseases 9, e0003864.

Cator, L.J., Arthur, B.J., Harrington, L.C., Hoy, R.R., 2009. Harmonic convergence in the love songs of the dengue vector mosquito. Science 323, 1077–1079.

Chamberlain, S.A., Bronstein, J.L., Rudgers, J.A., 2014. How context dependent are species interactions? Ecology Letters 17, 881–890.

Chesson, P., 2000. Mechanisms of maintenance of species diversity. Annual Review of Ecology and Systematics 31, 343–366.

Chouin-Carneiro, T., Vega-Rua, A., Vazeille, M., Yebakima, A., Girod, R., Goindin, D., Dupont-Rouzeyrol, M., Lourenço-de Oliveira, R., Failloux, A.B., 2016. Differential Susceptibilities of *Aedes aegypti* and *Aedes albopictus* from the Americas to Zika Virus. PLOS Neglected Tropical Diseases 10, e0004543.

Christofferson, R., Mores, C., 2015. A role for vector control in dengue vaccine programs. Vaccine 33, 7069–7074.

Cohen, J., 2016. The race for a Zika vaccine is on. Science 351, 543–544.

Colton, Y.M., Chadee, D.D., Severson, D.W., 2003. Natural skip oviposition of the mosquito *Aedes aegypti* indicated by codominant genetic markers. Medical and Veterinary Entomology 17, 195–204.

Cornel, A.J., Hunt, R.H., 1991. *Aedes albopictus* in Africa? First records of live specimens in imported tires in Cape Town. Journal of the American Mosquito Control Association 7, 107–108.

Costanzo, K.S., Kesavaraju, B., Juliano, S.A., 2005. Condition-specific competition in container mosquitoes: the role of noncompeting life-history stages. Ecology 86, 3289–3295.

Crainiceanu, C.M., Ruppert, D., Wand, M.P., 2005. Bayesian analysis for penalized spline regression using WinBUGS. Journal of Statistical Software 14, 1–24.

Daugherty, M.P., Alto, B.W., Juliano, S., 2000. Invertebrate carcasses as a resource for competing *Aedes albopictus* and *Aedes aegypti* (*Diptera: Culicidae*). Journal of medical entomology 37, 364–372.

Davis, T.J., Kaufman, P.E., Hogsette, J.A., Kline, D.L., 2015. The effects of larval habitat quality on *Aedes albopictus* skip oviposition . Journal of the American Mosquito Control Association 31, 321–328.

de Roos, A.M., Persson, L., 2003. Competition in size-structured populations: mechanisms inducing cohort formation and population cycles. Theoretical Population Biology 63, 1–16.

Delatte, H., Desvars, A., Bouétard, A., Bord, S., Gimonneau, G., Vourc'h, G., Fontenille, D., 2010. Blood-feeding behavior of *Aedes albopictus*, a vector of chikungunya on La Réunion. Vector-Borne and Zoonotic Diseases 10, 249–258.

Delatte, H., Gimonneau, G., Triboire, A., Fontenille, D., 2009. Influence of temperature on immature development, survival, longevity, fecundity, and gonotrophic cycles of *Ae. albopictus*, vector of chikungunya and dengue in the Indian Ocean. Journal of Medical Entomology 46, 33–41.

Dellaportas, P., Forster, J., Ntzoufras, I., 2000. Bayesian variable selection using the Gibbs sampler, in: Dey, D., Ghosh, S., Mallick, B. (Ed.), Generalized linear models: a Bayesian perspective. 5 ed.. Marcel Dekker, Inc., New York. volume 5, pp. 273–286.

Diniz, D.F.A., de Albuquerque, C.M.R., Oliva, L.O., de Melo-Santos, M.A.V., Ayres, C.F.J., 2017. Diapause and quiescence: dormancy mechanisms that contribute to the geographical expansion of mosquitoes and their evolutionary success. Parasites and Vectors 10, 1–13.

Dritsou, V., Topalis, P., Windbichler, N., Simoni, A., Hall, A., Lawson, D., Hinsley, M., Hughes, D., Napolioni, V., Crucianelli, F., Deligianni, E., Gasperi, G., Gomulski, L.M., Savini, G., Manni, M., Scolari, F., Malacrida, A.R., Arcà, B., Ribeiro, J.M., Lombardo, F., Saccone, G., Salvemini, M., Moretti, R., Aprea, G., Calvitti, M., Picciolini, M., Papathanos, P.A., Spaccapelo, R., Favia, G., Crisanti, A., Louis, C., 2015. A draft genome sequence of an invasive mosquito: an Italian *Aedes albopictus*. Pathogens and Global Health 109, 207–220.

Dye, C., 1982. Intraspecific competition amongst larval *Aedes aegypti*: food exploitation or chemical interference? Ecological Entomology 7, 39–46.

Dye, C., 1984a. Competition amongst larval *Aedes aegypti*: the role of interference. Ecological Entomology 9, 355–357.

Dye, C., 1984b. Models for the population dynamics of the yellow fever mosquito, *Aedes aegypti*. British Ecological Society 53, 247–268.

Dye, C., 1992. Transmission by bloodsucking insects. Annual Reviews Entomology 37, 1–19.

Edman, J.D., 1971. Host-feeding patterns of Florida mosquitoes I. *Aedes*, *Anopheles*, *Coquillettidia*, *Mansonia* and *Psorophora* (1). Journal of Medical Entomology 8, 687–695.

Eidex, R.B., 2004. History of thymoma and yellow fever vaccination. The Lancet 364, 936.

Elith, J., Leathwick, J.R., 2009. Species distribution models: ecological explanation and prediction across space and time. Annual Review of Ecology, Evolution, and Systematics 40, 677–697.

Erickson, R.A., Presley, S.M., Allen, L.J., Long, K.R., Cox, S.B., 2010a. A dengue model with a dynamic *Aedes albopictus* vector population. Ecological Modelling 221, 2899–2908.

Erickson, R.A., Presley, S.M., Allen, L.J., Long, K.R., Cox, S.B., 2010b. A stage-structured, *Aedes albopictus* population model. Ecological Modelling 221, 1273–1282.

Eritja, R., Palmer, J.R., Roiz, D., Sanpera-Calbet, I., Bartumeus, F., 2017. Direct evidence of adult *Aedes albopictus* dispersal by car. Scientific Reports 7, 1–15.

Ewing, D.A., Cobbold, C.A., Purse, B.V., Nunn, M.A., White, S.M., 2016. Modelling the effect of temperature on the seasonal population dynamics of temperate mosquitoes. Journal of Theoretical Biology 400, 65–79.

Ewing, D.A., Purse, B.V., Cobbold, C.A., Schäfer, S.M., White, S.M., 2019. Uncovering mechanisms behind mosquito seasonality by integrating mathematical models and daily empirical population data: *Culex pipiens* in the UK. Parasites and Vectors 12, 1–19.

Faria, N.R., Do Socorro Da Silva Azevedo, R., Kraemer, M.U., Souza, R., Cunha, M.S., Hill, S.C., Thézé, J., Bonsall, M.B., Bowden, T.A., Rissanen, I., Rocco, I.M., Nogueira, J.S., Maeda, A.Y., Da Silva Vasami, F.G., de Lima Macedo, F.L., Suzuki, A., Rodrigues, S.G., Cruz, A.C.R., Nunes, B.T., de Almeida Medeiros, D.B., Rodrigues, D.S.G., Queiroz, A.L.N., Da Silva, E.V.P., Henriques, D.F., Da Rosa, E.S.T., de Oliveira, C.S., Martins, L.C., Vasconcelos, H.B., Casseb, L.M.N., de Brito Simith, D., Messina, J.P., Abade, L., Lourenço, J., Alcantara, L.C., de Lima, M.M., Giovanetti, M., Hay, S.I., de Oliveira, R.S., Da Silva Lemos, P., de Oliveira, L.F., de Lima, C.P.S., Da Silva, S.P., de Vasconcelos, J.M., Franco, L., Cardoso, J.F., Da Silva Gonçalves Vianez-Júnior, J.L., Mir, D., Bello, G., Delatorre, E., Khan, K., Creatore, M., Coelho, G.E., de Oliveira, W.K., Tesh, R., Pybus, O.G., Nunes, M.R., Vasconcelos, P.F., 2016. Zika virus in the Americas: early epidemiological and genetic findings. Science 352, 345–349.

Farjana, T., Tuno, N., Higa, Y., 2012. Effects of temperature and diet on development and interspecies competition in *Aedes aegypti* and *Aedes albopictus*. Medical and Veterinary Entomology 26, 210–217.

Finlay, J.C., 1881. El mosquito hipoteticamente considerado como agente de trasmision de la fiebre amarilla. Anales de la Real Academia de Ciencias Médicas, Físicas y Naturales de la Habana 18, 147–169.

Focks, D.A., Haile, D.G., Daniels, E., Mount, G.A., 1993. Dynamic life table model for *Aedes aegypti* (*Diptera: Culicidae*): simulation results and validation. Journal of Medical Entomology 30, 1018–1028.

Gantz, V.M., Jasinskiene, N., Tatarenkova, O., Fazekas, A., Macias, V.M., Bier, E., James, A.A., 2015. Highly efficient Cas9-mediated gene drive for population modification of the malaria vector mosquito *Anopheles stephensi*. Proceedings of the National Academy of Sciences 112, E6736–E6743.

Garrett-Jones, C., 1964. The human blood index of malaria vectors in relation to epidemiological assessment. Bulletin of the World Health Organization 30, 241–61.

Gilotra, S.K., Rozeboom, L.E., Bhattacharya, N.C., 1967. Observations on possible competitive displacement between populations of *Aedes aegypti* Linnaeus and *Aedes albopictus* Skuse in Calcutta. Bulletin of the World Health Organization 37, 437–446.

Gorman, K., Young, J., Pineda, L., Márquez, R., Sosa, N., Bernal, D., Torres, R., Soto, Y., Lacroix, R., Naish, N., Kaiser, P., Tepedino, K., Philips, G., Kosmann, C., Cáceres, L., 2016. Short-term suppression of *Aedes aegypti* using genetic control does not facilitate *Aedes albopictus*. Pest Management Science 72, 618–628.

Gratz, N.G., 2004. Critical review of the vector status of *Aedes albopictus*. Medical and Veterinary Entomology 18, 215–227.

Gröning, J., Hochkirch, A., 2008. Reproductive interference between animal species. The Quarterly Review of Biology 83, 257–282.

Gubler, D., 1998a. Resurgent vector-borne diseases as a global health problem. Emerging Infectious Diseases 4, 442–450.

Gubler, D.J., 1998b. Dengue and dengue hemorrhagic fever, 1996. Clinical Microbiology Reviews 11, 480–496.

Gurney, W.S.C., Nisbet, R.M., Lawton, J.H., 1983. The systematic formulation of tractable single-species population models incorporating age structure. The Journal of Animal Ecology 52, 479.

Hancock, P.A., White, V.L., Callahan, A.G., Godfray, C.H., Hoffmann, A.A., Ritchie, S.A., 2016. Density-dependent population dynamics in *Aedes aegypti* slow the spread of wMel *Wolbachia*. Journal of Applied Ecology 53, 785–793.

Harris, A.F., McKemey, A.R., Nimmo, D., Curtis, Z., Black, I., Morgan, S.A., Oviedo, M.N., Lacroix, R., Naish, N., Morrison, N.I., Collado, A., Stevenson, J., Scaife, S., Dafa'Alla, T., Fu, G., Phillips, C., Miles, A., Raduan, N., Kelly, N., Beech, C., Donnelly, C.A., Petrie, W.D., Alphey, L., 2012. Successful suppression of a field mosquito population by sustained release of engineered male mosquitoes. Nature Biotechnology 30, 828–830.

Heath, K., Paton, R.S., Wilson, A.J., Bonsall, M.B., 2020. Resource availability, larval demographics and density-dependence in *Aedes aegypti*. Ecological Entomology .

Higham, D.J., 2001. An algorithmic introduction to numerical simulation of stochastic differential equations. SIAM Review 43, 525–546.

Hoffmann, A.A., Montgomery, B.L., Popovici, J., Iturbe-Ormaetxe, I., Johnson, P.H., Muzzi, F., Greenfield, M., Durkan, M., Leong, Y.S., Dong, Y., Cook, H., Axford, J., Callahan, A.G., Kenny, N., Omodei, C., McGraw, E.A., Ryan, P.A., Ritchie, S.A., Turelli, M., O'Neill, S.L., 2011. Successful establishment of *Wolbachia* in *Aedes* populations to suppress dengue transmission. Nature 476, 454–457.

Honório, N.A., Da Costa Silva, W., Leite, P.J., Gonçalves, J.M., Lounibos, L.P., Lourenço-de Oliveira, R., 2003. Dispersal of *Aedes aegypti* and *Aedes albopictus* (*Diptera: Culicidae*) in an urban endemic dengue area in the state of Rio de Janeiro, Brazil. Memorias do Instituto Oswaldo Cruz 98, 191–198.

Hutchinson, G.E., 1957. Concluding remarks. Cold Spring Harbor Symposia on Quantitative Biology 22, 415–427.

Jia, P., Liang, L., Tan, X., Chen, J., Chen, X., 2019. Potential effects of heat waves on the population dynamics of the dengue mosquito *Aedes albopictus*. PLOS Neglected Tropical Diseases 13, e0007528.

Jia, P., Lu, L., Chen, X., Chen, J., Guo, L., Yu, X., Liu, Q., 2016. A climate-driven mechanistic population model of *Aedes albopictus* with diapause. Parasites and Vectors 9, 1–15.

Juliano, S.a., 1998. Species introduction and replacement among mosquitoes: interspecific resource competition or apparent competition? Ecology 79, 255–268.

Juliano, S.A., 2009. Species interactions among larval mosquitoes: context dependence across habitat gradients. Annual Review of Entomology 54, 37–56.

Juliano, S.A., 2010. Coexistence, exclusion, or neutrality? A meta-analysis of competition between *Aedes albopictus* and resident mosquitoes. Israel Journal of Ecology and Evolution 56, 325–351.

Juliano, S.A., Lounibos, L.P., O'Meara, G.F., 2004. A field test for competitive effects of *Aedes albopictus* on *A. aegypti* in South Florida: differences between sites of coexistence and exclusion? Oecologia 139, 583–593.

Kaplan, L., Kendell, D., Robertson, D., Livdahl, T., Khatchikian, C., 2010. *Aedes aegypti* and *Aedes albopictus* in Bermuda: extinction, invasion and extinction. Biological Invasions 12, 3277–3288.

Kishi, S., Nakazawa, T., 2013. Analysis of species coexistence co-mediated by resource competition and reproductive interference. Population Ecology 55, 305–313.

Kishi, S., Nishida, T., Tsubaki, Y., 2009. Reproductive interference determines persistence and exclusion in species interactions. Journal of Animal Ecology 78, 1043–1049.

Knipling, E.F., 1959. Sterile-male method of population control. Science 130, 902–904.

Kohn, M., 1990. A survey on indoor resting mosquito species in Phnom Penh, Kampuchea. Folia Parasitologica 37, 165–174.

Kraemer, M.U., Reiner, R.C., Brady, O.J., Messina, J.P., Gilbert, M., Pigott, D.M., Yi, D., Johnson, K., Earl, L., Marczak, L.B., Shirude, S., Davis Weaver, N., Bisanzio, D., Perkins, T.A., Lai, S., Lu, X., Jones, P., Coelho, G.E., Carvalho, R.G., Van Bortel, W., Marsboom, C., Hendrickx, G., Schaffner, F., Moore, C.G., Nax, H.H., Bengtsson, L., Wetter, E., Tatem, A.J., Brownstein, J.S., Smith, D.L., Lambrechts, L., Cauchemez, S., Linard, C., Faria, N.R., Pybus, O.G., Scott, T.W., Liu, Q., Yu, H., Wint, G.R., Hay, S.I., Golding, N., 2019. Past and future spread of the arbovirus vectors *Aedes aegypti* and *Aedes albopictus*. Nature Microbiology 4, 854–863.

Kraemer, M.U., Sinka, M.E., Duda, K.A., Mylne, A.Q., Shearer, F.M., Barker, C.M., Moore, C.G., Carvalho, R.G., Coelho, G.E., Van Bortel, W., Hendrickx, G., Schaffner, F., Elyazar, I.R., Teng, H.J., Brady, O.J., Messina, J.P., Pigott, D.M., Scott, T.W., Smith, D.L., Wint, G.W., Golding, N., Hay, S.I., 2015. The global distribution of the arbovirus vectors *Aedes aegypti* and *Ae. albopictus*. eLife 4, 1–18.

Kruschke, J.K., 2015. Doing Bayesian data analysis, in: Kruschke, J.K. (Ed.), Doing Bayesian data analysis. second ed.. Academic Press, Boston, pp. 265–296.

Kuno, E., 1992. Competitive exclusion through reproductive interference. Researches on Population Ecology 34, 275–284.

Kyogoku, D., Sota, T., 2017. A generalized population dynamics model for reproductive interference with absolute density-dependence. Scientific Reports 7, 1–8.

Lacroix, R., McKemey, A.R., Raduan, N., Kwee Wee, L., Hong Ming, W., Guat Ney, T., Siti Rahidah, A.A., Salman, S., Subramaniam, S., Nordin, O., Norhaida Hanum, A.T., Angamuthu, C., Marlina Mansor, S., Lees, R.S., Naish, N., Scaife, S., Gray, P., Labbé, G., Beech, C., Nimmo, D., Alphey, L., Vasan, S.S., Han Lim, L., Wasi A., N., Murad, S., 2012. Open field release of genetically engineered sterile male *Aedes aegypti* in Malaysia. PLoS ONE 7, 1–9.

Lambrecht, F.L., 1971. Notes on the ecology of Seychelles mosquitoes. Bulletin of Entomological Research 60, 513–532.

Legros, M., Lloyd, A.L., Huang, Y., Gould, F., 2009. Density-dependent intraspecific competition in the larval stage of *Aedes aegypti* (*Diptera: Culicidae*): revisiting the current paradigm. Journal of Medical Entomology 46, 409–419.

Leisnham, P.T., Juliano, S.A., 2009. Spatial and temporal patterns of coexistence between competing *Aedes* mosquitoes in urban Florida. Oecologia 160, 343–352.

Leisnham, P.T., Lounibos, L.P., O'Meara, G.F., Juliano, S.A., 2009. Interpopulation divergence in competitive interactions of the mosquito *Aedes albopictus*. Ecology 90, 2405–2413.

Liang, G., Gao, X., Gould, E.A., 2015. Factors responsible for the emergence of arboviruses; strategies, challenges and limitations for their control. Emerging Microbes and Infections 4, 1–5.

Lindquist, D.A., Abusowa, M., Hall, M.J., 1992. The New World screwworm fly in Libya: a review of its introduction and eradication. Medical and veterinary entomology 6, 2–8.

Liu, N., 2015. Insecticide resistance in mosquitoes: impact, mechanisms, and research directions. Annual review of entomology 60, 537–559.

Liu-Helmersson, J., Stenlund, H., Wilder-Smith, A., Rocklöv, J., 2014. Vectorial capacity of *Aedes aegypti*: effects of temperature and implications for global dengue epidemic potential. PLoS ONE 9, e89783.

Lodewyckx, T., Kim, W., Lee, M.D., Tuerlinckx, F., Kuppens, P., Wagenmakers, E.J., 2011. A tutorial on Bayes factor estimation with the product space method. Journal of Mathematical Psychology 55, 331–347.

Lounibos, L.P., Bargielowski, I., Carrasquilla, M.C., Nishimura, N., 2016. Coexistence of *Aedes aegypti* and *Aedes albopictus* (*Diptera: Culicidae*) in Peninsular Florida Two Decades After Competitive Displacements. Journal of Medical Entomology 53, 1385–1390.

Lounibos, L.P., Juliano, S.A., 2018. Where vectors collide: the importance of mechanisms shaping the realized niche for modeling ranges of invasive *Aedes* mosquitoes. Biological Invasions 20, 1913–1929.

Lounibos, L.P., O'Meara, G.F., Juliano, S.A., Nishimura, N., Escher, R.L., Reiskind, M.H., Cutwa, M., Greene, K., 2010. Differential survivorship of invasive mosquito species in South Florida cemeteries: do site-specific microclimates explain patterns of coexistence and exclusion? Annals of the Entomological Society of America 103, 757–770.

Lyimo, I.N., Keegan, S.P., Ranford-Cartwright, L.C., Ferguson, H.M., 2012. The impact of uniform and mixed species blood meals on the fitness of the mosquito vector *Anopheles gambiae* s.s: does a specialist pay for diversifying its host species diet? Journal of Evolutionary Biology 25, 452–460.

MacDonald, G., 1957. The epidemiology and control of malaria. Oxford University Press.

Macdonald, W.W., 1956. *Aedes aegypti* in Malaya. Annals of Tropical Medicine Parasitology 50, 399–414.

Macdonald, W.W., 1962. The selection of a strain of *Aedes aegypti* susceptible to infection with semi-periodic Brugia Malayi. Annals of Tropical Medicine & Parasitology 56, 368–372.

Magori, K., Legros, M., Puente, M.E., Focks, D.A., Scott, T.W., Lloyd, A.L., Gould, F., 2009. Skeeter Buster: A stochastic, spatially explicit modeling tool for studying *Aedes aegypti* population replacement and population suppression strategies. PLoS Neglected Tropical Diseases 3.

Marcela, P., Hassan, A.A., Hamdan, A., Dieng, H., Kumara, T.K., 2015. Interspecific cross-mating between *Aedes aegypti* and *Aedes albopictus* laboratory strains: implication of population density on mating behaviors. Journal of the American Mosquito Control Association 31, 313–320.

Mattingly, P.F., 1967. Taxonomy of *Aedes aegypti* and related species. Bulletin of the World Health Organization 36, 552–554.

McCauley, E., Nelson, W.A., Nisbet, R.M., 2008. Small-amplitude cycles emerge from stage-structured interactions in daphnia-algal systems. Nature 455, 1240–1243.

McIntire, K.M., Juliano, S.A., 2018. How can mortality increase population size? A test of two mechanistic hypotheses. Ecology 99, 1660–1670.

McMeniman, C.J., Lane, R.V., Cass, B.N., Fong, A.W., Sidhu, M., Wang, Y.F., O'Neill, S.L., 2009. Stable introduction of a life-shortening *Wolbachia* infection into the mosquito *Aedes aegypti*. Science 323, 141–144.

Messina, J.P., Brady, O.J., Pigott, D.M., Golding, N., Kraemer, M.U., Scott, T.W., Wint, G.R., Smith, D.L., Hay, S.I., 2015. The many projected futures of dengue. Nature Reviews Microbiology 13, 230–239.

Moore, C.G., Fisher, B.R., 1969. Competition in mosquitoes: density and species ratio effects on growth, mortality, fecundity, and production of growth retardant. Annals of the Entomological Society of America 62, 1325–1331.

Moore, C.G., Whitacre, D.M., 1972. Competition in mosquitoes 2: production of *Aedes aegypti* larval growth retardant at various densities and nutrition levels. Annals of the Entomological Society of America 65, 915–918.

Mordecai, E.A., Cohen, J.M., Evans, M.V., Gudapati, P., Johnson, R., Lippi, C.A., Miazgowicz, K., Murdock, C.C., Rohr, J.R., Ryan, S.J., Savage, V., Shocket, M.S., Stewart Ibarra, A., Weikel, D.P., 2017. Detecting the impact of temperature on transmission of Zika, dengue, and chikungunya using mechanistic models. PLoS Negl Trop Dis 11, 1–18.

Moreira, L.A., Iturbe-Ormaetxe, I., Jeffery, J.A., Lu, G., Pyke, A.T., Hedges, L.M., Rocha, B.C., Hall-Mendelin, S., Day, A., Riegler, M., Hugo, L.E., Johnson, K.N., Kay, B.H., McGraw, E.A., van den Hurk, A.F., Ryan, P.A., O'Neill, S.L., 2009. A *Wolbachia* symbiont in *Aedes aegypti* limits infection with dengue, chikungunya, and *Plasmodium*. Cell 139, 1268–1278.

Morin, P.J., 2011. Community ecology. 2nd editio ed., John Wiley Sons, Ltd, Chichester, UK.

Moyes, C.L., Vontas, J., Martins, A.J., Ng, L.C., Koou, S.Y., Dusfour, I., Raghavendra, K., Pinto, J., Corbel, V., David, J.P., Weetman, D., 2017. Contemporary status of insecticide resistance in the major *Aedes* vectors of arboviruses infecting humans. PLoS Neglected Tropical Diseases 11, 1–20.

Muir, L.E., Kay, B.H., 1998. *Aedes aegypti* survival and dispersal estimated by mark-release-recapture in northern Australia. American Journal of Tropical Medicine and Hygiene 58, 277–282.

Murrell, E.G., Juliano, S.A., 2008. Detritus type alters the outcome of interspecific competition between *Aedes aegypti* and *Aedes albopictus* (*Diptera: Culicidae*). Journal of Medical Entomology 45, 375–383.

Nelson, M.L., 1986. *Aedes aegypti*: biology and ecology. Pan American Health Organization, Washington D.C.

Nisbet, R., Gurney, W., 1983. The systematic formulation of population models for insects with dynamically varying instar duration. Theoretical Population Biology 23, 114–135.

Nolting, B.C., Abbott, K.C., 2016. Balls, cups, and quasi-potentials: quantifying stability in stochastic systems. Ecology 97, 850–864.

O'Meara, G.F., Evans, J.L.F., Gettman, A.D., Cuda, J.P., 1995. Spread of *Aedes albopictus* and decline of *Ae. aegypti* (*Diptera: Culicidae*) in Florida. Journal of Medical Entomology 32, 554–562.

Pates, H., Takken, W., Stuke, K., Curtis, C., 2001. Differential behaviour of *Anopheles gambiae sensu stricto* (*Diptera: Culicidae*) to human and cow odours in the laboratory. Bulletin of Entomological Research 91, 289–296.

Paton, R.S., Bonsall, M.B., 2019. The ecological and epidemiological consequences of reproductive interference between the vectors *Aedes aegypti* and *Aedes albopictus*. Journal of The Royal Society Interface 16, 20190270.

Paupy, C., Delatte, H., Bagny, L., Corbel, V., Fontenille, D., 2009. *Aedes albopictus*, an arbovirus vector: from the darkness to the light. Microbes and Infection 11, 1177–1185.

Paupy, C., Ollomo, B., Kamgang, B., Moutailler, S., Rousset, D., Demanou, M., Hervé, J.P., Leroy, E., Simard, F., 2010. Comparative role of *Aedes albopictus* and *Aedes aegypti* in the emergence of dengue and chikungunya in Central Africa. Vector-Borne and Zoonotic Diseases 10, 259–266.

Phuc, H., Andreasen, M.H., Burton, R.S., Vass, C., Epton, M.J., Pape, G., Fu, G., Condon, K.C., Scaife, S., Donnelly, C.A., Coleman, P.G., White-Cooper, H., Alphey, L., 2007. Late-acting dominant lethal genetic systems and mosquito control. BMC Biology 5, 1–11.

Plummer, M., 2003. JAGS: a program for analysis of Bayesian graphical models using Gibbs sampling. Proceedings of the 3rd International Workshop on Distributed Statistical Computing (DSC 2003) , 20–22.

Ponlawat, A., Harrington, L.C., 2005. Blood feeding patterns of *Aedes aegypti* and *Aedes albopictus* in Thailand. Journal of Medical Entomology 42, 844–849.

Ponnusamy, L., Böröczky, K., Wesson, D.M., Schal, C., Apperson, C.S., 2011. Bacteria stimulate hatching of yellow fever mosquito eggs. PLoS ONE 6, e24409.

Powell, J.R., 2018. Perspective piece mosquito-borne human viral diseases: Why *Aedes aegypti*? American Journal of Tropical Medicine and Hygiene 98, 1563–1565.

R Core Team, 2019. R: a language and environment for statistical computing. R Foundation for Statistical Computing. Vienna, Austria.

Raftery, A.E., 1995. Bayesian model selection in social research. American Sociological Association 25, 111–163.

Raharimalala, F.N., Ravaomanarivo, L.H., Ravelonandro, P., Rafarasoa, L.S., Zouache, K., Tran-Van, V., Mousson, L., Failloux, A.B., Hellard, E., Moro, C.V., Ralisoa, B.O., Mavingui, P., 2012. Biogeography of the two major arbovirus mosquito vectors, *Aedes aegypti* and *Aedes albopictus* (Diptera, *Culicidae*), in Madagascar. Parasites Vectors 5, 56.

Ratsitorahina, M., Harisoa, J., Ratovonjato, J., Biacabe, S., Reynes, J.M., Zeller, H., Raoelina, Y., Talarmin, A., Richard, V., Soares, J.L., 2008. Outbreak of dengue and chikungunya fevers, Toamasina, Madagascar, 2006. Emerging Infectious Diseases 14, 1135–1137.

Real, L., 1977. The kinetics of functional response. The American Naturalist 111, 289–300.

Reiskin, M.H., Lounibos, L.P., 2009. Effects of intraspecific larval competition on adult longevity in the mosquitoes *Aedes aegypti* and *Aedes albopictus*. Medical and Veterinary Entomology 23, 62–68.

Reiskind, M.H., Zarrabi, A.A., Lounibos, L.P., 2012. Effects of combination of leaf resources on competition in container mosquito larvae. Bulletin of Entomological Research 102, 424–434.

Reiter, P., 2007. Oviposition, dispersal, and survival in *Aedes aegypti*: implications for the efficacy of control strategies. Vector-Borne and Zoonotic Diseases 7, 261–273.

Rey, J.R., Nishimura, N., Wagner, B., Braks, M.A.H., O'Connell, S.M., Lounibos, L.P., 2006. Habitat segregation of mosquito arbovirus vectors in south Florida. Journal of medical entomology 43, 1134–41.

Ribeiro, J.M.C., Spielman, A., 1986. The satyr effect: a model predicting parapatry and species extinction. The American Naturalist 128, 513–528.

Richards, S.L., Ponnusamy, L., Unnasch, T.R., Hassan, H.K., Apperson, C.S., 2006. Host-feeding patterns of *Aedes albopictus* (*Diptera: Culicidae*) in relation to availability of human and domestic animals in suburban landscapes of Central North Carolina. Journal of Medical Entomology 43, 543–551.

Rogers, D.J., Randolph, S.E., 1984. From a case study to a theoretical basis for tsetse control. International Journal of Tropical Insect Science 5, 419–423.

Ross, P.A., Ritchie, S.A., Axford, J.K., Hoffmann, A.A., 2019. Loss of cytoplasmic incompatibility in *Wolbachia*-infected *Aedes aegypti* under field conditions. PLOS Neglected Tropical Diseases 13, e0007357.

Ross, R., 1897. On some peculiar pigmented cells found in two mosquitos fed on malarial blood. BMJ 2, 1786–1788.

Ross, R., 1911. The prevention of malaria. Dutton.

Rudnick, A., 1965. Studies of the ecology of dengue in Malaysia: a preliminary report. Journal of Medical Entomology 2, 203–208.

Scott, T.W., Takken, W., 2012. Feeding strategies of anthropophilic mosquitoes result in increased risk of pathogen transmission. Trends in Parasitology 28, 114–121.

Shuker, D.M., Currie, N., Hoole, T., Burdfield-Steel, E.R., 2015. The extent and costs of reproductive interference among four species of true bug. Population Ecology 57, 321–331.

Simard, F., Nchoutpouen, E., Toto, J.C., Fontenille, D., 2005. Geographic distribution and breeding site preference of *Aedes albopictus* and *Aedes aegypti* (*Diptera: Culicidae*) in Cameroon, Central Africa. Journal of medical entomology 42, 726–731.

Sivan, A., Shriram, A.N., Sunish, I.P., Vidhya, P.T., 2015. Host-feeding pattern of *Aedes aegypti* and *Aedes albopictus* (*Diptera: Culicidae*) in heterogeneous landscapes of South Andaman, Andaman and Nicobar Islands, India. Parasitology Research 114, 3539–3546.

Snow, R., Lindsay, S., Hayes, R., Greenwood, B., 1988. Permethrin-treated bed nets (mosquito nets) prevent malaria in Gambian children. Transactions of the Royal Society of Tropical Medicine and Hygiene 82, 838–842.

Soetaert, K., Petzoldt, T., Setzer, R.W., 2010. Solving differential equations in R: package deSolve. Journal of Statistical Software 33, 1–25.

Southwood, T.R., Murdie, G., Yasuno, M., Tonn, R.J., Reader, P.M., 1972. Studies on the life budget of *Aedes aegypti* in Wat Samphaya, Bangkok, Thailand. Bulletin of the World Health Organization 46, 211–226.

Sparks, A.H., Hengl, T., Nelson, A., 2017. GSODR: global summary daily weather data in R. The Journal of Open Source Software 2.

Stanton, A.T., 1920. The mosquitoes of Far Eastern ports with special reference to the prevalence of *Stegomyia fasciata*, F. Bulletin of Entomological Research 10, 333–344.

Strong, D.R., 1986. Density-vague population change. Trends in Ecology and Evolution 1, 39–42.

Styer, L.M., Carey, J.R., Wang, J.L., Scott, T.W., 2007. Mosquitoes do senesce: departure from the paradigm of constant mortality. American Journal of Tropical Medicine and Hygiene 76, 111–117.

Sumpter, D.J.T., Broomhead, D.S., 2001. Relating individual behaviour to population dynamics. Proceedings of the Royal Society B: Biological Sciences 268, 925–932.

Takken, W., Verhulst, N.O., 2012. Host preferences of blood-feeding mosquitoes. Annual Review of Entomology 58, 433–453.

Tenan, S., O'Hara, R.B., Hendriks, I., Tavecchia, G., 2014. Bayesian model selection: the steepest mountain to climb. Ecological Modelling 283, 62–69.

Thomas, D.D., Donnelly, C.A., Wood, R.J., Alphey, L.S., 2000. Insect population control using a dominant, repressible, lethal genetic system. Science 287, 2474–2476.

Tripet, F., Lounibos, L.P., Robbins, D., Moran, J., Nishimura, N., Blosser, E.M., 2011. Competitive reduction by satyrization? Evidence for interspecific mating in nature and asymmetric reproductive competition between invasive mosquito vectors. American Journal of Tropical Medicine and Hygiene 85, 265–270.

Valerio, L., Marini, F., Bongiorno, G., Facchinelli, L., Pombi, M., Caputo, B., Maroli, M., della Torre, A., 2010. Host-feeding patterns of *Aedes albopictus* (*Diptera: Culicidae*) in urban and rural contexts within Rome province, Italy. Vector-Borne and Zoonotic Diseases 10, 291–294.

Weetman, D., Kamgang, B., Badolo, A., Moyes, C.L., Shearer, F.M., Coulibaly, M., Lambrechts, L., 2018. *Aedes* mosquitoes and *Aedes*-borne arboviruses in Africa : current and future threats. International journal of environmental reasearch and public health 15.

White, G.B., Magayuka, S.A., Boreham, P.F.L., 1972. Comparative studies on sibling species of the *Anopheles gambiae* Giles complex (Dipt., *Culicidae*): bionomics and vectorial activity of species A and species B at Segera, Tanzania. Bulletin of Entomological Research 62, 295.

White, S.M., Rohani, P., Sait, S.M., 2010. Modelling pulsed releases for sterile insect techniques: fitness costs of sterile and transgenic males and the effects on mosquito dynamics. Journal of Applied Ecology 47, 1329–1339.

Winchester, J.C., Kapan, D.D., 2013. History of *Aedes* mosquitoes in Hawaii. Journal of the American Mosquito Control Association 29, 154–163.

Wolfram Research, 2018. Mathematica.

Wood, S.N., 2006. Generalized additive models: an introduction with R. volume 170.

Yakob, L., 2016. How do biting disease vectors behaviourally respond to host availability? Parasites and Vectors 9, 1–9.

Yakob, L., Alphey, L., Bonsall, M.B., 2008. *Aedes aegypti* control: the concomitant role of competition, space and transgenic technologies. Journal of Applied Ecology 45, 1258–1265.

Yakob, L., Walker, T., 2016. Zika virus outbreak in the Americas: The need for novel mosquito control methods. The Lancet Global Health 4, e148–e149.

Yang, C.F., Hou, J.N., Chen, T.H., Chen, W.J., 2014. Discriminable roles of *Aedes aegypti* and *Aedes albopictus* in establishment of dengue outbreaks in Taiwan. Acta Tropica 130, 17–23.

Yen, C., Hyde, T.B., Costa, A.J., Fernandez, K., Tam, J.S., Hugonnet, S., Huvos, A.M., Duclos, P., Dietz, V.J., Burkholder, B.T., 2015. The development of global vaccine stockpiles. The Lancet Infectious Diseases 15, 340–347.

Yuval, B., 2006. Mating systems of blood-feeding flies. Annual Review of Entomology 51, 413–440.

# A | SUPPLEMENTARY MATERIAL FOR CHAPTER 3

## Isocline derivation for equations 3 and 4

In our methods, equations 3 and 4 describe the population dynamics of two competing mosquito species that use hosts according to a behavioural response, $f_i(Q)$:

$$\frac{dA(t)}{dt} = r_A A(t)\left((1 - f_A(Q)) + \frac{f_A(Q)A(t)}{A(t) + \delta_A f_B(Q)B(t)}\right) - \alpha_A A(t-\tau_A)[A(t-\tau_A) + \beta_A B(t-\tau_A)] - d_A A(t) \quad (3)$$

$$\frac{dB(t)}{dt} = r_B B(t)\left((1 - f_B(Q)) + \frac{f_B(Q)B(t)}{B(t) + \delta_B f_A(Q)A(t)}\right) - \alpha_B B(t-\tau_B)[B(t-\tau_B) + \beta_B A(t-\tau_B)] - d_B B(t) \quad (4)$$

Solving equations 3 and 4 for $\frac{dA}{dt} = 0$ and $\frac{dB}{dt} = 0$ respectively and factorising yields two expressions:

$$0 = \alpha A^2 + (\alpha B(\beta_A + \delta_A)f_B(Q) + d - r) + (B\delta_A f_B(Q)(\alpha B\beta_A + d + (f_A(Q) - 1)r)) \quad (A1)$$

$$0 = \alpha B^2 + (\alpha A(\beta_B + \delta_B)f_A(Q) + d - r) + (A\delta_B f_A(Q)(\alpha A\beta_B + d + (f_B(Q) - 1)r)) \quad (A2)$$

The solutions to equations A1 and A2 are simply the positive solutions of the quadratic formula. This gives an expression for the population sizes for each population ($A^*$ and $B^*$):

$$A^* = \frac{-(\alpha B(\beta_A + \delta_A)f_B(Q) + d - r)}{2\alpha} + \frac{\sqrt{(\alpha B(\beta_A + \delta_A)f_B(Q) + d - r)^2 + 4\alpha(B\delta_A f_B(Q)(\alpha B\beta_A + d + (f_A(Q) - 1)r))}}{2\alpha} \quad (A3)$$

$$B^* = \frac{-(\alpha B(\beta_B + \delta_B)f_A(Q) + d - r)}{2\alpha} + \frac{\sqrt{(\alpha A(\beta_B + \delta_B)f_A(Q) + d - r)^2 + 4\alpha(A\delta_B f_A(Q)(\alpha A\beta_B + d + (f_B(Q) - 1)r))}}{2\alpha} \quad (A4)$$

The necessary conditions for coexistence can be examined by substituting equation A3 into A4 and vice-versa. This yields a cubic polynomial for each species, and is included in the supplementary Mathematica file. The discriminant of the resultant expressions reveals the nature of the roots of the polynomial.

## Derivation of the pathogen intrinsic growth rate, $R$

The intrinsic growth rate, $R$, of a pathogen in this multi-vector system can be determined from the determinant of the Jacobian matrix of the linearised system. This calculation is based on equations 7 to 9 in the text:

$$\frac{dI_A(t)}{dt} = \rho_A \kappa_A f_A(Q)[A(t) - I_A(t)]\frac{I_H(t)}{H} - d_A I_A(t) \tag{7}$$

$$\frac{dI_B(t)}{dt} = \rho_B \kappa_B f_B(Q)[B(t) - I_B(t)]\frac{I_H(t)}{H} - d_B I_B(t) \tag{8}$$

$$\frac{dI_H(t)}{dt} = (\rho_A \gamma_A f_A(Q) I_A(t) + \rho_B \gamma_B f_B(Q) I_B(t))\left[\frac{H - I_H(t)}{H}\right] - m I_H(t) \tag{9}$$

We can write the Jacobian as:

$$R = Det\begin{bmatrix} \frac{\partial(dI_H/dt)}{\partial I_H} & \frac{\partial(dI_H/dt)}{\partial I_A} & \frac{\partial(dI_H/dt)}{\partial I_B} \\ \frac{\partial(dI_A/dt)}{\partial I_H} & \frac{\partial(dI_A/dt)}{\partial I_A} & \frac{\partial(dI_A/dt)}{\partial I_B} \\ \frac{\partial(dI_B/dt)}{\partial I_H} & \frac{\partial(dI_B/dt)}{\partial I_A} & \frac{\partial(dI_B/dt)}{\partial I_B} \end{bmatrix} \tag{A5}$$

Then, calculating the partial derivatives:

$$R = Det\begin{bmatrix} \frac{-\rho_A \gamma_A f_A(Q) I_A(t) + \rho_B \gamma_B f_B(Q) I_B(t)}{H} - m & \rho_A \gamma_A f_A(Q)\left[\frac{H - I_H(t)}{H}\right] & \rho_B \gamma_B f_B(Q)\left[\frac{H - I_H(t)}{H}\right] \\ \frac{\rho_A f_A(Q) \kappa_A}{H}[A(t) - I_A(t)] & -\rho_A f_A(Q)\kappa_A \frac{I_H(t)}{H} - d_A & 0 \\ \frac{\rho_B f_B(Q) \kappa_B}{H}[B(t) - I_B(t)] & 0 & -\rho_B f_B(Q)\kappa_B \frac{I_H(t)}{H} - d_B \end{bmatrix} \tag{A6}$$

Assuming that the pathogen invades an entirely healthy population ($I_A(t)$, $I_B(t)$ and $I_H(t) \longrightarrow 0$) and vector population sizes are at equilibrium ($A(t) = A^*$ and $B(t) = B^*$) then $R$ is:

$$R = Det\begin{bmatrix} -m & \rho_A \gamma_A f_A(Q) & \rho_B \gamma_B f_B(Q) \\ \frac{\rho_A \kappa_A f_A(Q) A^*}{H} & -d_A & 0 \\ \frac{\rho_B \kappa_B f_B(Q) B^*}{H} & 0 & -d_B \end{bmatrix} \tag{A7}$$

# B | SUPPLEMENTARY MATERIAL FOR CHAPTER 3

## Pilot study

In order to choose an appropriate feeding regime for the main experiments, it was necessary to find the baseline per-capita nutritional requirements of both species. We therefore explored, on a per-capita basis, how much liver powder was required for a larvae to successfully develop.

### Procedure

Eggs of each species were vacuum hatched for approximately 1.5 hours in tap water. The wells of a 6-well-plate were filled with 9ml reverse-osmosis filtered water. A single larvae was placed into each well of a six-well plate. A dilution of liver powder corresponding to 0.05, 0.2, 0.35, 0.5, 0.65 and 0.8 mg per larvae was added to each well, bringing the total volume to 10ml. The larvae were fed again with 1ml of this solution on the 2nd and 4th day after hatching (evaporation was thought to maintain the volume at approximately 10 ml). Each day the larvae were checked to see if they had pupated or died. Larvae were given a three weeks to develop, after which time they were assumed dead. This process was repeated for each species, across 3 replicates.

A binomially-distributed logit-link generalised linear model was used to analyse the survival data, and a step-wise down model selection procedure using log-likelihood ratio tests (LRT) was used to determine the optimal set of predictors.

### Results

Food treatment had a significant (LRT: $\Delta df = 1, p = 2.1\text{x}10^{-16}$) positive effect ($0.0143 \pm 0.0025$, logit scale) on survivorship, but the effect did not significantly differ between species (LRT: $\Delta df = 1, p = 0.1299$). The relationship is shown in Figure B.1.

### Conclusions

Both species responded to the availability to the liver power in the same way. The estimated probability of survival asymptotically approached 1 from approximately 0.5mg/La. We therefore elected to set our feeding regime at 0.55mg/La, to ensure that there were adequate food resources to maintain all larvae in the population.

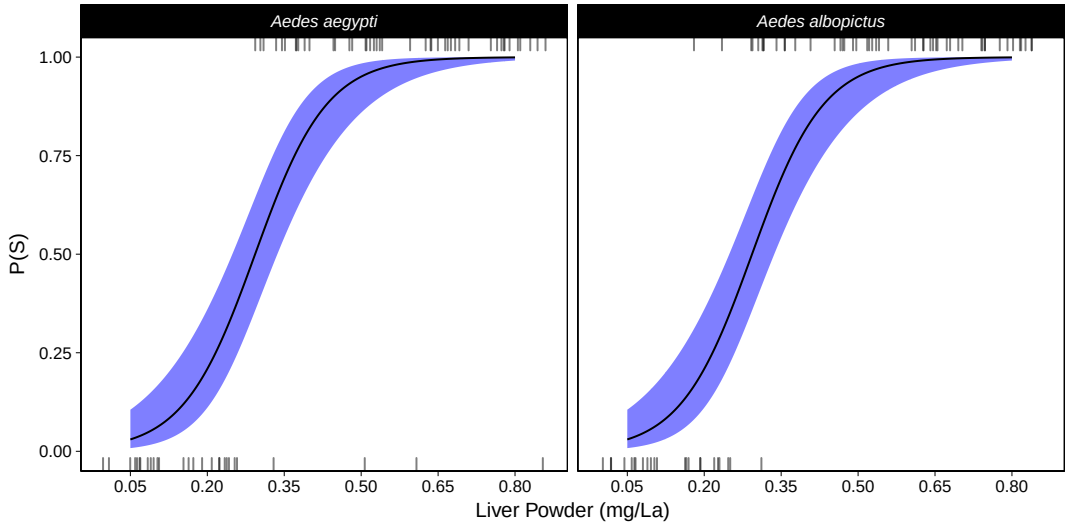



Figure B.1: Experimental data for the pilot studies examining the survivorship of *Ae. aegypti* and *Ae. albopictus*. Rugs show the jittered survival data across all replicates. Note that there is a positive effect of food availability on survivorship that it is consistent across both species.

## Priors

Model priors are given in table B.1.

| **Survival** | | **Development** | |
|---|---|---|---|
| *Variable(s)* | *Distribution* | *Variable(s)* | *Distribution* |
| Intercept | $\mathcal{N}(2.7, 1)$ | Intercept | $\mathcal{N}(2.079, 1)$ |
| Linear predictors | $\mathcal{N}(0, 1)$ | Linear predictors | $\mathcal{N}(0, 0.3)$ |
| Smoothing parameters | $\Gamma(1, 0.001)$ | Standard deviation | $\Gamma(1.28, 0.23)$ |
| Certainty, $\theta$ (beta-binomial) | $\Gamma(1, 1000)$ | - | - |

Table B.1: Priors used for fitting the binomial, beta binomial and development time models. Both intercepts were taken from pilot runs of the experiment, as was the standard deviation for development time.

## Gibbs Variable Selection (GVS)

Results for the GVS procedure are reported for the two survivorship model structures (binomial in Table B.2 and beta-binomial in Table B.3), and the gamma model of development times (Table B.4). The frequencies with which predictor combinations were selected are reported, along with the absolute number of iterations. Parameter combinations selected less than 1% of the iterations are not included in the tables. The fits corresponding to each of the best fitting model are given in Figures B.2 and B.3 for the two survival models, and B.4 for the development time model.

Binomial model of larval survival

| Rank | Predictor combinations | *N* | % |
|---|---|---|---|
| 1 | $Int + Sp + D_{aeg} + D_{alb} + Sp : D_{alb} + f(D_{aeg})$ | 633723 | 15.84 |
| 2 | $Int + Sp + D_{aeg} + Sp : D_{aeg} + D_{alb} + Sp : D_{alb} + f(D_{aeg})$ | 402459 | 10.06 |
| 3 | $Int + Sp + D_{aeg} + Sp : D_{aeg} + D_{alb} + D_{aeg} : D_{aeg} + f(D_{aeg})$ | 326178 | 8.15 |
| 4 | $Int + Sp + D_{aeg} + Sp : D_{aeg} + D_{alb}$ | 295250 | 7.38 |
| 5 | $Int + Sp + D_{aeg} + Sp : D_{aeg} + D_{alb} + Sp : D_{alb}$ | 240442 | 6.01 |
| 6 | $Int + Sp + D_{aeg} + D_{alb} + D_{aeg} : D_{aeg} + f(D_{aeg})$ | 213651 | 5.34 |
| 7 | $Int + Sp + D_{aeg} + D_{alb} + f(D_{aeg})$ | 212110 | 5.30 |
| 8 | $Int + Sp + D_{aeg} + Sp : D_{aeg} + D_{alb} + Sp : D_{alb} + D_{aeg} : D_{aeg} + f(D_{aeg})$ | 202547 | 5.06 |
| 9 | $Int + Sp + D_{aeg} + D_{alb} + Sp : D_{alb} + D_{aeg} : D_{aeg} + f(D_{aeg})$ | 179147 | 4.48 |
| 10 | $Int + Sp + D_{aeg} + Sp : D_{aeg} + D_{alb} + Sp : D_{alb} + Sp : D_{aeg} : D_{alb} + f(D_{aeg})$ | 173728 | 4.34 |
| 11 | $Int + Sp + D_{aeg} + Sp : D_{aeg} + D_{alb} + f(D_{aeg})$ | 152175 | 3.80 |
| 12 | $Int + Sp + D_{aeg} + D_{alb} + Sp : D_{alb} + Sp : D_{aeg} : D_{alb} + f(D_{aeg})$ | 107058 | 2.68 |
| 13 | $Int + Sp + D_{aeg} + Sp : D_{aeg} + D_{alb} + D_{aeg} : D_{aeg} + Sp : D_{aeg} : D_{alb} + f(D_{aeg})$ | 57074 | 1.43 |
| 14 | $Int + Sp + D_{aeg} + Sp : D_{aeg} + D_{alb} + Sp : D_{alb} + Sp : D_{aeg} : D_{alb}$ | 53330 | 1.33 |
| 15 | $Int + Sp + D_{aeg} + Sp : D_{aeg} + D_{alb} + Sp : D_{aeg} : D_{alb}$ | 53317 | 1.33 |
| 16 | $Int + Sp + D_{aeg} + Sp : D_{aeg} + D_{alb} + Sp : D_{alb} + D_{aeg} : D_{aeg} + Sp : D_{aeg} : D_{alb} + f(D_{aeg})$ | 48099 | 1.20 |
| 17 | $Int + Sp + D_{aeg} + D_{alb} + D_{aeg} : D_{aeg} + Sp : D_{aeg} : D_{alb} + f(D_{aeg})$ | 46015 | 1.15 |

Table B.2: Frequencies with which combinations of predictors were selected for the binomial model during GVS. *N* denotes for how many samples particular variable combinations were active, and the percentages calculated as *N* divided by the total number of iterations ($4x10^6$). *Int* is the intercept, *Sp* the species, $D_{aeg}$ the density of *Ae. aegypti* and $D_{alb}$ the density of *Ae. albopictus*. Interactions between variables are denoted by :, while $f()$ denotes that the term is a smooth function of the predictor in brackets. Each smooth functions had 5 knots. The most frequently selected model is given in row 1, and included a species-specific intercept, a linear species specific response to *Ae. albopictus* density and a linear and smooth term for *Ae. aegypti* density.

Beta-binomial model of larval survival

| Rank | Predictor combinations | *N* | % |
|---|---|---|---|
| 1 | $Int + Sp + D_{aeg} + Sp : D_{aeg} + D_{alb}$ | 1340494 | 33.51 |
| 2 | $Int + Sp + D_{aeg} + Sp : D_{aeg} + D_{alb} + Sp : D_{alb}$ | 968011 | 24.20 |
| 3 | $Int + Sp + D_{aeg} + D_{alb}$ | 533692 | 13.34 |
| 4 | $Int + Sp + D_{aeg} + D_{alb} + Sp : D_{alb}$ | 355619 | 8.89 |
| 5 | $Int + Sp + D_{aeg} + Sp : D_{aeg} + D_{alb} + D_{aeg} : D_{alb}$ | 184094 | 4.60 |
| 6 | $Int + Sp + D_{aeg} + D_{alb} + Sp : D_{alb} + D_{aeg} : D_{alb}$ | 116732 | 2.92 |
| 7 | $Int + Sp + D_{aeg} + D_{alb} + D_{aeg} : D_{alb}$ | 97547 | 2.44 |
| 8 | $Int + Sp + D_{aeg} + Sp : D_{aeg} + D_{alb} + Sp : D_{alb} + D_{aeg} : D_{alb}$ | 81131 | 2.03 |
| 9 | $Int + Sp + D_{aeg} + D_{alb} + Sp : D_{alb} + f(D_{aeg})$ | 42801 | 1.07 |
| 10 | $Int + D_{aeg} + D_{alb}$ | 41163 | 1.03 |

Table B.3: Frequencies with which combinations of predictors were selected for the beta-binomial model during GVS. *N* denotes for how many samples particular variable combinations were active, and the percentages calculated as *N* divided by the total number of iterations ($4x10^6$). *Int* is the intercept, *Sp* the species, $D_{aeg}$ the density of *Ae. aegypti* and $D_{alb}$ the density of *Ae. albopictus*. Interactions between variables are denoted by :, while $f()$ denotes that the term is a smooth function of the predictor in brackets. Each smooth functions had 5 knots. The most frequently selected model is given in row 1, and included a species-specific intercept, a linear species-specific response to *Ae. aegypti* density and a linear *Ae. albopictus* density.

Gamma distributed model of development time

| Rank | Predictor combinations | *N* | % |
|---|---|---|---|
| 1 | $Int + Sp + Sx + D_{aeg} + D_{alb} + D_{aeg} : D_{alb} + Sp : D_{aeg} + Sp : D_{alb} + Sp : D_{aeg} : D_{alb}$ | 916754 | 22.92 |
| 2 | $Int + Sp + Sx + D_{aeg} + D_{alb}$ | 877931 | 21.95 |
| 3 | $Int + Sp + Sx + D_{aeg} + D_{alb} + D_{aeg} : D_{alb} + Sp : D_{aeg} + Sp : D_{alb} + Sx : D_{alb} + Sp : D_{aeg} : D_{alb}$ | 347898 | 8.70 |
| 4 | $Int + Sp + Sx + D_{aeg} + D_{alb} + Sx : D_{alb}$ | 340935 | 8.52 |
| 5 | $Int + Sp + Sx + D_{aeg} + D_{alb} + Sp : D_{aeg}$ | 173395 | 4.33 |
| 6 | $Int + Sp + Sx + D_{aeg} + D_{alb} + D_{aeg} : D_{alb} + Sp : D_{aeg} + Sx : D_{aeg} + Sp : D_{alb} + Sp : D_{aeg} : D_{alb}$ | 154349 | 3.86 |
| 7 | $Int + Sp + Sx + D_{aeg} + D_{alb} + Sp : D_{alb}$ | 153422 | 3.84 |
| 8 | $Int + Sp + Sx + D_{aeg} + D_{alb} + Sx : D_{aeg}$ | 145638 | 3.64 |
| 9 | $Int + Sp + Sx + Sp : Sx + D_{aeg} + D_{alb}$ | 92416 | 2.31 |
| 10 | $Int + Sp + Sx + Sp : Sx + D_{aeg} + D_{alb} + D_{aeg} : D_{alb} + Sp : D_{aeg} + Sp : D_{alb} + Sp : D_{aeg} : D_{alb}$ | 88255 | 2.21 |
| 11 | $Int + Sp + Sx + D_{aeg} + D_{alb} + D_{aeg} : D_{alb}$ | 79092 | 1.98 |
| 12 | $Int + Sp + Sx + D_{aeg} + D_{alb} + Sp : D_{aeg} + Sx : D_{alb}$ | 66902 | 1.67 |
| 13 | $Int + Sp + Sx + D_{aeg} + D_{alb} + Sp : D_{alb} + Sx : D_{alb}$ | 58694 | 1.47 |
| 14 | $Int + Sp + Sx + D_{aeg} + D_{alb} + D_{aeg} : D_{alb} + Sp : D_{alb}$ | 47654 | 1.19 |
| 15 | $Int + Sp + Sx + D_{aeg} + D_{alb} + Sx : D_{aeg} + Sx : D_{alb}$ | 46270 | 1.16 |

Table B.4: Frequencies with which combinations of predictors were selected for the gamma GLM during GVS. *N* denotes for how many samples particular variable combinations were active, and the percentages are *N* divided by the total number of iterations ($4x10^6$). *Int* is the Intercept, *Sp* the species (categorical), *Sx* the sex (categorical), $D_{aeg}$ the density of *Ae. aegypti* and $D_{alb}$ the density of *Ae. albopictus*. Interactions between variables are denoted by colon. The most selected model is given in the first row, and included a sex-specific intercept, as well as

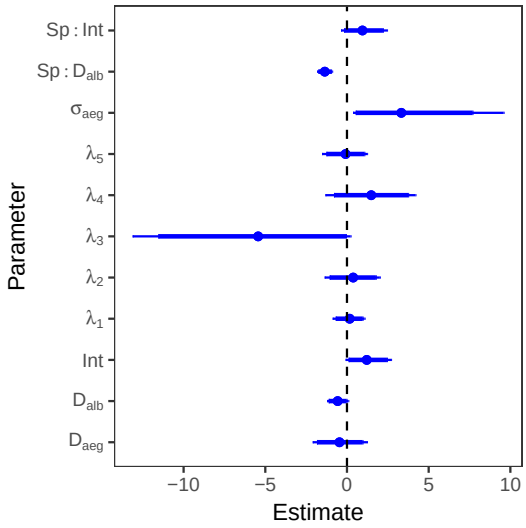



Figure B.2: Parameter estimates for the binomial model, after the predictors had been selected by GVS. Dots denote medians, thick lines the 90% HDIs and thin lines the 95% HDIs. In this model, $\sigma_{aeg}$ is the standard deviation of the normal distribution used to estimate the smoothing parameters ($\lambda_{1-5}$) of the 5-knot smooth function of *Ae. aegypti* density (Crainiceanu et al., 2005). Colons denote interactions, "Sp" the intercept change for *Ae. albopictus* and "Int" the intercept. $D_{aeg}$ and $D_{alb}$ are the densities of *Ae. aegypti* and *Ae. albopictus* respectively. This model was compared to the beta-binomial model (Figure B.3).

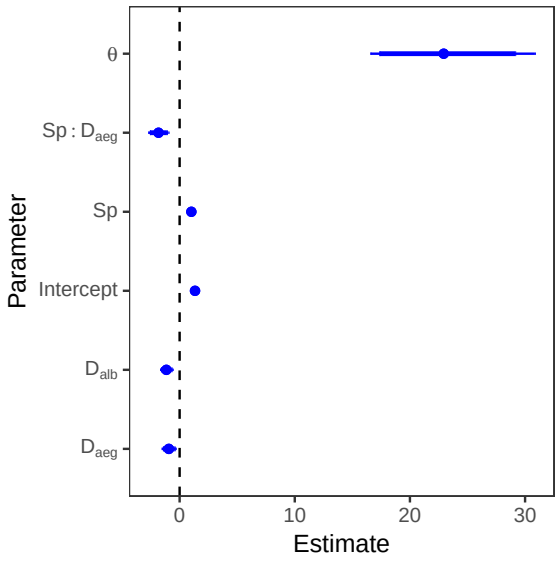



Figure B.3: Parameter estimates for the beta-binomial model, after the predictors have been selected by GVS. Dots denote medians, thick lines the 90% HDIs, and thin lines the 95% HDIs. In this model, $\theta$ is the certainty parameter, as mentioned in the reparametrisation of the beta distribution in (Kruschke, 2015). Colons denote interactions, "Sp" the intercept change for *Ae. albopictus* and "Int" the intercept. $D_{aeg}$ and $D_{alb}$ are the densities of *Ae. aegypti* and *Ae. albopictus* respectively. This model was compared to the beta-binomial model (Figure B.2). These estimates are also given in Table 3.2 in the main text.

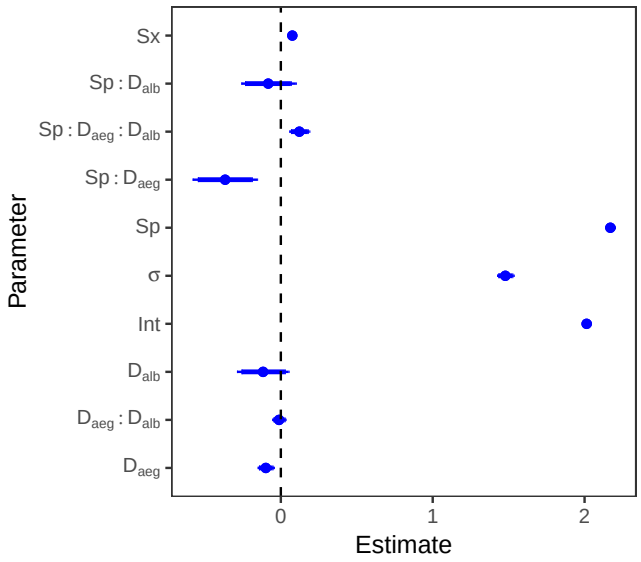



Figure B.4: Parameter estimates for the development time model after the predictors have been selected by GVS. Dots denote medians, thick lines the 90% HDIs, and thin lines the 95% HDIs. Colons denote interactions, "Sp" the intercept change for *Ae. albopictus* and "Int" the intercept. $D_{aeg}$ and $D_{alb}$ are the densities of *Ae. aegypti* and *Ae. albopictus* respectively. These four models were then compared using the PSM to decide on the best structure.

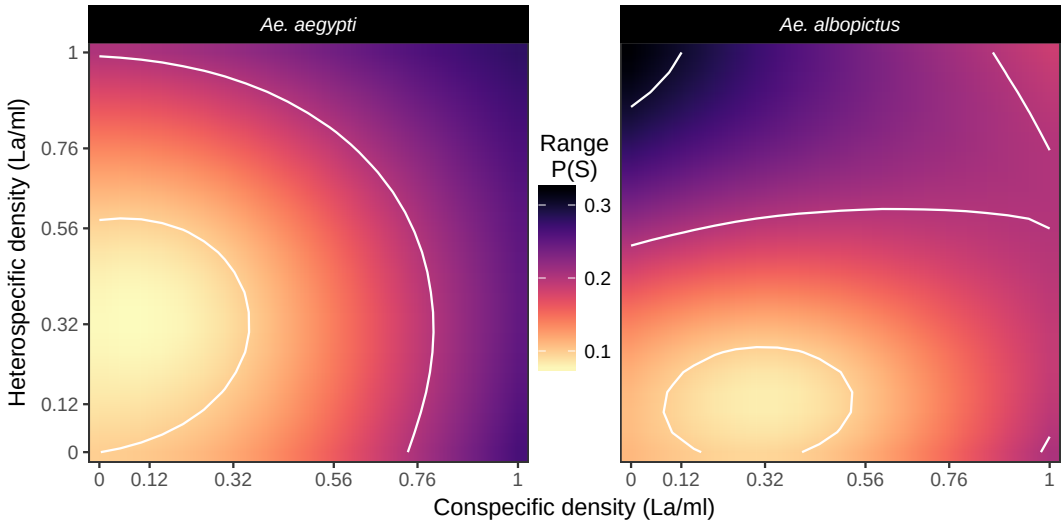



Figure B.5: Plot showing the distribution of uncertainty (as a range in survival probability) across the predicted response surfaces in Figure 3.3.

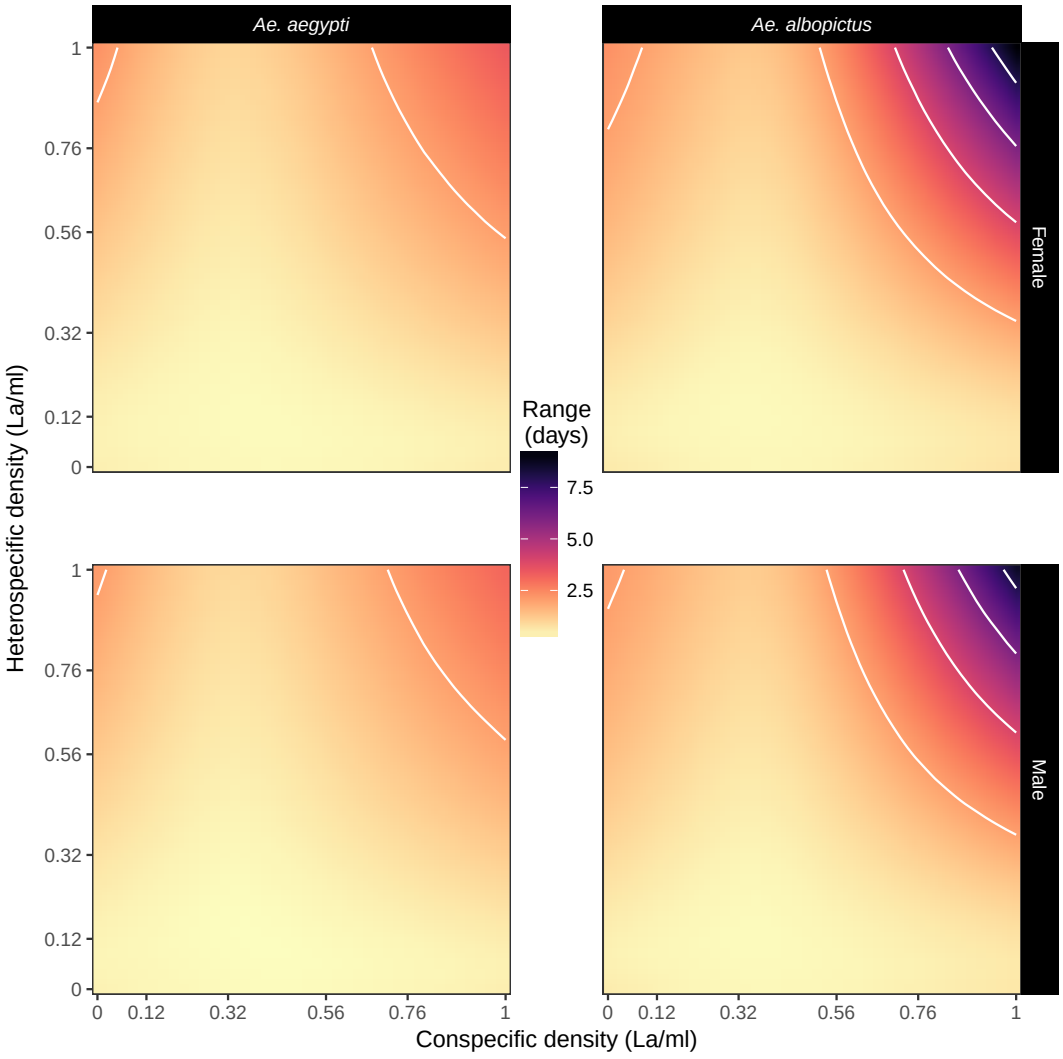



Figure B.6: Plot showing the distribution of uncertainty (as a range in days) across the predicted response surfaces in Figure 3.5.

# C | SUPPLEMENTARY MATERIAL FOR CHAPTER 4

## Model derivation

Gurney et al. (1983) derive a model framework that expresses stage-structured populations as a system of delay-differential equations. In their paper, they move from a system of partial differential equations that describe a population with a continuous age distribution, to one where individuals enter and leave discrete age-classes at distinct time points (deemed the lumped age-class formalism). Nisbet and Gurney (1983) go on to develop this framework to include variable delays; that is to say that the time spent in each stage (say $\tau$) is allowed to vary through time, changing as a function of a variable ($\tau(t) = g(t)$). This is challenging, as the survival through classes will also be affected – being exposed to a dynamic mortality rate across a variable-length stage duration needs to be accounted for. The authors were motivated by the fact that in many insects specific metrics – such as weight gain – trigger transitions between stages rather than chronological age. In our case, we were motivated to use this framework as the variable delay approach allows is to alter a stages duration with temperature. They give the rate of change in a state-duration as:

$$\frac{d\tau(t)}{dt} = 1 - \frac{g(t)}{g(t-\tau(t))}. \tag{C.1}$$

The proportion of individuals surviving through a stage can be given as:

$$S_i(t) = exp\left( - \int_{t-\tau(t)}^{t} \phi(t) \right) \tag{C.2}$$

where $\phi$ is the mortality rate which is integrated across the the duration of the stage ($\tau$). In order to determine the rate of change in survival ($\frac{dS(t)}{dt}$), we must differentiate with respect to time:

$$\frac{S_i(t)}{dt} = S(t)\left[ \frac{d}{dt}\left( - \int_{t-\tau(t)}^{t} \phi(t) \right) \right]. \tag{C.3}$$

$$\frac{S_i(t)}{dt} = S(t)\left[ \frac{d}{dt}(t-\tau(t))\phi(t-\tau(t)) - \phi(t) \right]. \tag{C.4}$$

$$\frac{S_i(t)}{dt} = S(t)\left[ 1 - \left( \frac{d\tau(t)}{dt} \right)\phi(t-\tau(t)) - \phi(t) \right]. \tag{C.5}$$

Given we know that $\frac{d\tau(t)}{dt} = 1 - \frac{g(t)}{g(t-\tau(t))}$, the expression becomes

$$\frac{S_i(t)}{dt} = S(t)\left[ \frac{g(t)}{g(t-\tau(t))}\phi(t-\tau(t)) - \phi(t) \right]. \tag{C.6}$$

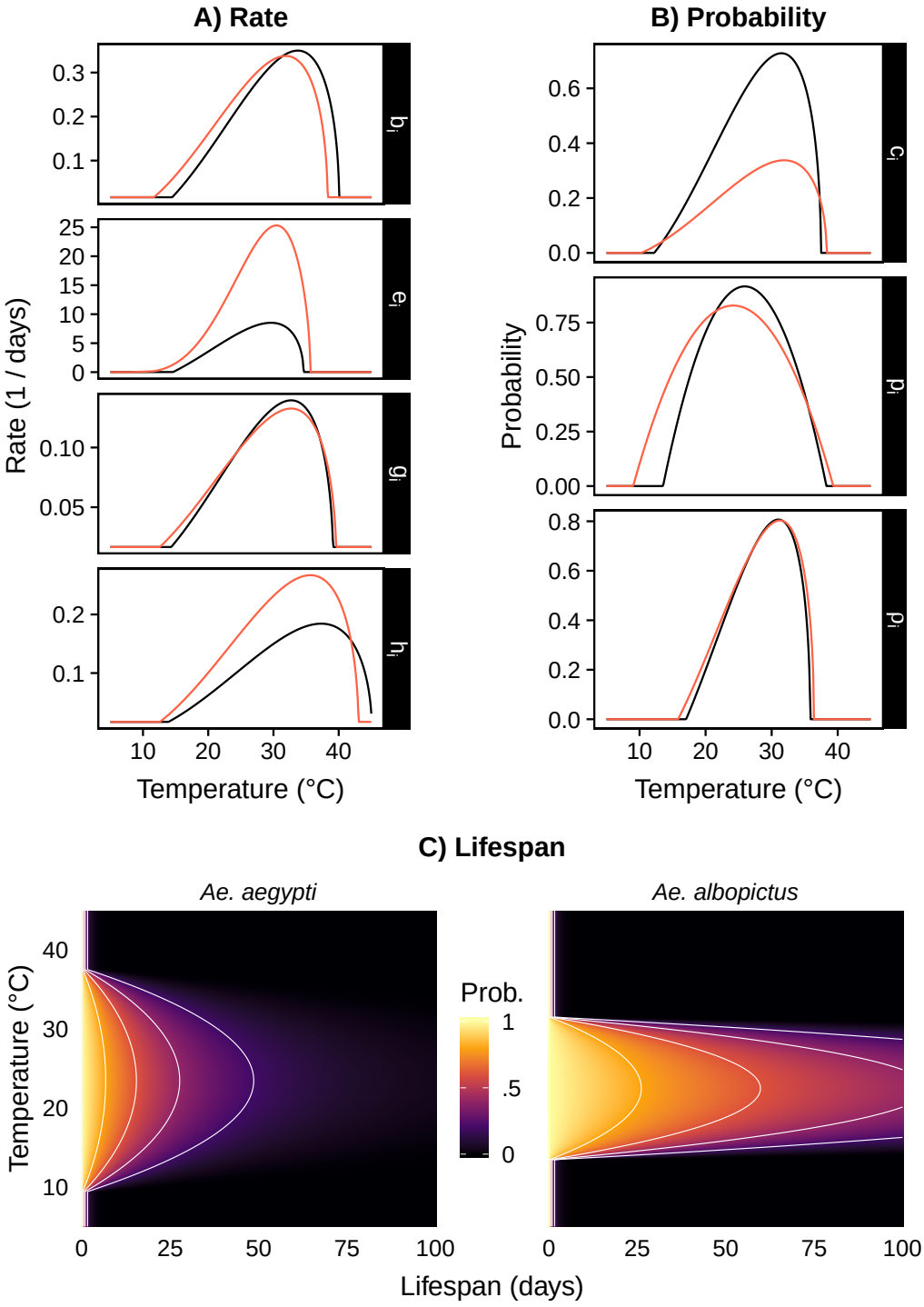



Figure C.1: Temperature responses for *Ae. aegypti* and *Ae. albopictus* taken from Mordecai et al. (2017). Set A shows how rates change with temperature; these are the biting rate ($b_i$), the egg-laying rate ($e_i$), the egg-to-adult development rate ($g_i$) and the extrinsic incubation rate ($h_i$). The response of *Ae. aegypti* is given in black and *Ae. albopictus* in red. Set B shows how the probabilities of egg to adult survival ($c_i$), the mosquito becoming infected from a bite on an infected host ($p_i$) and a mosquito transmitting infection to a host ($\rho_i$) changes as a function of temperature. Again, the response of *Ae. aegypti* are given in black and *Ae. albopictus* in red. Set C shows how the lifespan of adult mosquitoes changes with temperature. The probability of an adult mosquito being alive at a particular time after emergence is given by the colour scale. A minimum lifespan of 1 day was imposed, so even at the limits of the thermal range, at least some mosquitoes would still briefly survive. The parameters used in for these functions (and any limits imposed on them) are given in appendix Table C.1

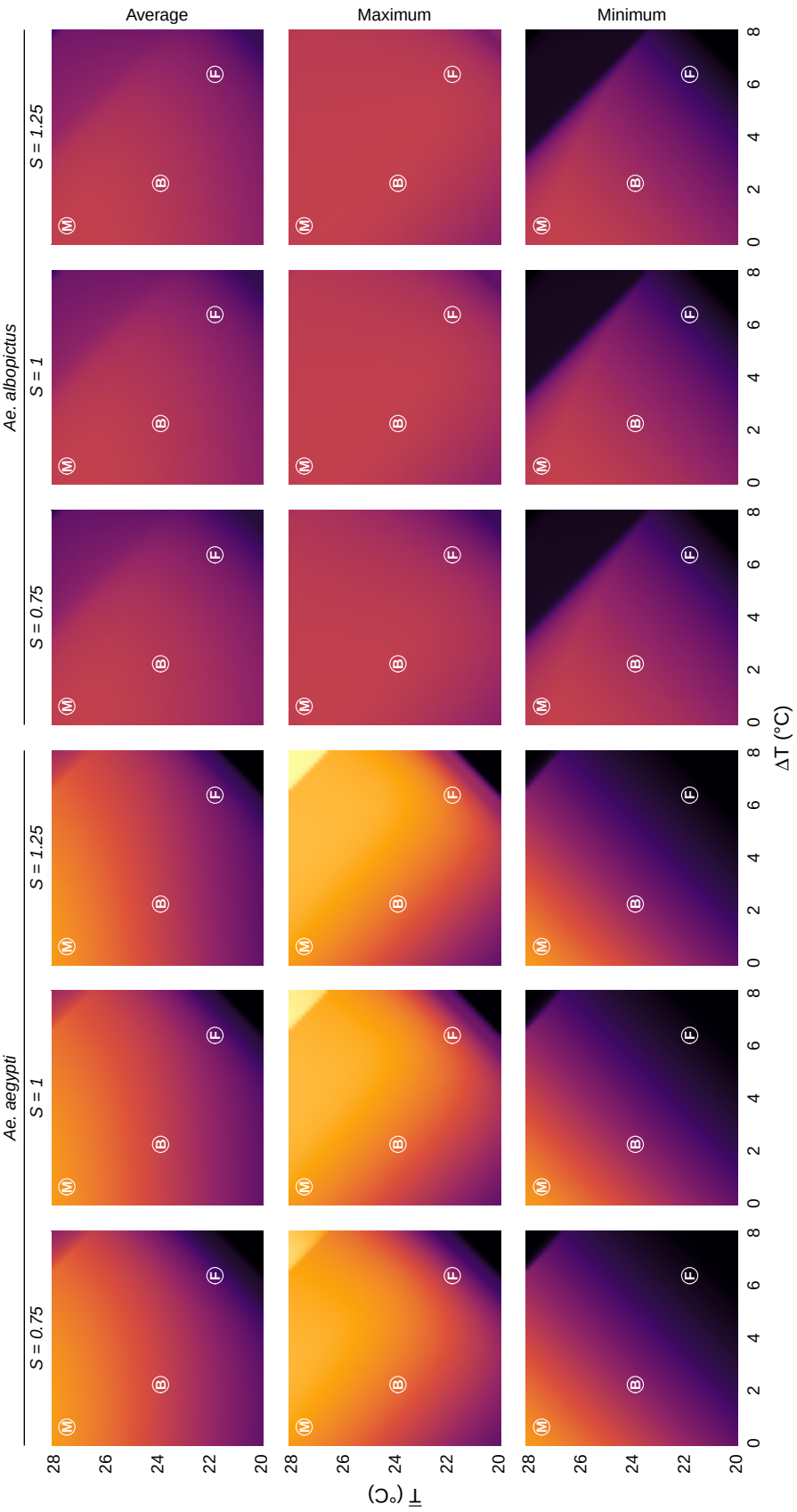



Figure C.2: Surfaces showing how the adult female population size (indicated by colour) of *Ae. aegypti* and *Ae. albopictus* change in response to average temperature ($\overline{T}$), the amplitude of annual temperature fluctuations ($\Delta T$) and the sharpness of the temperature change ($S$). The effect size of sharpness is shown across the column facets. In the first row, population sizes are averaged across the final three years of simulations, with maximum and minimum population sizes given in rows two and three. The letters M, B and F denote where the climates of Malaysia, Brazil and Florida sit within this parameter space. In this plot, $\alpha = 1 \times 10^{-6}$, $\gamma = 1$, $P = 0.5$ and $S = 1$.

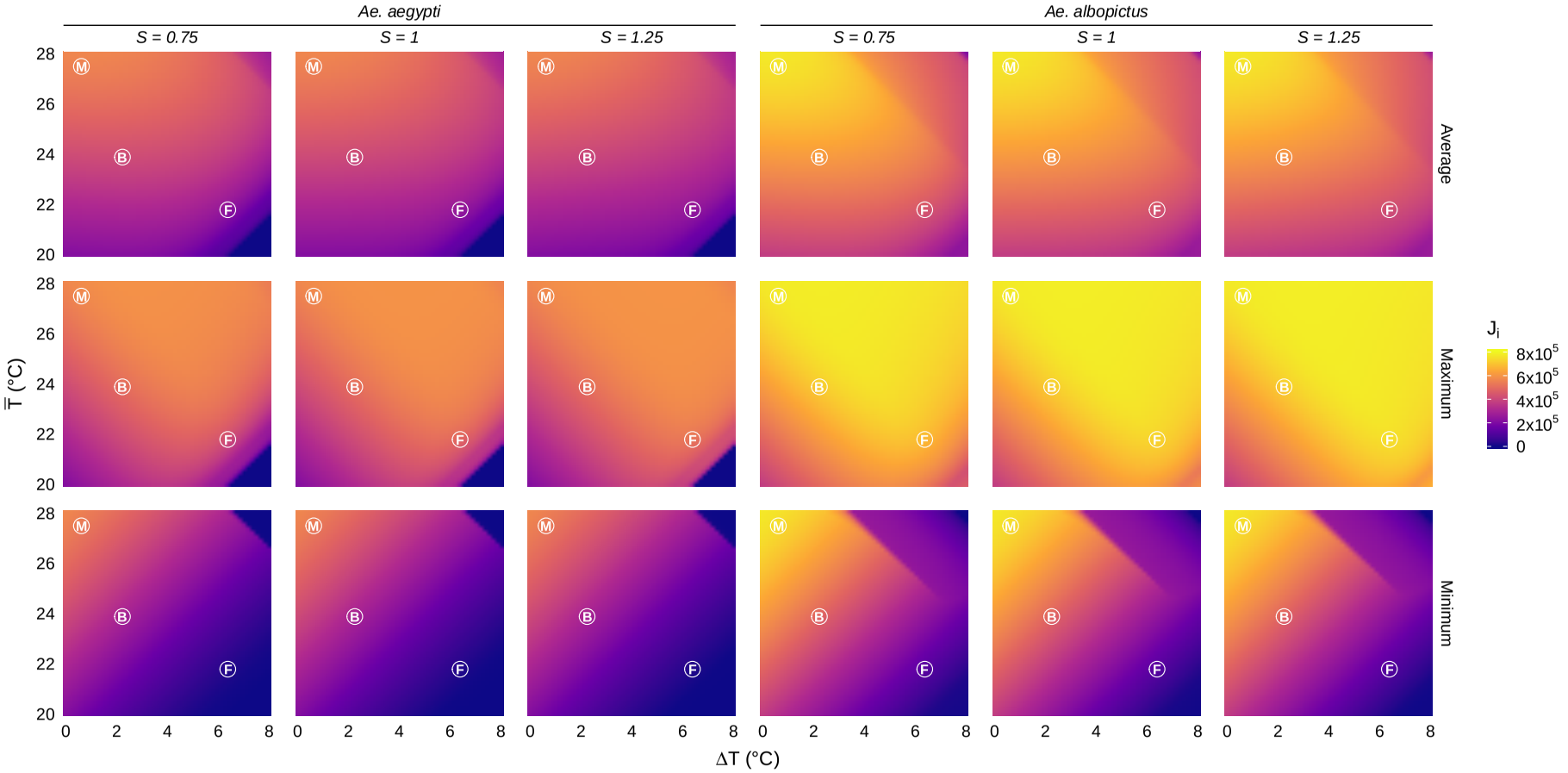



Figure C.3: Surfaces showing how the juvenile population size (indicated by colour) of *Ae. aegypti* and *Ae. albopictus* change in response to average temperature ($\overline{T}$), the amplitude of annual temperature fluctuations ($\Delta T$) and the sharpness of the temperature change ($S$). The effect size of sharpness is shown across the column facets. In the first row, population sizes are averaged across the final three years of simulations, with maximum and minimum population sizes given in rows two and three. The letters M, B and F denote where the climates of Malaysia, Brazil and Florida sit within this parameter space. In this plot, $\alpha = 1 \times 10^{-6}$, $\gamma = 1$, $P = 0.5$ and $S = 1$.

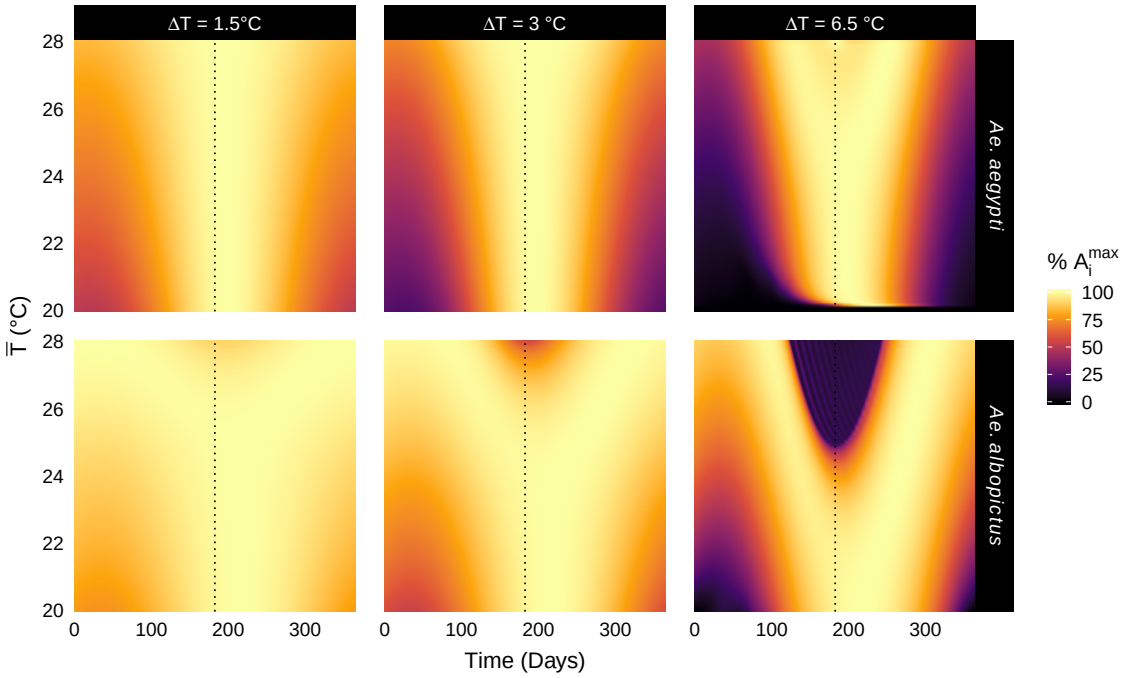



Figure C.4: Time series showing the timing of peak adult population size. The average temperature is shown on the y-axis ($\overline{T}$) and the day of the year on the x-axis (only the final year is plotted). The colour temperature of the surfaces indicates what percentage of the maximum population size the population is at for a given time. The dotted line denotes $P$, the point at which the maximum temperature is reached.

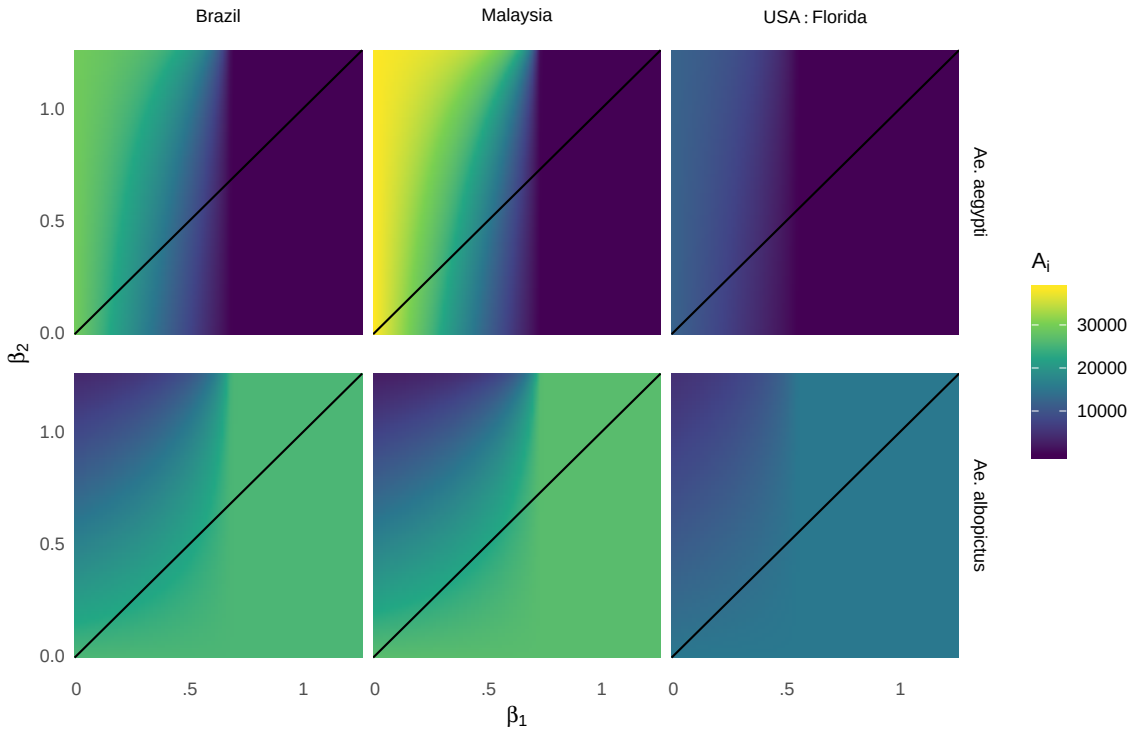



Figure C.5: Surfaces showing how the average densities of *Ae. aegypti* and *Ae. albopictus* change in response to different levels of larval competition.

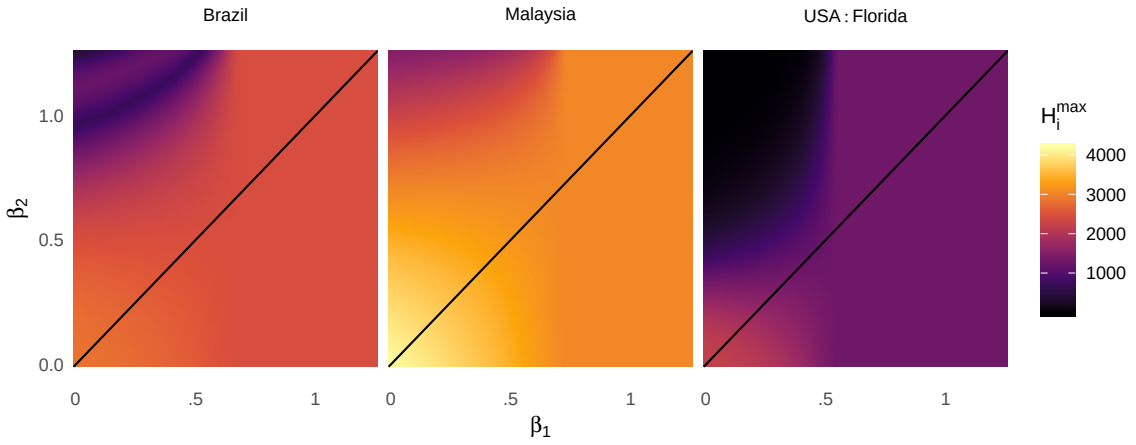



Figure C.6: Surfaces showing how the peak outbreak size changes in response to different levels of larval competition.

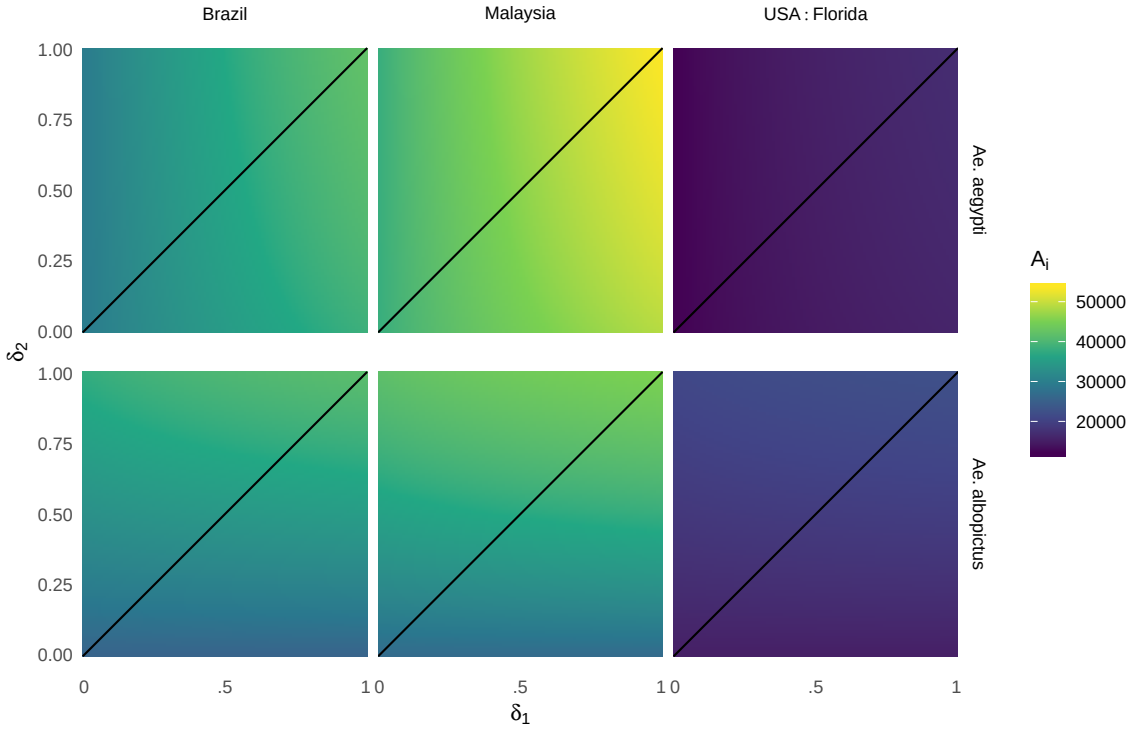



Figure C.7: Surfaces showing how the average densities of *Ae. aegypti* and *Ae. albopictus* change in response to different levels of reproductive interference. Note that interspecific larval competition is absence in these simulations.

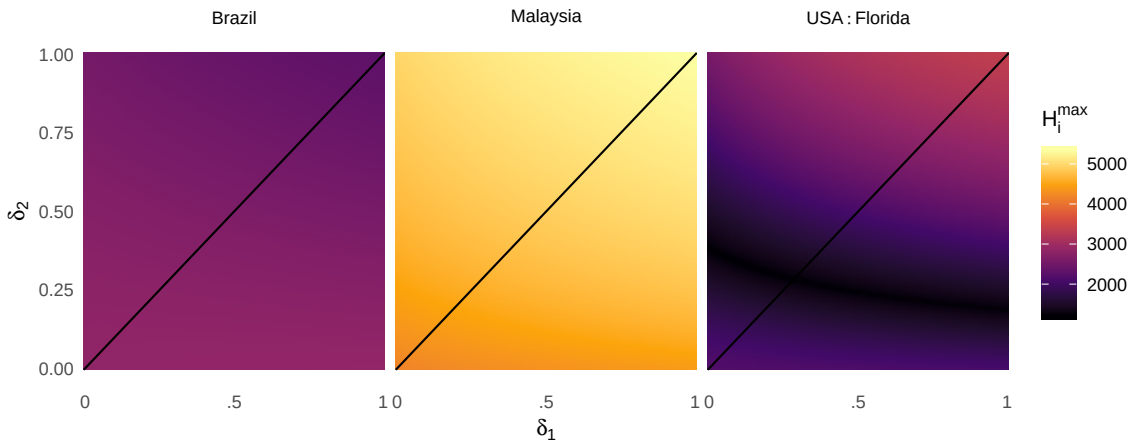



Figure C.8: Surfaces showing how the peak outbreak size changes in response to different levels of reproductive interference.

| trait | function | definition | $r$ | $T_m$ (°C) | $T_M$ (°C) | min |
|---|---|---|---|---|---|---|
| *Ae. aegypti* | | | | | | |
| $g$ | Bieré | the development rate of juveniles | $7.86 \times 10^{-5}$ | 11.36 | 39.17 | $\frac{1}{60}$ |
| $c$ | Quadratic | egg-to-adult survival probability | $5.99 \times 10^{-3}$ | 13.56 | 38.29 | 0 |
| $e$ | Bieré | egg-laying rate (eggs / female / day) | $8.56 \times 10^{-3}$ | 14.58 | 34.61 | 0 |
| $\frac{1}{d_A}$ | Quadratic | adult mosquito lifespan | $1.48 \times 10^{-1}$ | 9.16 | 37.73 | 1 day |
| $h$ | Bieré | the extrinsic incubation rate | $6.65 \times 10^{-5}$ | 10.68 | 45.09 | $\frac{1}{60}$ |
| $p$ | Bieré | probability of a mosquito becoming infected after a blood meal from an infected host | $4.91 \times 10^{-4}$ | 12.22 | 37.46 | 0 |
| $\rho$ | Bieré | probability of a bite from an infected mosquito transmitting the infection to the host | $8.49 \times 10^{-4}$ | 17.05 | 35.83 | 0 |
| $b$ | Bieré | the mosquito biting rate | $2.02 \times 10^{-4}$ | 13.35 | 40.08 | 0 |
| *Ae. albopictus* | | | | | | |
| $g$ | Bieré | the development rate of juveniles | $6.38 \times 10^{-5}$ | 8.60 | 39.66 | $\frac{1}{60}$ |
| $c$ | Quadratic | egg-to-adult survival probability | $3.61 \times 10^{-3}$ | 9.04 | 39.33 | 0 |
| $e$ | Bieré | egg-laying rate (eggs / female / gonotrophic cycle) | $4.88 \times 10^{-2}$ | 8.02 | 35.65 | 0 |
| $\frac{1}{d_A}$ | Quadratic | adult mosquito lifespan | 1.43 | 13.41 | 31.51 | 1 day |
| $h$ | Bieré | the extrinsic incubation rate | $1.09 \times 10^{-4}$ | 10.39 | 43.05 | $\frac{1}{60}$ |
| $p$ | Bieré | probability of a mosquito becoming infected after a blood meal from an infected host | $4.39 \times 10^{-4}$ | 3.62 | 36.82 | 0 |
| $\rho$ | Bieré | probability of a bite from an infected mosquito transmitting the infection to the host | $7.35 \times 10^{-4}$ | 15.84 | 36.40 | 0 |
| $b$ | Bieré | the mosquito biting rate | $1.93 \times 10^{-4}$ | 10.25 | 38.32 | 0 |

Table C.1: Model parameters estimated by Mordecai et al. (2017) from their literature review of the data on temperature-sensitive mosquito traits. Note that for *Ae. aegypti* egg-laying rates are estimated as a daily rate, whereas they are estimated per gonotrophic cycle for *Ae. albopictus*. In the model, we therefore correct the function $e_2$ (the egg-laying rate of *Ae. albopictus*) by multiplying by the biting rate at that time (as it can be assumed that the rate at which blood meals are taken will determine the rate at which eggs can be laid). When temperatures fell below or exceeded the thermal limits ($T < T_m$ or $T > T_m$) we specified a minimum value for the functions. Minimum juvenile development rates and extrinsic incubation rate were set to $\frac{1}{60}$ (i.e. the maximum period was 60 days), while the minimum adult lifespan was set to 1 day. Illustrations of these functions are given in Figure C.1.

| parameter | value | highest density interval |
|---|---|---|
| *Brazil* | | |
| $\overline{T}$ | 23.872 | 23.754-23.988 |
| $\Delta T$ | 2.239 | 2.143-2.342 |
| $P$ | 0.011 | 0.006-0.016 |
| $S$ | 0.510 | 0.460-0.564 |
| *Malaysia* | | |
| $\overline{T}$ | 27.487 | 27.437-27.534 |
| $\Delta T$ | 0.623 | 0.585-0.659 |
| $P$ | 0.407 | 0.395-0.417 |
| $S$ | 1.40 | 1.164-1.674 |
| *USA – Florida* | | |
| $\overline{T}$ | 21.775 | 21.491-22.039 |
| $\Delta T$ | 6.384 | 6.165-6.593 |
| $P$ | 0.556 | 0.552-0.561 |
| $S$ | 0.716 | 0.653-0.782 |

Table C.2: Table of parameter values estimated by fitting equation 18 to weather station data from Brazil, Malaysia and Florida. The value column corresponds to the median of the MCMC chains and the 95% highest density intervals given in the third column. Model fits are presented in Figure 4.1